

AFOSR 67-0753

A New Model for "Impulsive"  
Phenomena: Application to  
Atmospheric-Noise Communication  
Channels

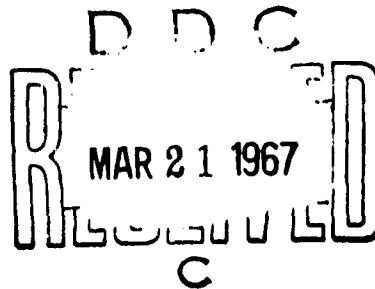
AD 64 by  
Harry M. Hall

August 1966

Technical Report No. 3412-8

Technical Report No. 7050-7

Prepared under  
U.S. Air Force Office of Scientific Research  
Grants AFOSR-783-65 and 783-66  
U.S. Air Force Office of Scientific Research  
Contract AF49(638)-1517  
Tri-Service Contract Nonr-225(83)



**RADIOSCIENCE LABORATORY**

**STANFORD ELECTRONICS LABORATORIES**

STANFORD UNIVERSITY • STANFORD, CALIFORNIA

ARCHIVE COPY



SEL-66-052

A NEW MODEL FOR "IMPULSIVE" PHENOMENA:  
APPLICATION TO ATMOSPHERIC-NOISE COMMUNICATION CHANNELS

by  
Harry M. Hall

August 1966

Reproduction in whole or in part  
is permitted for any purpose of  
the United States Government.

Technical Report No. 3412-8

Technical Report No. 7050-7

Prepared under

U.S. Air Force Office of Scientific Research  
Grants AFOSR-783-65 and 783-66

U.S. Air Force Office of Scientific Research  
Contract AF 49(638)1517  
Tri-Service Contract Nonr-225(83)

Radioscience Laboratory  
Systems Theory Laboratory  
Stanford Electronics Laboratories  
Stanford University                      Stanford, California

### ABSTRACT

This work is concerned with the development and application of an analytical model for "impulsive" phenomena. Specifically, a new model is developed for atmospheric noise, which is radio noise that originates in lightning discharges. This model is applied to the detection of known signals in additive atmospheric noise.

The modeling approach used here is based on the observation that a gaussian model is inappropriate for received atmospheric noise, primarily because gaussian noise does not have the large dynamic range exhibited by the received noise power. The generalized "t" model resulting from the approach used in this work is in good agreement with measured data, and describes the received atmospheric noise  $y(t)$  as

$$y(t) = a(t) n(t)$$

where  $n(t)$  is a narrowband gaussian process and  $a(t)$  is a slowly varying process, independent of  $n(t)$ , that modulates  $n(t)$ .

The detection of known signals in additive generalized "t" noise--i.e., in the presence of additive noise described by the generalized "t" model, is considered, and the receiver that minimizes the probability of error is found to be a "logarithmic-correlator" receiver that implements the rule:

Decide that the known signal is present iff

$$\int_0^T \ln[|x(t)|^2 + \gamma^2] dt \geq \int_0^T \ln[|x(t) - \mu(t)|^2 + \gamma^2] dt ,$$

where  $m(t)$  is the known signal,  $x(t)$  is the received signal,  $|x(t)|$  is the envelope of  $x(t)$ , and  $|x(t) - \mu(t)|$  is the envelope of  $[x(t) - m(t)]$ . An "exponentially correct" estimate of the probability of error achieved by this receiver is given by

$$P_e \approx K \exp\left[-\frac{1.35 E}{Y_0}\right]$$

where  $E$  is the energy of the known signal,  $Y_0 = 2\gamma^2/B$  is proportional to the average noise energy, and  $K$  is a polynomial in  $(2TB)^{-1/2}$ .

The performance of the log-correlator receiver is compared with that achieved by other receiver forms in the presence of additive generalized "t" noise. Analytical results indicate that the log-correlator receiver performs significantly better than any linear receiver in the presence of additive atmospheric noise. Available experimental data support this conclusion.

## CONTENTS

	<u>Page</u>
I. INTRODUCTION . . . . .	1
A. Purpose . . . . .	1
B. Background . . . . .	1
C. Contributions of This Work . . . . .	2
II. THE GENERALIZED "t" MODEL . . . . .	3
A. Introduction . . . . .	3
1. Physical Description of Atmospheric Noise . . . . .	3
2. Summary of Existing Models for Atmospheric Noise . . . . .	4
B. Development of the New Model . . . . .	10
1. Specification of the Generalized "t" Model . . . . .	11
C. Verification of Applicability of the Generalized "t" Model . . . . .	17
1. First-Order Distributions of Envelope and Phase . . . . .	19
2. Average Intensity of Envelope Level Crossings . . . . .	53
3. The Distribution of Envelope Level Crossings . . . . .	62
D. Summary and Conclusions . . . . .	75
III. APPLICATION OF THE GENERALIZED "t" MODEL . . . . .	78
A. Introduction . . . . .	78
1. Summary of Known Results . . . . .	78
B. Case I: Short-Duration Signals, $a(t) = a, 0 \leq t \leq T$ . . . . .	82
1. Calculation of the Likelihood Ratio . . . . .	84
2. Discussion of the Optimal Receiver Rule . . . . .	87
3. Case $I_m$ : Modified Generalized "t" Noise . . . . .	89
4. Calculation of the Probability of Error for Case I and Case $I_m$ . . . . .	92
5. Generalized "t" Noise . . . . .	94
6. Modified Generalized "t" Noise . . . . .	98
7. Discussion of Probability-of-Error Results . . . . .	101
C. Case II: Long-Duration Signals; The General Case . . . . .	102
1. Calculation of the Likelihood Ratio . . . . .	104
D. Case IIa: Complex Envelope Representation . . . . .	107
1. Calculation of the Likelihood Ratio for Case IIa . . . . .	108
2. Discussion of Optimal Receiver Rule (Case IIa) . . . . .	113
3. Calculation of the Probability of Error (Case IIa) . . . . .	116
4. Discussion of Probability-of-Error Results (Case IIa) . . . . .	129

## CONTENTS (Cont)

	<u>Page</u>
E. Summary and Conclusions . . . . .	134
IV. RELATED TOPICS . . . . .	138
A. Comparison of the Log-Correlator with Another Receiver Form . . . . .	138
B. Detection and Analysis of Whistler-Mode Signals . . . . .	140
1. Analysis of Typical Whistler Receivers . . . . .	141
2. Conclusions . . . . .	143
V. SUMMARY AND CONCLUSIONS . . . . .	145
A. The Generalized "t" Model for Received Atmospheric Noise	145
B. Detection of Known Signals in Additive Atmospheric Noise	146
1. Case I: Short-Duration Signals . . . . .	146
2. Case II: Long-Duration Signals, The General Case . .	147
C. Recommendations for Future Work . . . . .	149
APPENDIX A. EVALUATION OF INTEGRALS . . . . .	151
APPENDIX B. PROOF THAT EQ. (3.126), $\mu_N^1(s) = 0$ , IS UNIQUELY SATISFIED BY $s = 1$ . . . . .	155
APPENDIX C. PROOF THAT INFINITE RECEIVER BANDWIDTH ( $2B = \infty$ ) MINIMIZES THE CASE IIa $P_e$ RESULT . . . . .	159
REFERENCES . . . . .	161

## ILLUSTRATIONS

<u>Figure</u>	<u>Page</u>
1. Waveform and spectrum of the radiated field of a lightning discharge . . . . .	5
2. Hilbert transforming filter . . . . .	20
3. Typical Fourier transforms, $A(f)$ and $N(f)$ , of $a(t)$ and $n(t)$ . . . . .	20
4. Probability distribution function of the envelope of received vlf atmospheric noise: comparison of model results with data measured at Point Barrow, Alaska, Sept. 16, 1955 . . . .	26
5. Probability distribution function of the envelope of received vlf atmospheric noise: comparison of model results with data measured at Point Barrow, Alaska, Sept. 10, 1955 . . . . .	28
6. Probability distribution function of the envelope of received vlf atmospheric noise: comparison of model results with data measured at Boulder, Colorado, Aug. 5, 1955 . . . . .	30
7. Probability distribution function of the envelope of received vlf atmospheric noise: comparison of model results with data measured at Boulder, Colorado, Mar. 23, 1956 . . . . .	32
8. Probability distribution function of the envelope of received vlf atmospheric noise: comparison of model results with data measured at Balboa, C.Z., Oct. 27, 1955 . . . . .	34
9. Probability distribution function of the envelope of received vlf atmospheric noise: comparison of model results with data measured at Balboa, C.Z., Oct. 28, 1955 . . . . .	36
10. Composite probability distribution function of the envelope of received vlf atmospheric noise: comparison of model results with data measured at Slough, England and at Singapore . . . .	33
11. Composite probability distribution function of the envelope of received lf atmospheric noise: comparison of model results with data measured at Slough, England and at Singapore . . . .	40
12. Composite probability distribution function of the envelope of received hf atmospheric noise: comparison of model results with data measured at Slough, England and at Singapore . . . .	42
13. Composite probability distribution function of the envelope of received hf atmospheric noise: comparison of model results with data measured at Slough, England and at Singapore . . . .	44
14. Probability distribution function of the envelope of received hf atmospheric noise: demonstration of effect of a pre-dominant local noise source . . . . .	46
15. Average rate of envelope level crossings: comparison of model results with measured vlf data . . . . .	56

## ILLUSTRATIONS (Cont)

<u>Figure</u>	<u>Page</u>
16. Definition of $q_i(t)$ , $i = 0, \dots, N$ , where $t_i \triangleq \left(i - \frac{1}{2}\right) \Delta t$	63
17. Probability distribution of the time interval between envelope level crossings: comparison of model results with measured vlf data . . . . .	68
18. Probability distribution of the time interval between envelope level crossings: comparison of model results with measured .lf data . . . . .	70
19. Description of additive-atmospheric-noise communication channel . . . . .	78
20. Description of "known"-signals detection problem . . . . .	81
21. Geometrical picture of spherical symmetry of the probability distribution of the Case I additive-noise vector . . . . .	93
22. "Short-duration" signal (Case I) performance: comparison of error curves achievable by optimal matched filter receiver in presence of various additive noises . . . . .	96
23. Block diagram of optimal logarithmic-correlator receiver . .	113
24. Receiver performance in presence of additive atmospheric noise: comparison of predicted error curves with measured performance of an FSK system operating at vlf . . . . .	130
25. Block diagram of receiver commonly used in presence of additive atmospheric noise . . . . .	139
26. Block diagram of clipper receiver commonly used to analyze whistler signals . . . . .	141
27. Description of contour of integration used to evaluate Eq. (A.5) . . . . .	153

# LIST OF SYMBOLS

$a(t)$	modulating function appearing in the generalized "t" model for atmospheric noise
$b(t)$	$1/a(t)$
$2B$	receiver radio-frequency (rf) bandwidth centered about $f_0$
$B_c$	$\int_{-\infty}^{\infty} f^2 \frac{S_c(f)}{R_c(0)} df$ ; root-mean-square (rms) bandwidth
$B_0/2$	$\sigma^2$ ; "width" parameter of the chi distribution specifying the first order statistics of $b(t)$
$E$	energy of the transmitted signal
$E(t)$	envelope of the gaussian process $n(t)$
$E[x]$	$\int_{-\infty}^{\infty} \tau p_x(\tau) d\tau$ ; expected value of the random variable $x$
$\text{erfc}(x)$	$\int_x^{\infty} (2\pi)^{-1/2} \exp(-\tau^2/2) d\tau$ ; area under tail of the normal distribution with zero mean and unity variance
$f_0$	band center frequency
$g_i(s)$	$E[\exp(s \ln z_i)]$ ; moment-generating function of $\ln z_i$
$g_N(s)$	moment-generating function of the sum of independent random variables $\sum_{i=1}^N \ln z_i$
$L(x)$	$w(x h^{(1)})/w(x h^{(2)})$ ; the likelihood ratio
$\ln x$	logarithm of $x$ to the base $e$
$m$	parameter of the chi distribution $\chi(m, \sigma)$
$m(t)$	transmitted signal
$n(t)$	zero-mean gaussian process with covariance $R_n(\tau)$ appearing in the generalized "t" model
$N_0/2$	$R_n(0) = \sigma_1^2$ ; variance of $n(t)$
$\overline{N_V(V_0)}$	average number of crossings of the level $V_0$ by the envelope $V(t)$ per second

$p_x(\cdot)$	probability density function of the random variable $x$
$P(x)$	$\int_{-\infty}^x p_x(\tau) d\tau$ ; probability distribution function of the random variable $x$
$P_0(x)$	$1 - P(x)$
$P_e$	probability of error
$Pr$	probability
$q_1(t)$	pulse "basis" function appearing in signal representations
$Q$	average transmitted signal power
$S_n(f)$	power spectral density of the random process $n(t)$ ; i.e., the Fourier transform of $R_n(\tau)$
SNR	signal-to-noise energy ratio
$\Delta t$	time increment
$T$	a fixed length of time (denotes length of either observation or signaling interval)
$\text{var}(x)$	variance of the random variable $x$
$V(t)$	envelope of $y(t)$
$w(x h^{(i)})$	probability density function of $x$ under hypothesis $i$
$x(t)$	received sum of transmitted signal plus additive noise
$y(t)$	observed atmospheric noise
$Y_0$	$4\xi^2$ ; parameter proportional to the average noise energy received in the time interval $\Delta t$
$z_i$	$\frac{ \eta_1 ^2 + \xi^2}{ \eta_1 - \mu_1 ^2 + \xi^2}$ ; random variable appearing in probability of error calculations for Case IIa.
$\beta$	truncation parameter specifying the modified generalized "t" model
$\gamma$	$\sqrt{m} \frac{\sigma_1}{\sigma}$ ; parameter specifying "width" of the generalized "t" distribution
$\Gamma(n)$	$\int_0^{\infty} \tau^{n-1} \exp(-\tau) d\tau$ ; the gamma function

$\delta_{ij}$	$\begin{cases} 1, & i = j, \\ 0, & \text{otherwise;} \end{cases}$ <p>the Kronecker delta</p>
$\eta(t)$	complex envelope of $y(t)$
$\theta$	$m+1$ ; parameter specifying slope of the tail of the generalized "t" distribution
$\Lambda$	an arbitrary square matrix
$\mu(t)$	complex envelope of $m(t)$
$\mu_N(s)$	$\ln[g_N(s)]$
$\mu_N'(s)$	$\frac{d}{ds} [\mu_N(s)]$ ; derivative of $\mu_N(s)$ with respect to $s$
$v(t)$	complex envelope of $n(t)$
$\xi^2$	$\gamma^2 \Delta t = m \frac{N_0}{B_0} \Delta t$ ; parameter proportional to the average noise energy received in the time interval $\Delta t$
$\sigma$	parameter of the chi distribution $x(m, \sigma)$
$\sigma_1$	parameter of the normal distribution $N(0, \sigma_1^2)$
$\varphi(t)$	phase of $y(t)$
$\varphi_1(t)$	eigenfunction of $R_n(t, s)$
$x(t)$	complex envelope of $x(t)$
$x(m, \sigma)$	chi distribution having parameters $m$ and $\sigma$
$x_2(m, \sigma)$	two-sided chi distribution having parameters $m$ and $\sigma$
$\forall$	for all
$\triangleq$	is defined as
$\approx$	is approximately equal to

#### Some Conventions and Notations

Convolution of  $x_1(t)$  with  $x_2(t)$ :

$$x_1(t) * x_2(t) = \int_{-\infty}^{\infty} x_1(\tau) x_2(t-\tau) d\tau$$

Fourier transform of  $x(t)$ :

$$X(f) = \int_{-\infty}^{\infty} x(t) \exp(-i2\pi ft) dt$$

Hilbert transform of  $x(t)$ :

$$\tilde{x}(t) = \int_{-\infty}^{\infty} \frac{x(\tau)}{\pi(t-\tau)} d\tau \quad (\text{Cauchy principal value})$$

Vector notation:

$$\underline{x} = \begin{bmatrix} x_1 \\ \vdots \\ x_N \end{bmatrix}; \quad \text{a column vector}$$

Other notation:

$\underline{x}_t$	the transpose of $\underline{x}$
$\ \underline{x}\ $	the norm of $\underline{x}$
$\langle \underline{x}_1, \underline{x}_2 \rangle$	the inner product of the vectors $\underline{x}_1$ and $\underline{x}_2$
$\langle \underline{x}_1, \underline{x}_2 \rangle_{\Lambda}$	the bilinear form $\underline{x}_1 \Lambda \underline{x}_2$
$\dot{x}(t)$	$\frac{d}{dt} [x(t)]$ ; time derivative of $x(t)$
$x^*$	complex conjugate of $x$

#### ACKNOWLEDGMENTS

The author wishes to acknowledge the guidance of Professor Thomas Kailath both as a research advisor and as a teacher. I am very grateful for his direction and encouragement throughout the course of this work.

I am much indebted to Professor R. A. Helliwell for his interest in this work and for providing a research environment in which the author was free to devote full attention to this research problem.

Acknowledgments are due to the many experimentalists who have provided measured data upon which the research presented here is based. Particular gratitude is due Mr. A. D. Watt and Mr. E. L. Maxwell whose excellent data are drawn upon heavily throughout this work.

This research was supported in part by the U.S. Air Force under grants AFOSR 783-65 and 783-66, monitored by the Air Force Office of Scientific Research of the Office of Aerospace Research, in part by the U.S. Air Force under AFOSR Contract AF 49(638)1517, and in part by Tri-Service Contract Nonr-225(83), jointly supported by the U.S. Army Signal Corps., the U.S. Air Force, and the U.S. Navy (Office of Naval Research).

## I. INTRODUCTION

### A. PURPOSE

The purpose of this work is two-fold: 1) to develop an analytical model for "impulsive" phenomena, i.e., phenomena having impulse characteristics, and 2) to apply this model to the study of communication channels having additive impulse noise. In particular, this work focuses on a specific impulsive phenomenon, atmospheric radio noise. Atmospheric radio noise is selected as a case of special interest because: 1) there is a reasonable amount of experimental data available against which proposed models can be checked, and 2) additive-atmospheric-noise channels are important both for communication purposes and as a source of information on naturally occurring signals of scientific interest. (An example of such signals is the whistler-mode signal discussed in Chapter IV.)

### B. BACKGROUND

Atmospheric noise, which is described in more detail in Chapter II, is radio noise that originates in lightning discharges. At a representative receiving site, lightning discharges are typically observed to occur at a rate of the order of 10 discharges per second, although it is emphasized that this typical rate can vary from about one per second to nearly 100 per second dependent on several factors mentioned in Chapter II. Since the principal noise pulse produced by each discharge has a duration of about 100  $\mu$ sec, it follows that the observed noise has a distinctive impulsive character. Various analytical models have been proposed for received atmospheric noise, and these usually are derived from one of two points of view, which will be discussed in more detail in Chapter II. Briefly, the most interesting approach from a physical point of view takes the received noise to be the weighted sum of contributions from individual lightning discharges. Although this approach is well motivated physically, it has the disadvantage that the resulting models are not analytically tractable. The alternative approach is an empirical method that yields analytical models chosen to fit the measured statistics of the noise. However, in addition to the lack of direct physical support

for this procedure, the existing empirical models suffer from the fact that they consider only the first-order statistics of the noise, while neglecting the higher-order statistics.

Although several models for received atmospheric noise have been proposed in the literature, very few analytical results are available on problems of signal detection or estimation in the presence of additive atmospheric noise. The published results, which are discussed in detail in Chapter III, fall into two categories:

1. A signal-to-noise ratio (SNR) criterion has been used to compare specific receiving techniques.
2. Several workers have employed empirical models to calculate the probability of error resulting from the use of linear receivers in the presence of additive atmospheric noise.

#### C. CONTRIBUTIONS OF THIS WORK

Using an approach which differs from both of those mentioned above, a new analytical model for received atmospheric noise is developed in Chapter II. This model, called the generalized "t" model, is attractive from an analytical point of view and also provides a good fit to the measured statistics of received atmospheric noise, including statistics of higher-order as well as those of first-order. This model is applied in Chapter III to the detection of known signals in additive atmospheric noise. A receiver called the "logarithmic-correlator" receiver is found to minimize the probability of error in the presence of additive generalized "t" noise. The probability of error achievable using this receiver is calculated and provides the only theoretical estimate known to the author of the error performance achievable in the presence of additive atmospheric noise. In Chapter IV, the performance of the log-correlator receiver is compared with that of receivers commonly used in practice in the presence of additive atmospheric noise.

## II. THE GENERALIZED "t" MODEL

### A. INTRODUCTION

The purpose of the work described in this chapter is to obtain a class of nongaussian random processes that can serve as a model for certain impulsive phenomena observed in nature. Specifically, it is desired to develop a model for certain impulsive noises observed in communications engineering, with particular emphasis on the additive impulse noise, commonly termed atmospheric noise, observed on radio circuits operating at frequencies below approximately 100 Mc. The work in this chapter is concerned with the formulation of a model for impulsive phenomena, and the verification of the applicability of this model, when appropriately specialized, as a model for received atmospheric noise.

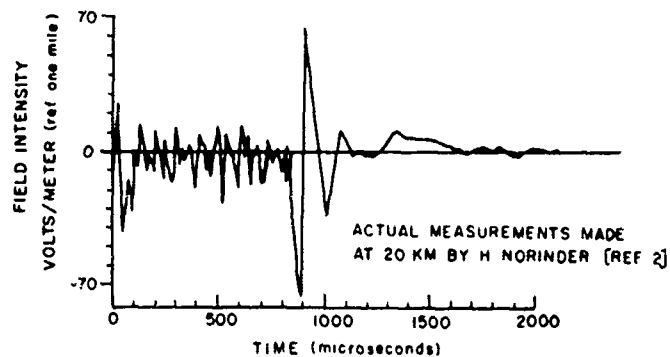
#### 1. Physical Description of Atmospheric Noise

Before proceeding with the modeling problem, a brief physical description of atmospheric noise is presented as follows: Atmospheric noise is taken here to be radio noise that has its source in lightning discharges. A descriptive discussion of both this noise and its lightning sources is presented by Watt and Maxwell [Ref. 1], who point out that the lightning discharge consists essentially of a slowly developing leader stroke (predischARGE) of about one msec duration followed by a return stroke (main discharge) of about 100  $\mu$ sec duration. Although the details of the discharge are complicated, the observed noise can be explained by noting that the leader stroke is actually made up of a series of discrete leaders occurring at a rate of one every 25 to 100  $\mu$ sec. Each of these leaders travels over a successive 30 ft to 200 ft portion of the cloud-to-ground path, producing a current pulse of about one  $\mu$ sec duration with an intensity of the order of 300 amp. The result of this recurrent process is that the energy radiated by the predischARGE has a 3-db bandwidth of the order of 40 kc centered at a frequency of approximately 30 kc. Following this predischARGE, the single return stroke takes place, producing a current pulse of about 100  $\mu$ sec duration having an average peak intensity of 20 kiloamperes. The energy radiated by this return stroke, which accounts for about 95 percent of the total energy radiated by the lightning

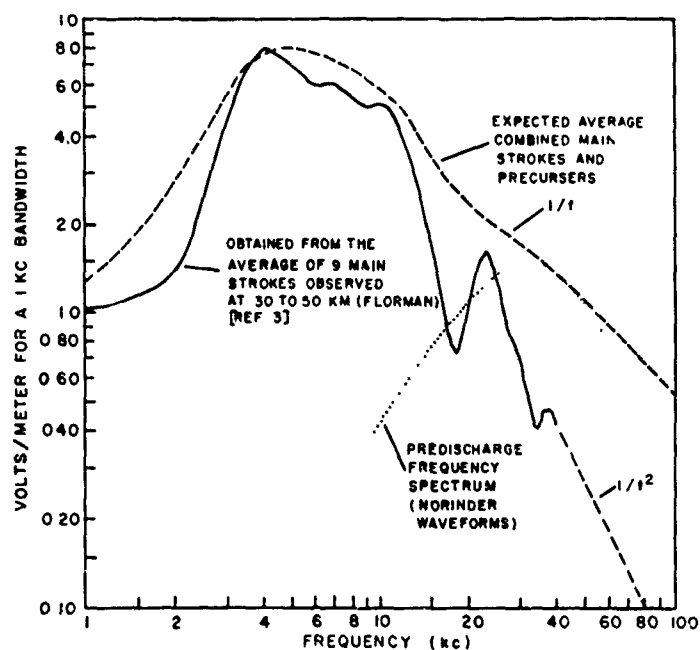
discharge, has a 3-db bandwidth of the order of 10 kc centered at a frequency of approximately 10 kc. This behavior of the lightning discharge as a function of time and frequency is illustrated in Fig. 1 (taken from Watt and Maxwell) which shows both the waveform and the spectrum of the radiated field (see also Refs. 2 and 3). The total energy radiated by a single lightning discharge is of the order of 200,000 joules [Ref. 4]; therefore it is not surprising that the resulting atmospheric noise is the predominant radio noise at vlf and lf. However, because the spectrum of the lightning discharge is approximately proportional to  $1/f$  at frequencies above the upper "3-db-down point," as indicated in Fig. 1, it is often true that atmospheric noise is the predominant radio noise even at hf. It should be noted, however, that hf atmospheric noise differs from vlf atmospheric noise in that the former is primarily the result of the predischARGE with its discrete fine structure, whereas the latter is predominantly the result of the return stroke. With the above description of the individual lightning discharge in mind, and noting that the average number of lightning discharges observed per unit time at a receiving site typically lies in the range from one per second to 100 per second, it is clear, in agreement with experience, that the received atmospheric noise will be impulsive in nature. It is pointed out that the large range exhibited by the average rate of observed lightning discharges is the result of several factors detailed in the next section. Of particular importance among these factors is the geographical position of the receiver. For example, the average rate can vary from about one distinguishable discharge per second at temperate latitudes to nearly 100 per second in the tropics.

## 2. Summary of Existing Models for Atmospheric Noise

Turning attention now to the problem of developing a model for received atmospheric noise, it is seen that this noise is always observed through the passband of some receiver filter. Thus the noise observed at any instant of time is the resultant of several lightning discharges spaced in time and location of occurrence, with the observed number and intensity of the lightning discharges dependent upon a number of factors. Notable among these factors are receiver bandwidth and band center frequency,



a. Waveform



b. Spectrum

FIG. 1. WAVEFORM AND SPECTRUM OF THE RADIATED FIELD OF A LIGHTNING DISCHARGE. (Referred to a distance of one mile.)

receiver location, thunderstorm activity, and propagation conditions. These factors must be taken into consideration in the model.

To provide motivation for the development of a new model for atmospheric noise, a brief summary of available models is now presented. It is reasonable to categorize the available models for observed atmospheric noise into two groups, to be called here the filtered-impulse models and the empirical models, respectively.

a. The Filtered-Impulse Models

The filtered-impulse models [Refs. 5, 6, 7, 8] are well motivated physically and are similar to one another in that they all take the received noise  $n(t)$  to have essentially the form

$$n(t) = \sum_{i=1}^N a_i p(t-t_i), \quad (2.1)$$

where the  $a_i$  are independent, identically distributed random variables whose distribution is deduced primarily from lightning discharge statistics as affected by receiver location and propagation considerations;  $p(t)$  gives the form of the noise pulse resulting from an individual lightning stroke as shaped by an assumed filter in the front end of the receiver; and the  $t_i$  are the occurrence times of the  $N$  individual lightning strokes. With this formulation for the received noise, and with the assumption that the contributions to the received noise by the individual lightning strokes are statistically independent, various results [Refs. 6, 7, 8] have been obtained on the first-order statistics of the received noise using the method of characteristic functions. In particular, the workers referenced above have focused on the problem of determining the probability distribution of the envelope of the received noise, since this distribution has been measured quite extensively [Refs. 6, 9, 10, 11, 12]. Although the analytical results vary in their agreement with the measured data as a function of both the choice of  $p(t)$  and the choice of the statistics of  $N$ , of the  $t_i$ , and of the  $a_i$ , the following conclusions on the filtered-impulse models appear to be warranted in general: The strong point of the filtered impulse approach is of course that the

model is well motivated physically. Thus it is possible to specify the model and to determine the degree to which the received noise is expected to be nongaussian in terms of physically meaningful parameters. On the other hand, there are several disadvantages that arise as a consequence of the filtered-impulse approach. These can be summarized as follows:

1. The resulting probability distributions are quite complicated, and one is not able to put them in closed form except in certain limiting situations. As a result of the complexity of these distributions, they are not of much use in the consideration of the statistical detection problem at the receiver. The available results [Ref. 7] are achieved by resorting to a signal-to-noise ratio SNR argument as a criterion for comparing specific receiving techniques; it is well known that SNR is not necessarily a good measure of the ability of a receiver to process digital information.
2. The assumption that the contributions of the individual lightning strokes to the received noise are statistically independent of one another, which is crucial to the solution for the first-order statistics of  $n(t)$ , does not appear to be true, at least for vlf atmospheric noise. This conclusion follows from the experimental results obtained by Watt and Maxwell [Ref. 9] on the distribution of the time interval between crossings of a fixed level by the envelope of vlf atmospheric noise in which it has been found that received noise pulses are usually statistically dependent on preceding pulses.

The second disadvantage is particularly disturbing, because the strongest argument in support of the filtered-impulse models has been the closeness of their approximation to the physics of the noise. In this regard it is noted that the filtered-impulse models in the literature have typically been based on the assumption, either that the number of noise pulses influencing the received noise is known [Ref. 8], or that the noise pulses occur in a Poisson fashion [Refs. 5, 6, 7]. The latter assumption, which enables one to think of the received noise as a filtered Poisson process, seems quite reasonable, but does not admit the particular type of statistical dependence between adjacent noise pulses that is usually observed in practice.

One approach that may be useful in introducing this dependence into the filtered-impulse model is that taken by Furutsu and Ishida [Ref. 6], who have considered the case of Poisson-Poisson noise. In this case the noise is assumed to consist of clusters of noise pulses, where the pulses within the cluster occur in a Poisson fashion with mean rate  $\nu$ ,

while the clusters themselves occur in a Poisson fashion with mean rate  $\nu'$ , where  $\nu' < \nu$ . It is to be noted that Furutsu and Ishida were primarily studying hf atmospheric noise, and introduced the Poisson-Poisson noise model as a means of representing the fine structure of the leader stroke. It has not yet been demonstrated that the Poisson-Poisson model yields the distribution of inter-level-crossing intervals observed by Watt and Maxwell at vlf; but it seems reasonable as a model which imitates the tendency of received atmospheric noise to consist of clusters of noise pulses.

Finally, it should be mentioned as noted by Galejs [Ref. 8] that the filtered-impulse models may be most useful as a method for studying the problem (the inverse of that being studied here) of using the relatively large amount of data on received atmospheric noise to determine the statistics of the lightning source itself.

#### b. The Empirical Models

The empirical models differ fundamentally in their concept from the filtered-impulse models in that they result from an attempt to construct a mathematical expression that fits the observed data without regard for the physics of the noise source. In every case, these empirical models consist of mathematical expressions constructed in an attempt to fit the measured data on the first-order statistics of the envelope of the received noise. A recent summary of the various empirical models that have been proposed is presented by Ibukun [Ref. 12]. Despite the diversity of these models, the following conclusions appear to be warranted in general: The principal advantage that accrues from use of the empirical modeling procedure is that the resulting model for the first-order statistics of the received noise is much simpler than that obtained from any of the filtered-impulse models. Hopefully, this simplicity will make the empirical model useful in the consideration of the signal-detection problem at the receiver. On the other hand, disadvantages that result from use of the empirical modeling procedure are:

1. It may not be possible to justify the empirical model on physical grounds.
2. By the nature of their construction, the empirical models consider only the first-order statistics of the noise. In order to extend

these models to the point that one has a model for the random process, it is necessary to make further assumptions concerning the higher-order statistics of the noise. Because of the distinctly nongaussian nature of the noise, it appears that the assumptions required to produce an analytically tractable model must include the assumption that the contributions of individual lightning strokes to the received noise are statistically independent. As discussed earlier, this assumption is not in agreement with measured results.

Although (1) above is a fundamental disadvantage of the empirical approach, it is noted that several workers [Refs. 13, 14, 15] have had some success in finding physical justification for empirical models. Perhaps the most interesting of these, because of its simplicity and its closeness of fit to measured data, is the model that takes the envelope of the received atmospheric noise to be Rayleigh-distributed at low values of the envelope and log-normally distributed at high values. Beckmann [Ref. 14] has given a physical argument which supports this model, particularly in the situation where there is little local thunderstorm activity. It is noted that several workers [Refs. 12, 14, 15, 16] have proposed models similar to that considered by Beckmann, although they differ in regard to how the two distributions should be combined to give the best resultant model.

With this brief summary of available models in mind, the development of a new model called the generalized "t" model will proceed in the next section from a point of view different than those leading to either the filtered-impulse models or the empirical models discussed above.

It is noted at this point, however, that the generalized "t" model will be seen to give some physical support to perhaps the simplest of the empirical models. This empirical model is the one [Refs. 12, 17] that takes the probability  $P_0(V)$  that the noise envelope exceeds the value  $V$  to be

$$P_0(V) = \left[ 1 + \left( \frac{\alpha V}{\bar{V}} \right)^r \right]^{-1} \quad (2.2)$$

where  $\bar{V}$  is the average value of the envelope and  $\alpha$  and  $r$  are two parameters to be chosen. This empirical model is also essentially identical

to the model studied in detail by Mertz [Refs. 18, 19]. In addition to the fact that the first-order statistics of the generalized "t" model agree closely with this class of empirical models, it will be shown that the generalized "t" model has the advantage over the empirical models in general that it can be specified to also give a good fit to the higher-order statistics of the noise.

Before proceeding with the development of a new model for impulsive phenomena, it is acknowledged that the conceptual motivation for this development derives from the work of Mandelbrot [Ref. 20] on the applicability of a class of "self-similar" random processes as a model for certain intermittent phenomena. Mandelbrot introduces the concept of a random process that is controlled by one "regime" for the duration of observation, where this regime is itself a random variable. Although the class of "self-similar" random processes considered by Mandelbrot is not of interest as a model for atmospheric noise, the regime concept will be useful in suggesting a model of the form of the generalized "t" model.

#### B. DEVELOPMENT OF THE NEW MODEL

Before mathematically formulating a new model for impulsive phenomena, a physical discussion focusing on the particular case of received atmospheric noise is presented in order to lend physical significance to the mathematical formulation. Although this discussion is based on experience with received atmospheric noise, it is seen that similar models may be applicable to other impulsive phenomena, e.g., to the impulse noise observed on telephone lines.

As mentioned in Section A2, the atmospheric noise observed at an instant in time through the passband of a linear receiver is dependent on a number of factors; notably receiver bandwidth and band center frequency, receiver location, thunderstorm activity, and propagation conditions. Now, if the receiver is sufficiently narrowband, it is reasonable to assume that the noise at the receiver output is modeled well as a gaussian process. This follows because of the fact that the filtered noise is the sum of contributions from a large number of independent lightning discharges, none of which is dominant at the filter output. However, experimental data [Ref. 9] indicate that the bandwidth required to achieve this condition at

vlf is substantially less than one cps, so that a gaussian assumption is not physically viable at vlf. The goal of the model development here is the formulation of an analytical model that is both an accurate description of the received noise and suitable for application to the statistical detection problem at the receiver. As far as the detection problem is concerned, it appears necessary to model the atmospheric noise prior to the performance of any receiver operations, so that a gaussian assumption is certainly not justified.

Although the gaussian assumption cannot be justified, the modeling problem can nevertheless be simplified by noting that in practice attention can be restricted to receiver bandwidths substantially smaller than the band center frequency. This result, which enables the received atmospheric noise to be thought of as a narrowband random process, follows from the fact of limited spectrum availability at the frequencies where atmospheric noise is predominant. This limited spectrum availability means that the receiver bandwidth must be sufficiently restricted to validate the assumption that interference from strong adjacent channel signals is negligible. Further, it is noted that this "narrowband" assumption is precisely what is needed to enable verification of the accuracy of the analytical model, since almost all available experimental data [Refs. 6, 9, 10, 11, 12] have been obtained in narrowband situations.

#### 1. Specification of the Generalized "t" Model

With the above general features of the atmospheric noise in mind, the formulation of the generalized "t" model proceeds as follows: Although the gaussian assumption is not justified for the atmospheric noise of interest, it is conjectured, following loosely the intuitive notion of regime suggested by Mandelbrot [Refs. 20, 21], that this may be closely related to the fact that the regime of sources controlling the received noise varies with time over a large dynamic range. That is, the gaussian model may be inappropriate principally because the received noise at an instant in time is controlled by a few lightning discharges that vary in intensity and location as a function of time. Continuing with this line of reasoning, it is proposed that a model for received atmospheric noise worth consideration is one that takes the received noise to be a narrowband gaussian noise multiplied by a weighting factor that varies with time

in accordance with the regime of sources in control of the noise. Thus it is proposed that the narrowband received atmospheric noise  $y(t)$  be considered to have the form

$$y(t) = a(t) n(t) , \quad (2.3)$$

where  $n(t)$  is a zero-mean narrowband gaussian process with covariance function  $R_n(\tau)$ ; and  $a(t)$ , the "regime" process, is a stationary random process, independent of  $n(t)$ , whose statistics are to be chosen so that the product  $a(t) n(t)$  is an accurate description of the received atmospheric noise. It is noted that the above discussion leading to this model formulation suggests that  $a(t)$  will be a slowly varying random process as compared to the narrowband process  $n(t)$ . It will be shown below that this is indeed the case in the sense that for a good fit to measured data the power spectrum of the lowpass function  $a(t)$  needs to have negligible overlap with the power spectrum of the band-centered gaussian process  $n(t)$ .

Before attempting to specify the statistics of the regime process  $a(t)$ , an alternate argument suggesting the existence of such a regime process is presented in support of the model proposed in Eq. (2.3). Setting aside the regime notion and observing the narrowband atmospheric noise that it is desired to model, it is interesting to note that a gaussian model is inappropriate primarily for the following two reasons [Refs. 9, 17]:

1. The atmospheric noise process does not tend to deliver energy at a constant rate as would a gaussian process.
2. The contribution of a single source component may not be small compared to the total received energy.

Further, it is known [Ref. 17] that in almost every case where the received noise satisfies requirement 1, so that excursions far above the rms value are extremely unlikely, the process can be well approximated as a gaussian process despite the fact that it may exhibit a preferred waveform in violation of requirement 2. This is particularly true in narrowband situations where the signal shape is essentially a sinusoid at the band center frequency, and in fact an example of this result is that in most calculations a sinusoid is well approximated by a narrowband gaussian process.

Thus it is concluded that it is primarily the large dynamic range of atmospheric noise that makes a gaussian model inappropriate. Now, noting that it is desirable from an analytical point of view to model the received atmospheric noise in terms of gaussian processes, it seems natural to ask how we can operate on a gaussian model to introduce the large dynamic range observed in atmospheric noise. One possibility, which in fact appears to be the simplest feasible possibility, is to multiply (modulate) the narrowband gaussian process by a process having the desired dynamic range. Noting that this modulating process is expected to vary as the envelope of the narrowband atmospheric noise, we are again led to a model of the form given by Eq. (2.3), where  $a(t)$  is now thought of as a slowly varying modulating function.

The above discussion based on the physical characteristics of received atmospheric noise has been presented to give physical support to the model proposed in Eq. (2.3) and to indicate the existence of the modulating process  $a(t)$ . It remains to specify the statistics of  $a(t)$ , and this crucial step will now be considered from an empirical point of view.

Recalling that  $a(t)$  is expected to be a slowly varying random process, whereas  $n(t)$  is a narrowband gaussian process, it is assumed that the envelope  $V(t)$  of the received atmospheric noise  $y(t)$  is given by

$$V(t) = |a(t)| E(t), \quad (2.4)$$

where  $E(t)$  is the envelope of  $n(t)$ . It is now observed that the first-order statistics of the product  $|a(t)| E(t)$  have the following "reproducing" property: If the probability density function of  $|a|$  has the form

$$\lim_{x \rightarrow \infty} p_{|a|}(x) \propto \frac{1}{x^\beta} \quad (2.5)$$

where  $\beta > 1$ , then the probability density function of  $V = |a| E$  has the form

$$\lim_{x \rightarrow \infty} p_V(x) \propto \frac{1}{x^\beta} \quad (2.6)$$

Now, it is seen that the hyperbolic distribution specific to Eq. (2.6) is asymptotically identical in form to perhaps the simplest of the empirical models [Refs. 12, 17, 18, 19] proposed from observation of measured data on the envelope of received atmospheric noise [see Eq. (2.2)]. Thus it is concluded that Eq. (2.5) gives a reasonable specification of the asymptotic behavior of the first-order statistics of  $a(t)$ .

It is next observed that if a random variable  $b$  is defined to be distributed according to the "two-sided" chi distribution

$$p_b(b) = \frac{\left(\frac{m}{2}\right)^{m/2}}{\sigma^m \Gamma\left(\frac{m}{2}\right)} |b|^{m-1} \exp\left[-\frac{m}{2\sigma^2} b^2\right], \quad -\infty < b < \infty \quad (2.7)$$

designated as  $\chi_2(m, \sigma)$ ,<sup>†</sup> then the random variable  $a = 1/b$  is distributed according to

$$p_a(a) = \frac{1}{a} p_b\left(\frac{1}{a}\right) = \frac{\left(\frac{m}{2}\right)^{m/2}}{\sigma^m \Gamma\left(\frac{m}{2}\right)} \frac{1}{|a|^{m+1}} \exp\left[-\frac{m}{2\sigma^2} \frac{1}{a^2}\right], \quad -\infty < a < \infty. \quad (2.8)$$

Thus it is seen that  $p_a(a)$  given by Eq. (2.8) has precisely the asymptotic behavior specified by Eq. (2.5). Now it is certainly true that other distributions could be formulated having this same asymptotic behavior, but that given by Eq. (2.8) is preferred in the model development here for the following reasons:

1.  $a(t)$  distributed according to Eq. (2.8) provides a distribution for  $a(t) n(t)$  that agrees very well with available measured data on the first-order statistics of received atmospheric noise. This is demonstrated in detail in Section C1.
2. The model development to this point has considered only the first-order statistics of the noise. However, the fact that  $\chi_2(1, \sigma)$  is identical to  $N(0, \sigma^2)$  means that  $b(t) = 1/a(t)$  is a gaussian process in this special case. Thus the model becomes the quotient

<sup>†</sup>This designation follows from the fact that  $|b|$  is distributed according to the well-known chi distribution [Ref. 22].

of two gaussian processes, and it is anticipated that this fact will be useful in fitting the model to the observed higher-order statistics of the noise.

Now, with the above specification of the first-order statistics of  $a(t)$  [or equivalently  $b(t)$ ], a direct solution can be obtained for the first-order statistics of  $y(t) = a(t) n(t)$  as follows: Since  $n(t)$  and  $b(t)$  are assumed to be statistically independent, it follows that [Ref. 22]:

$$\begin{aligned} p_y(y) &= \int_{-\infty}^{\infty} dx |x| p_{n,b}(yx, x), \\ &= \int_{-\infty}^{\infty} dx |x| p_n(yx) p_b(x), \quad -\infty < y < \infty, \end{aligned} \quad (2.9)$$

where

$$p_n(n) = N[0, R_n(0)], \quad R_n(0) \triangleq \sigma_1^2,$$

so that

$$p_n(n) = \frac{1}{\sqrt{2\pi\sigma_1^2}} \exp\left[-\frac{n^2}{2\sigma_1^2}\right], \quad -\infty < n < \infty \quad (2.10)$$

and  $p_b(b)$  is given by Eq. (2.7). Thus, using Dwight [Ref. 23], item 860.17, this gives

$$p_y(y) = \frac{\Gamma\left(\frac{m+1}{2}\right)}{\Gamma\left(\frac{m}{2}\right)} \frac{\left(m^{1/2} \frac{\sigma_1}{\sigma}\right)^n}{\pi^{1/2}} \frac{1}{\left[y^2 + m \frac{\sigma_1^2}{\sigma^2}\right]^{(m+1)/2}}, \quad m > 0, \quad (2.11)$$

which is conveniently written as

$$p_y(y) = \frac{\Gamma\left(\frac{\theta}{2}\right)}{\Gamma\left(\frac{\theta-1}{2}\right)} \frac{\gamma^{\theta-1}}{\pi^{1/2}} \frac{1}{[y^2 + \gamma^2]^{\theta/2}}, \quad -\infty < y < \infty \quad (2.12)$$

where  $\gamma \triangleq m^{1/2} \sigma_1 / \sigma$  and  $\theta \triangleq m+1 > 1$ . Now, noting that in the special case  $\sigma_1 = \sigma$ ,  $p_y(y)$  given by Eq. (2.11) is Student's "t" distribution [Ref. 22, p. 180] with parameter  $m$ , it will henceforth be said that the first-order statistics of  $y(t)$  are given by the generalized "t" distribution defined by Eq. (2.12) with parameters  $\theta$  and  $\gamma$ .

Before proceeding to check the validity of the generalized "t" model as a model for atmospheric noise by comparing it with measured statistical data, there are several points of interest to note concerning the model. In conjunction with the modulating function  $b(t)$  whose first-order statistics are given by the  $x_2$  distribution specified in Eq. (2.7), it is interesting to note [Ref. 22] that if  $x_1, x_2, \dots, x_n$  are independent gaussian variables, each distributed as  $N(0, \sigma^2)$ , then

$$Y = \left[ \frac{1}{n} \sum_{k=1}^n x_k^2 \right]^{1/2} \quad (2.13)$$

is distributed as  $\chi(n, \sigma)$ . Thus it is seen that  $|b(t)|$  has a relationship to a combination of gaussian variables that may be useful in later calculations. It will be shown below that  $\theta$  in the range  $2 < \theta \leq 4$  is appropriate to fit measured data on atmospheric noise, with  $\theta \approx 3$  being appropriate to fit a large body of data at vlf and lf. Now

$$p_y(y) \Big|_{\theta=3} = \frac{\gamma^2}{2} \frac{1}{[y^2 + \gamma^2]^{3/2}}, \quad -\infty < y < \infty, \quad (2.14)$$

so that  $E[y]_{\theta=3} = 0$  and  $\text{var}(y)_{\theta=3} = \infty$ . Thus it is seen that  $\theta=3$  results in an infinite variance, so that this is not a model for a physical noise, although it will be found to fit the data very closely. This problem of infinite variance will be considered in detail in Section C, and it will be shown that there are two possible solutions to the difficulty:

1. The measured data actually requires  $\theta > 3$  for an optimum fit at large values of  $y$ , so that  $\text{var}(y)$  is bounded; or
2. The generalized "t" model as formulated in this development requires modification in that the measured data depart from the model for cumulative envelope probabilities greater than about one minus  $10^{-5}$ . It will be shown that the measured data in this region of envelope probabilities, which is somewhat suspect because of the tremendous dynamic range required for its observation, can be fitted well by truncating  $p_a(a)$  given by Eq. (2.8) at some point. This truncation will have negligible effect on  $p_y(y)$  as determined above in Eq. (2.12) for cumulative probabilities smaller than about  $1-10^{-5}$ , so that the truncation is not of practical significance in most problems of interest.

It should be mentioned that the above discussion, which indicates that the atmospheric noise has very large average power, agrees in principle with the results of Mandelbrot [Ref. 21] in which he notes that intermittent phenomena often appear to have barely convergent, or even divergent, second moments dependent strongly on sample size. Mandelbrot [Ref. 21] also gives an excellent discussion of how the mathematical result of infinite variance is to be interpreted in a physical application.

Finally, it is noted that  $p_y(y)$  as given by Eq. (2.12) is a function only of the two parameters  $\theta$  and  $\gamma$ . This result is in agreement with measured data [Refs. 9, 10, 11] on the first-order statistics of atmospheric noise, in which it is found that these statistics are adequately described by the rms value of the noise together with the ratio of this rms value to the average value of the noise envelope.

#### C. VERIFICATION OF APPLICABILITY OF THE GENERALIZED "t" MODEL

Although a heuristic argument indicating the plausibility of choosing a model of the type of the generalized "t" model accompanied the development of this model, it remains to be shown that a specific form of the model is in fact of any practical use as a model for received atmospheric noise.

Since we are attempting to develop a model for a random process, the measurements required to check the validity of the model fall into two categories, as follows:

The first of these categories, and the one for which the greatest amount of experimental data are available, is concerned with the first-order statistics of the random process. The particular measurements in this category that have been reported in the literature are measurements of the probability distribution of the envelope of the received noise [Refs. 6, 9, 10, 11, 12], and measurements of the average number of level crossings per unit time of a fixed level by the envelope of the received noise [Refs. 9, 10]. Relatively extensive measurements have been made of the probability distribution function of the envelope, and these measurements have been used exclusively in the verification of the empirical models discussed in Section A2. Thus, as the first step in the verification of the applicability of the generalized "t" model, the probability distribution function of the envelope will be calculated. Particular interest will center on the fit of the model as a function of band center frequency and receiver bandwidth. Because of the fact that we are interested in modeling the atmospheric noise in as wide a bandwidth as possible subject to the interfering signal constraint discussed in the model development, the model will be checked using the widest bandwidth data available. It is noted, however, that all reported data have been obtained in bandwidths justifying a narrowband assumption for the received noise. In this narrowband case, the envelope  $V(t)$  and phase  $\phi(t)$  of the received noise waveform have an unambiguous and physical (operationally meaningful) significance. Further, the available data on the first-order statistics of  $V(t)$ , plus the intuitive notion that  $\phi(t)$  must be uniformly distributed in the interval  $[0, 2\pi]$ , provide the opportunity to check conclusively the applicability of the generalized "t" model as far as the first-order statistics are concerned.

As a further check on the first-order statistics of the model, the average number of level crossings by the envelope per unit time will be calculated. This calculation is of interest, because it bears out the experimental fact that the average number of level crossings per unit time for the case of atmospheric noise is not given by the product of the

probability density function of the envelope with a suitable bandwidth factor, as it would be if the noise were a gaussian process [Ref. 24]. It is noted that this calculation has not been carried out for any of the empirical models discussed in Section A2, although Nakai [Ref. 25] has obtained numerical results in agreement with the experimental data of Watt and Maxwell for a filtered-impulse model in which the noise pulses occur in a Poisson fashion.

The second category of measured data, and the one where much less data are available, is concerned with the second- and higher-order statistics of the random process. The particular measurements that have been reported in this category are measurements of the probability distribution of the time interval between crossings of a specified level by the envelope of the noise [Ref. 9]. While available experimental data are sparse, being restricted to a few measurements at vlf, it is also true that the analytical derivation of these statistics is complicated, requiring machine computation in the general case. Nevertheless, this derivation will be considered in detail in Section C3 and limiting cases will be presented to demonstrate that the higher-order statistics of the generalized "t" model can be selected to fit the measured data. It is noted that the interpretation that the generalized "t" model is made up of a narrowband gaussian noise modulated by a slowly varying random process will be useful in the specification of these higher-order statistics.

#### 1. First-Order Distributions of Envelope and Phase

As discussed above, the significance of the representation

$$y(t) = V(t) \cos[\omega_0 t + \phi(t)] \quad (2.15)$$

for narrowband received noise is clear. In order to check the applicability of the generalized "t" model as far as the first-order statistics are concerned, it is sufficient to calculate the joint probability density  $p_{V,\phi}(V,\phi)$  of envelope and phase which can be accomplished as follows: It is well known that [Ref. 26]

$$p_{V,\phi}(V,\phi) = V p_{y,\dot{y}}(V \cos \phi, V \sin \phi), \quad (2.16)$$

where  $V = (y^2 + \tilde{y}^2)^{1/2}$ ,  $\varphi = \tan^{-1}(\tilde{y}/y)$ , and  $\tilde{y}(t)$  is the quadrature component corresponding to  $y(t)$  which can be found by taking the Hilbert transform<sup>†</sup> of  $y(t)$ . Perhaps the easiest way of finding  $\tilde{y}(t)$  here is to pass  $y(t)$  through a Hilbert transforming filter as shown in Fig. 2. Now, recalling that

$$y(t) = a(t) n(t), \quad (2.3)$$

where  $n(t)$  is a zero-mean stationary narrowband gaussian process and  $a(t)$  is assumed to be a slowly varying stationary random process, it is useful to make the specific assumption, depicted in Fig. 3, that in fact

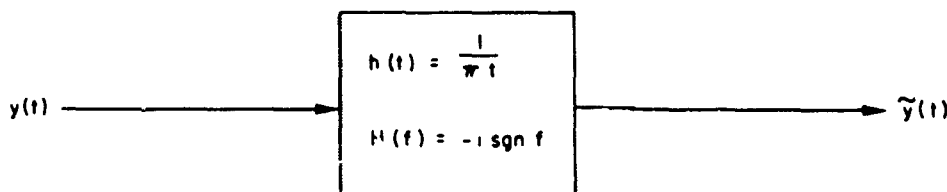


FIG. 2. HILBERT TRANSFORMING FILTER.

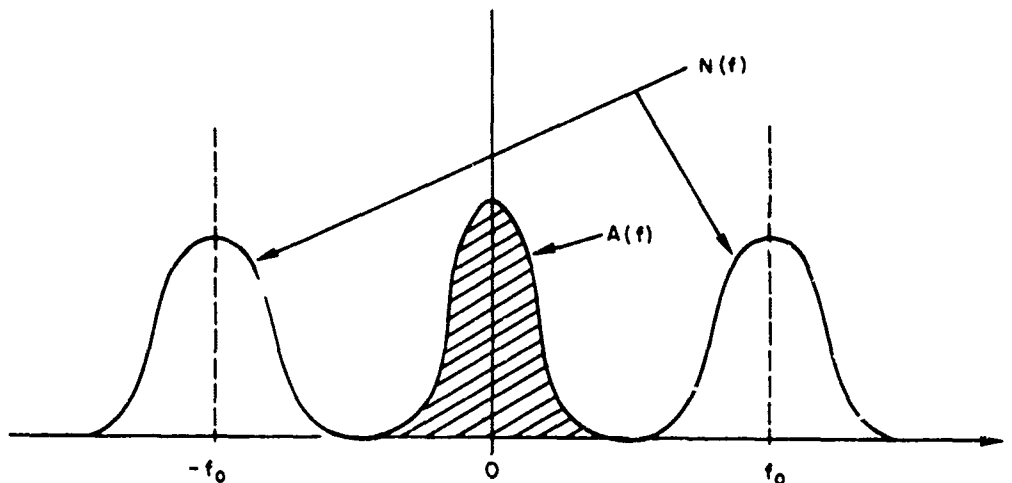


FIG. 3. TYPICAL FOURIER TRANSFORMS,  $A(f)$  AND  $N(f)$ , OF  $a(t)$  AND  $n(t)$ . (Magnitude only)

<sup>†</sup> See "Conventions," p. xi.

the Fourier transform<sup>†</sup>  $A(f)$  of  $a(t)$  has, with high probability, negligible overlap in the frequency domain with the Fourier transform  $N(f)$  of  $n(t)$ .

Define  $Y(f)$  as the Fourier transform of  $y(t)$ ; then with the above assumption, it follows directly that  $\tilde{Y}(f)$ , the Fourier transform of  $\tilde{y}(t)$ , is given by

$$\begin{aligned}\tilde{Y}(f) &= (-i \operatorname{sgn} f) Y(f) \\ &\approx i \int_{-\infty}^0 N(\alpha) A(f-\alpha) d\alpha - i \int_0^{\infty} N(\alpha) A(f-\alpha) d\alpha \\ &\approx A(f) * \tilde{N}(f), \quad i = \sqrt{-1},\end{aligned}\tag{2.17}$$

where  $*$  signifies the convolution of  $A(f)$  with  $\tilde{N}(f)$ .<sup>†</sup> Thus it is found that, with the assumption of negligible overlap of  $A(f)$  and  $N(f)$  (which is intuitively reasonable for the noise of interest),

$$\tilde{y}(t) \approx a(t) \tilde{n}(t). \tag{2.18}$$

Now,  $n(t)$  being a gaussian process implies that  $\tilde{n}(t)$  is a gaussian process where it is easily shown that  $n(t)$  and  $\tilde{n}(t)$  at the same time instant  $t$  are independent and identically distributed random variables. Thus it follows that

$$\begin{aligned}p_{y, \tilde{y}}(y, \tilde{y}) &= p_{an, a\tilde{n}}(y, \tilde{y}) \\ &= \int_{-\infty}^{\infty} dx \frac{1}{x} p_{a, n, \tilde{n}}\left(x, \frac{y}{x}, \frac{\tilde{y}}{x}\right) \\ &= \int_{-\infty}^{\infty} dx \frac{1}{x} p_a(x) p_n\left(\frac{y}{x}\right) p_{\tilde{n}}\left(\frac{\tilde{y}}{x}\right),\end{aligned}\tag{2.19}$$

<sup>†</sup>See "Conventions," p. xi.

where

$$p_n(x) = p_{\tilde{n}}(x) = (2\pi\sigma_1^2)^{-1/2} \exp\left(-\frac{x^2}{2\sigma_1^2}\right),$$

and where  $p_a(x)$  is given by Eq. (2.8). Making a change of variable and using Dwight, item 860.17, this yields

$$p_{y,\tilde{y}}(y,\tilde{y}) = \frac{(\theta-1)\gamma^{\theta-1}}{2\pi} \frac{1}{[y^2 + \tilde{y}^2 + \gamma^2]^{(\theta+1)/2}}, \quad (2.20)$$

where  $\gamma$  and  $\theta$  are defined in Eq. (2.12). Now, substituting Eq. (2.20) into Eq. (2.16):

$$\begin{aligned} p_{V,\varphi}(V,\varphi) &= \frac{(\theta-1)\gamma^{\theta-1}}{2\pi} \frac{V}{[V^2 + \gamma^2]^{(\theta+1)/2}}, \\ &= p_V(V) p_{\varphi}(\varphi) \quad 0 \leq V < \infty, \quad 0 \leq \varphi \leq 2\pi. \end{aligned} \quad (2.21)$$

Thus, finally:

$$p_V(V) = (\theta-1)\gamma^{\theta-1} \frac{V}{[V^2 + \gamma^2]^{(\theta+1)/2}}, \quad 0 \leq V < \infty \quad (2.22)$$

and

$$p_{\varphi}(\varphi) = \frac{1}{2\pi}, \quad 0 \leq \varphi \leq 2\pi. \quad (2.23)$$

#### a. Discussion of Calculated Results

The results calculated above lead to the following comments and conclusions:

1. As anticipated,  $\varphi(t)$  is found to be uniformly distributed in the interval  $[0, 2\pi]$  in accord with intuition.
2. It is noted that the results on  $p_V(V)$  and  $p_\varphi(\varphi)$  straightforwardly calculated above could have been deduced directly using the formulation assumed in Eq. (2.4) along with the reasonable assumption that the phase is uniformly distributed in  $[0, 2\pi]$ .
3. Finally, it is important to note, in support of the generalized "t" model as a model for received atmospheric noise, the following asymptotic forms of  $p_V(V)$ :

$$\lim_{V \rightarrow \infty} p_V(V) = (\theta - 1) \gamma^{\theta - 1} \frac{1}{V^\theta} \quad (2.24)$$

$$\lim_{V \rightarrow 0} p_V(V) = (\theta - 1) \frac{V}{\gamma} = \lim_{V \rightarrow 0} \frac{V}{\sigma_2} \exp\left(-\frac{V^2}{2\sigma_2^2}\right), \quad (2.25)$$

where

$$\sigma_2^2 = \frac{\gamma^2}{\theta - 1}.$$

Thus it is seen that for large  $V/\gamma$  the generalized "t" model has precisely the desired behavior specified by Eq. (2.6), while for small  $V/\gamma$  the envelope of the generalized "t" model behaves as if it were Rayleigh-distributed. This is of course in agreement with both experimental results and intuition, since the noise at low levels is expected to be the result of contributions from a large number of independent noise sources.

Now, to proceed with the comparison of the distribution of the envelope given by the generalized "t" model with available measured data, it is necessary to compute the complement of the envelope probability distribution function, i.e., go find  $P_0(V)$ , where

$$P_0(V) = 1 - P(V) = \int_V^{\infty} p_V(x) dx, \quad (2.26)$$

in which  $p_V(x)$  is given by Eq. (2.22). Evaluation of this integral gives

$$P_0(V) = \frac{\gamma^{\theta-1}}{(V^2 + \gamma^2)^{(\theta-1)/2}}, \quad (2.27)$$

$P_0(V)$  calculated as above is plotted in Figs 4 through 13 along with measured data from Watt and Maxwell [Ref. 9] (Figs. 4-9) and Clarke et al [Ref. 10] (Figs. 10-13). (Note that in the figures,  $\log|\log P_0(V)|$  is plotted vs  $\log V$ . This choice of scales has the interesting property that the Rayleigh-distributed envelope plots as a straight line.) In addition, Fig. 14 using data from Furutsu and Ishida [Ref. 6] is presented to demonstrate the variation observed in the statistics of the received noise at hf where the choice of an appropriate noise model is strongly a function of local thunderstorm activity.

In order to produce these plots, it was necessary to specify values to be taken on by the two parameters of the model  $\gamma$  and  $\theta$ . The plots in these figures were produced by letting  $\theta$  take on integer values as labeled, while  $\gamma$  was chosen in the following manner: For the case  $\theta = 3$ ,  $\gamma$  was chosen to make  $E[V] = V_{avg}$ , where  $E[V]$  is the expected value of the envelope as given by the model, and  $V_{avg}$  is the time average of the envelope of the received noise obtained by direct measurement.<sup>†</sup> Now

$$E[V] \Big|_{\theta=3} = \int_0^V v p_V(v) \Big|_{\theta=3} dv, \quad (2.28)$$

<sup>†</sup> For Figs. 10 and 11,  $V_{avg}$  was obtained by using the ratio  $V_{rms}/V_{avg}$  presented by Clarke, et al in their Section 3.1.

Figures 4 through 14  
appear on the following pages.

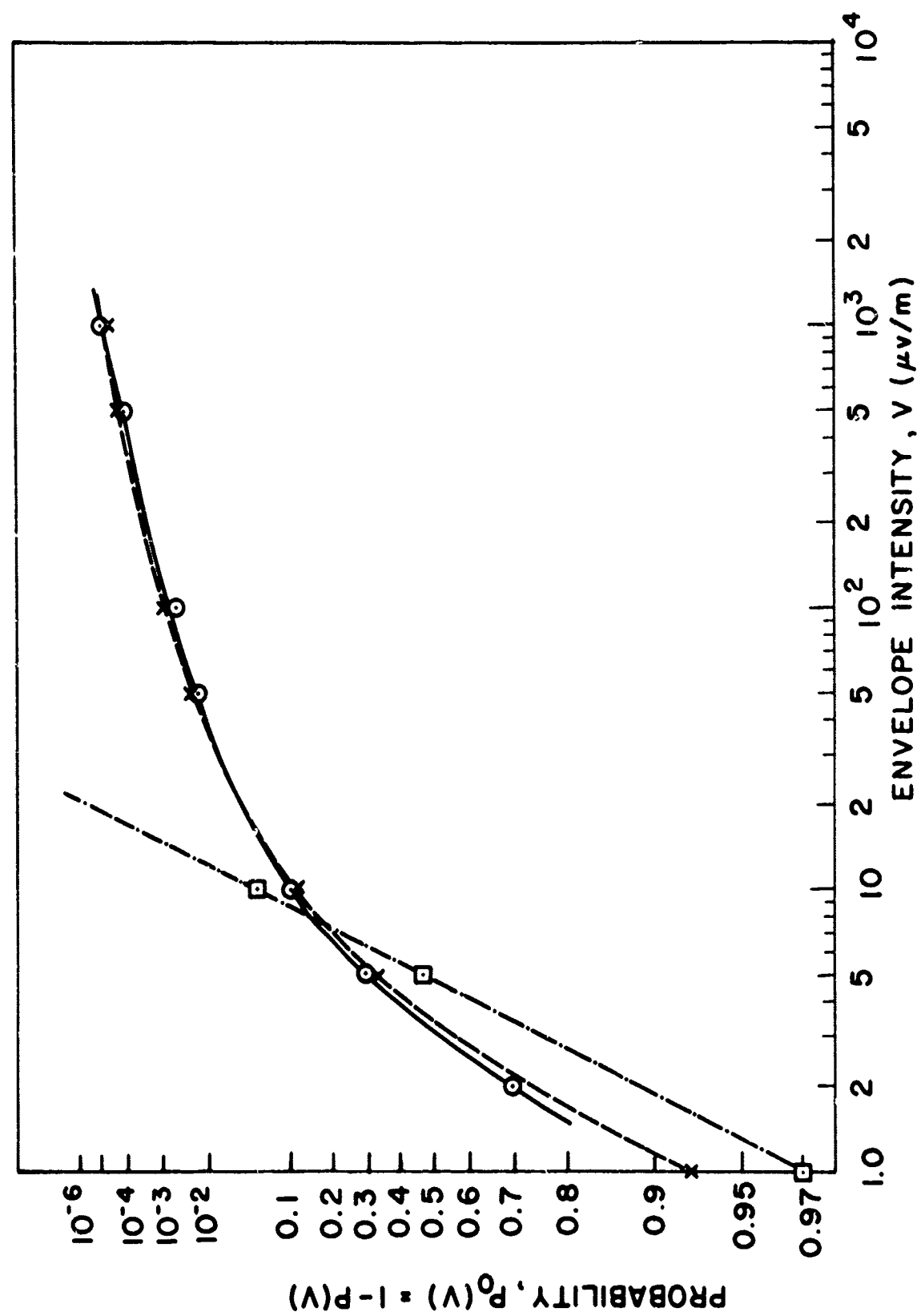


FIG. 4. PROBABILITY DISTRIBUTION FUNCTION OF THE ENVELOPE OF RECEIVED VLF ATMOSPHERIC NOISE:  
COMPARISON OF MODEL RESULTS WITH DATA MEASURED AT POINT BARROW, ALASKA, SEPT. 16, 1955.

$P_0(V)$  = Probability that envelope intensity  $V$   
exceeds abscissa value.

[Note: Vertical scale is  $\log|\log P_0(V)|$ .]

LEGEND:

———— Measured data (Watt and Maxwell [Ref. 9])

Band center frequency,  $f_0 = 22$  kc

Receiver 6-db bandwidth = 1000 cps

$V_{avg} \approx 5.5 \mu v/m$   
(lowest avg. power observed)

--- Generalized "t" model

$\theta = 3$

$\gamma = 3.5 \times 10^{-6}$

$E[V] = 5.5 \mu v/m$

--- Rayleigh-distributed envelope

$E[V] = 5.0 \mu v/m$

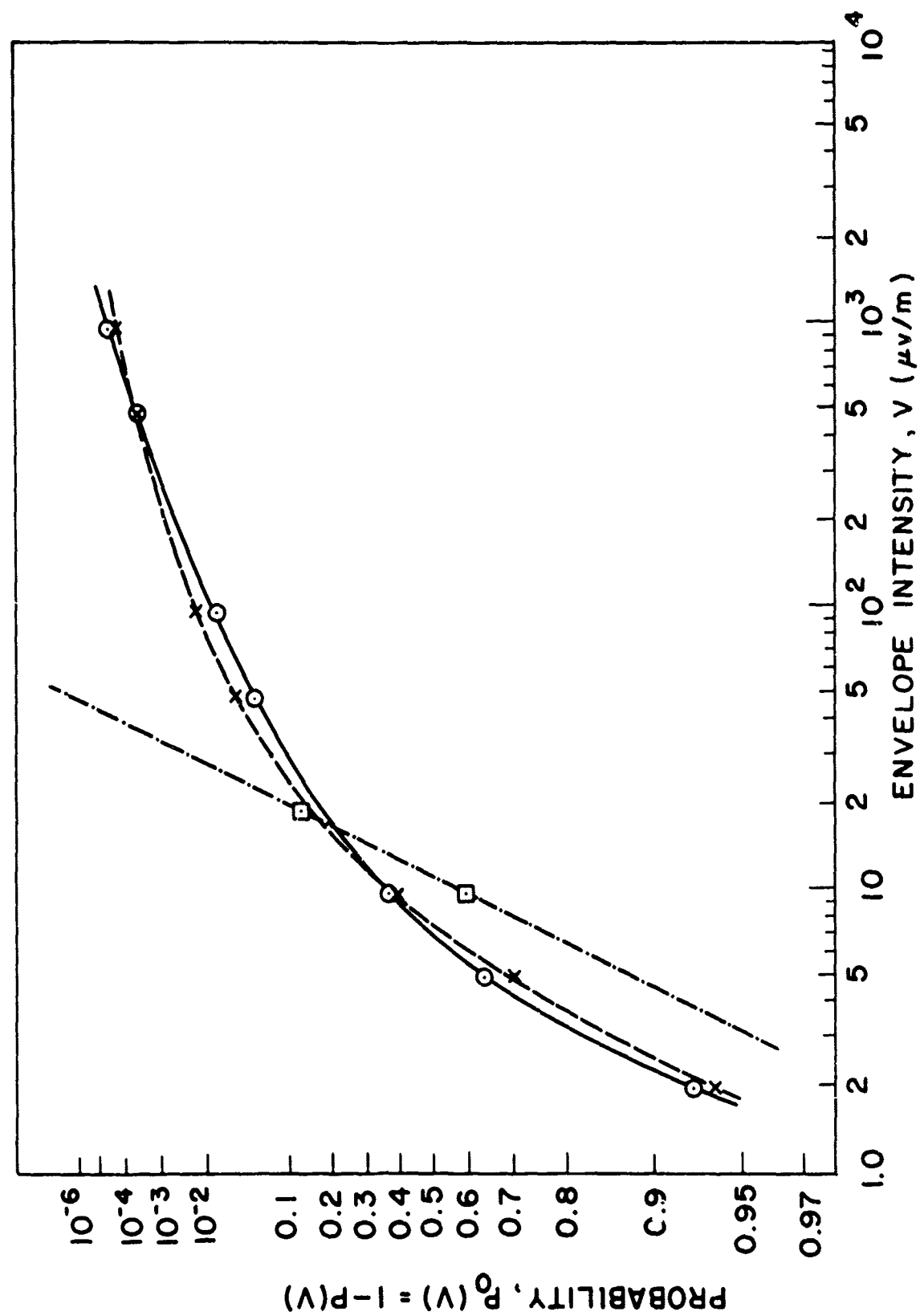


FIG. 5. PROBABILITY DISTRIBUTION FUNCTION OF THE ENVELOPE OF RECEIVED VLF ATMOSPHERIC NOISE:  
COMPARISON OF MODEL RESULTS WITH DATA MEASURED AT POINT BARROW, ALASKA, SEPT. 10, 1955.

$P_0(V)$  = Probability that envelope intensity  $V$   
exceeds abscissa value.

[Note: Vertical scale is  $\log|\log P_0(V)|$ .]

LEGEND:

———— Measured data (Watt and Maxwell [Ref. 9])

Band center frequency,  $f_0 = 22$  kc

Receiver 6-db bandwidth = 1000 cps

$V_{avg} \approx 12 \mu\text{v/m}$

— — — Generalized "t" model

$\theta = 3$

$\gamma = 7.63 \times 10^{-6}$

$E[V] = 12 \mu\text{v/m}$

— . . . Rayleigh-distributed envelope

$E[V] = 12 \mu\text{v/m}$

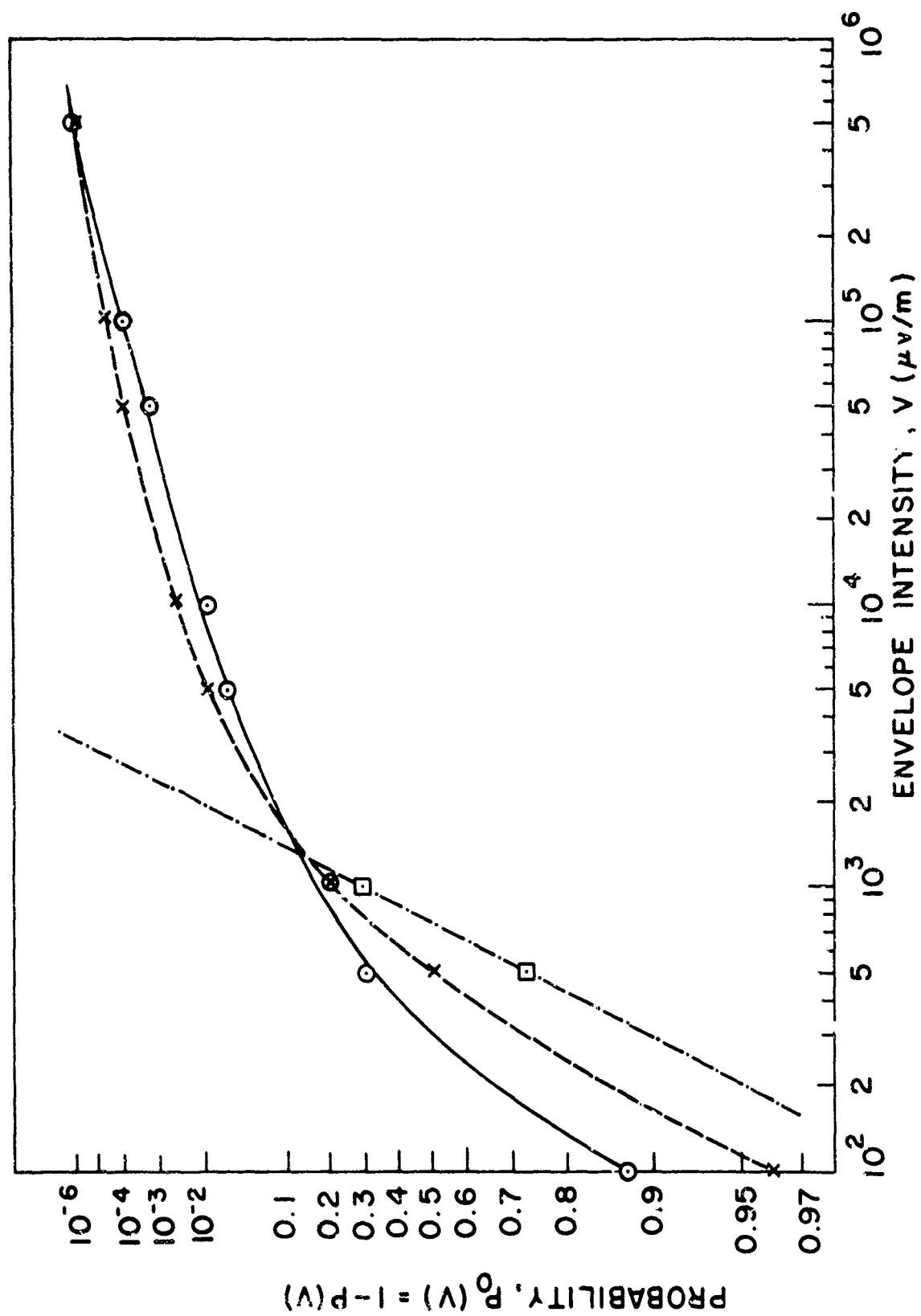


FIG. 6. PROBABILITY DISTRIBUTION FUNCTION OF THE ENVELOPE OF RECEIVED VLF ATMOSPHERIC NOISE:  
COMPARISON OF MODEL RESULTS WITH DATA MEASURED AT BOULDER, COLORADO, AUG. 5, 1955.

$P_0(V)$  = Probability that envelope intensity  $V$   
exceeds abscissa value.

[Note: Vertical scale is  $\log|\log P_0(V)|$ .]

LEGEND:

—— Measured data (Watt and Maxwell [Ref. 9])

Band center frequency,  $f_0 = 21$  kc

Receiver 6-db bandwidth  $\approx 1000$  cps

$V_{avg} \approx 800 \mu v/m$

(highest avg. power observed)

--- Generalized "l" model

$\theta = 3$

$\gamma = 509 \times 10^{-6}$

$E[V] = 800 \mu v/m$

--- Rayleigh-distributed envelope

$E[V] = 800 \mu v/m$

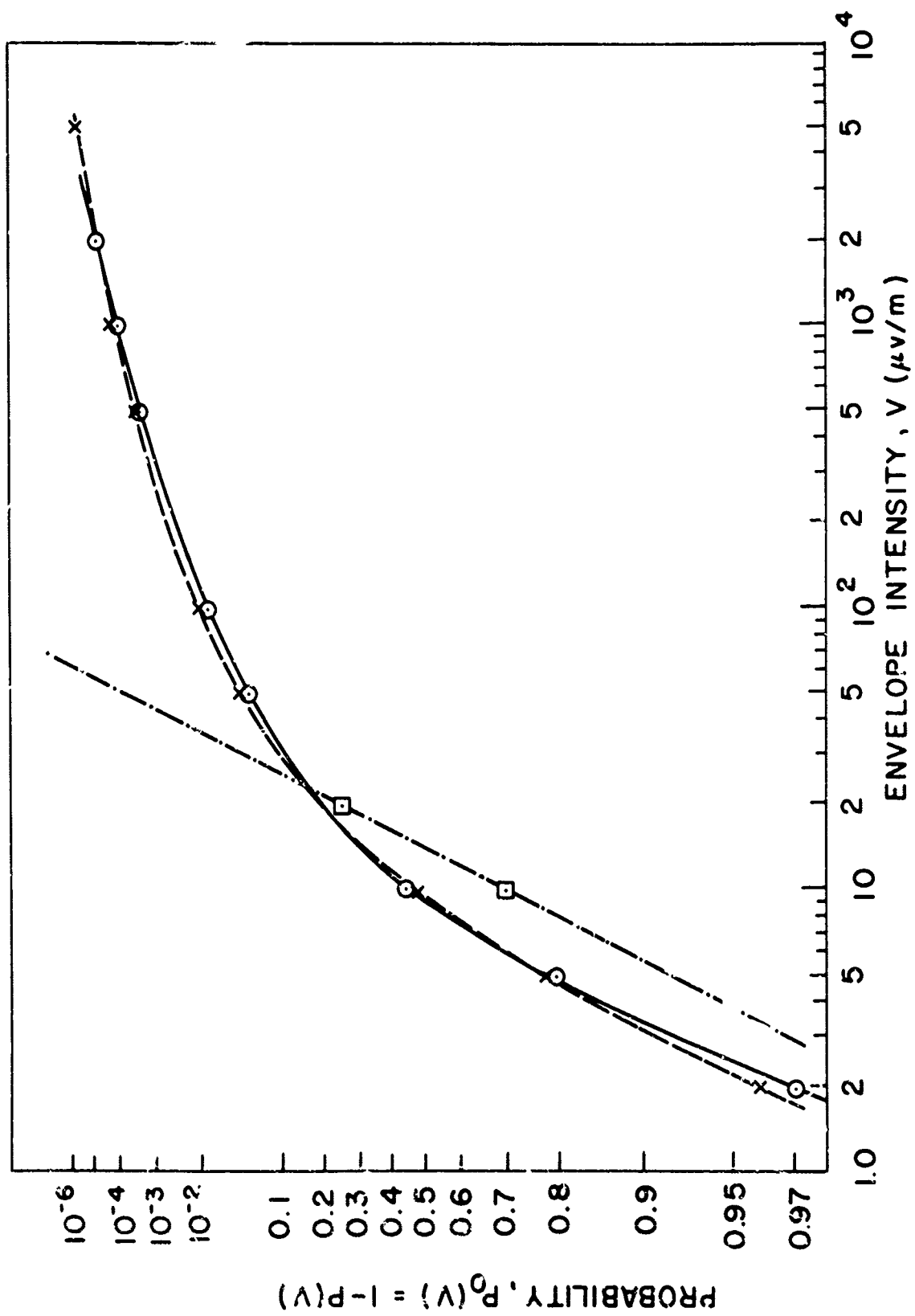


FIG. 7. PROBABILITY DISTRIBUTION FUNCTION OF THE ENVELOPE OF RECEIVED VLF ATMOSPHERIC NOISE:  
COMPARISON OF MODEL RESULTS WITH DATA MEASURED AT BOULDER, COLORADO, MAR. 23, 1956.

$P_0(V)$  : Probability that envelope intensity  $V$   
exceeds abscissa value.

[Note: Vertical scale is  $\log|\log P_0(V)|$ .]

LEGEND:

———— Measured data (Watt and Maxwell [Ref. 9])

Band center frequency,  $f_0 = 22$  kc

Receiver 6-db bandwidth = 1100 cps

$V_{avg} \approx 15 \mu v/m$

— — — — Generalized "t" model

$\theta = 3$

$\gamma = 9.5 \times 10^{-6}$

$E[V] = 15 \mu v/m$

— · — · — · Rayleigh-distributed envelope

$E[V] = 15 \mu v/m$

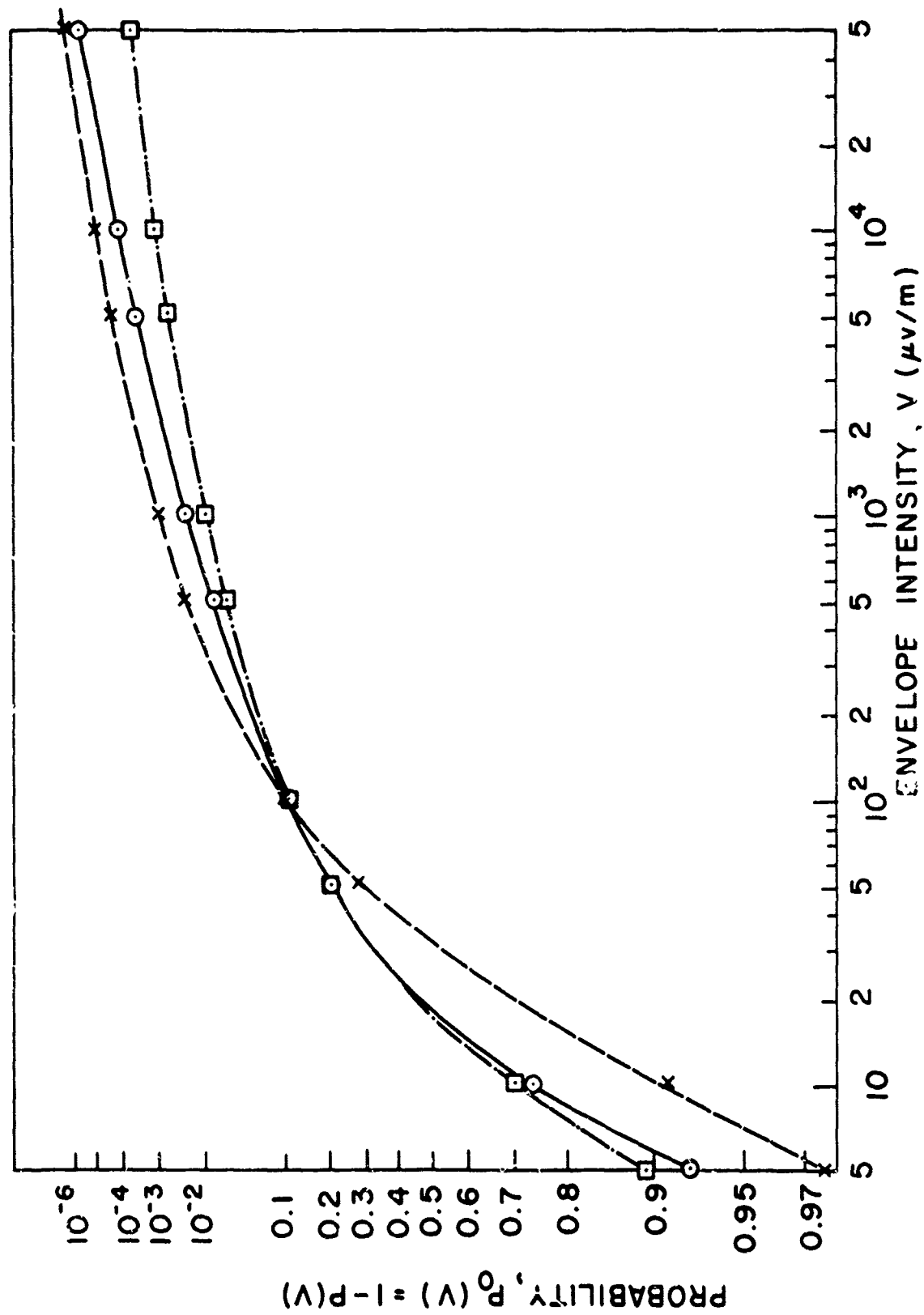


FIG. 8. PROBABILITY DISTRIBUTION FUNCTION OF THE ENVELOPE OF RECEIVED VLF ATMOSPHERIC NOISE:  
COMPARISON OF MODEL RESULTS WITH DATA MEASURED AT BALBOA, C.Z., OCT. 27, 1955.

$P_0(V)$  = Probability that envelope intensity  $V$   
exceeds abscissa value.

[Note: Vertical scale is  $\log|\log P_0(V)|$ .]

LEGEND:

———— Measured data (Watt and Maxwell [Ref. 9])

Band center frequency,  $f_0 = 22$  kc

Receiver 6-db bandwidth = 1331 cps

$V_{avg} \approx 50 \mu\text{V/m}$

--- Generalized "t" model

$\theta = 3$

$\gamma = 31.8 \times 10^{-6}$

$E[V] = 50 \mu\text{V/m}$

--- Generalized "t" model

$\theta = 2$

$\gamma = 10^{-5}$

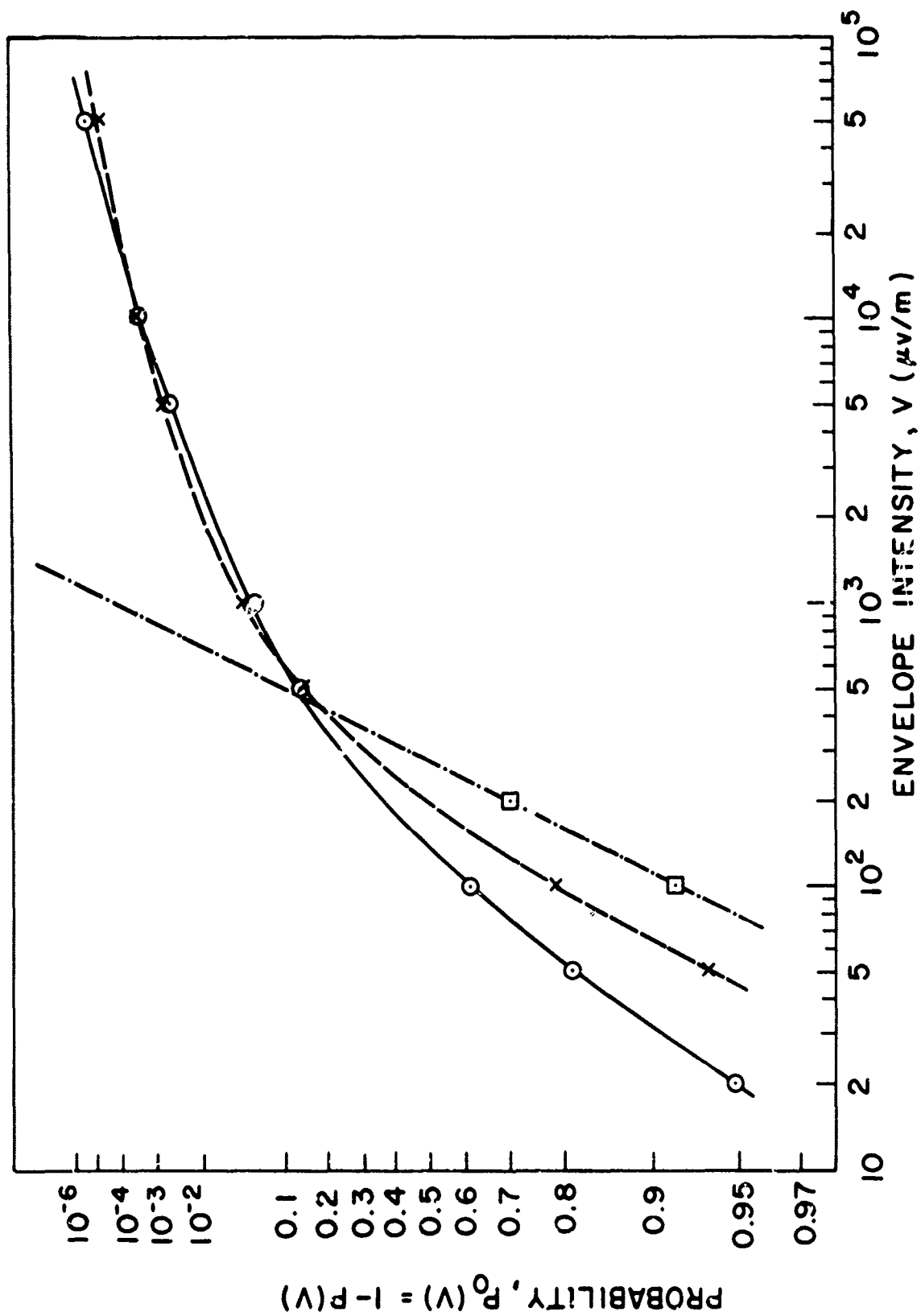


FIG. 9. PROBABILITY DISTRIBUTION FUNCTION OF THE ENVELOPE OF RECEIVED VLF ATMOSPHERIC NOISE:  
COMPARISON OF MODEL RESULTS WITH DATA MEASURED AT BALBOA, C.Z., OCT. 28, 1955.

$P_0(V)$  = Probability that envelope intensity  $V$   
exceeds abscissa value.

[Note: Vertical scale is  $\log|\log P_0(V)|$ .]

LEGEND:

———— Measured data (Watt and Maxwell [Ref. 9])

Band center frequency,  $f_0 = 22$  kc

Receiver 6-db bandwidth = 1331 cps

$V_{avg} \approx 300 \mu v/m$

----- Generalized "t" model

$\theta = 3$

$\gamma = 191 \times 10^{-6}$

$E[V] = 300 \mu v/m$

..... Rayleigh-distributed envelope

$E[V] = 300 \mu v/m$

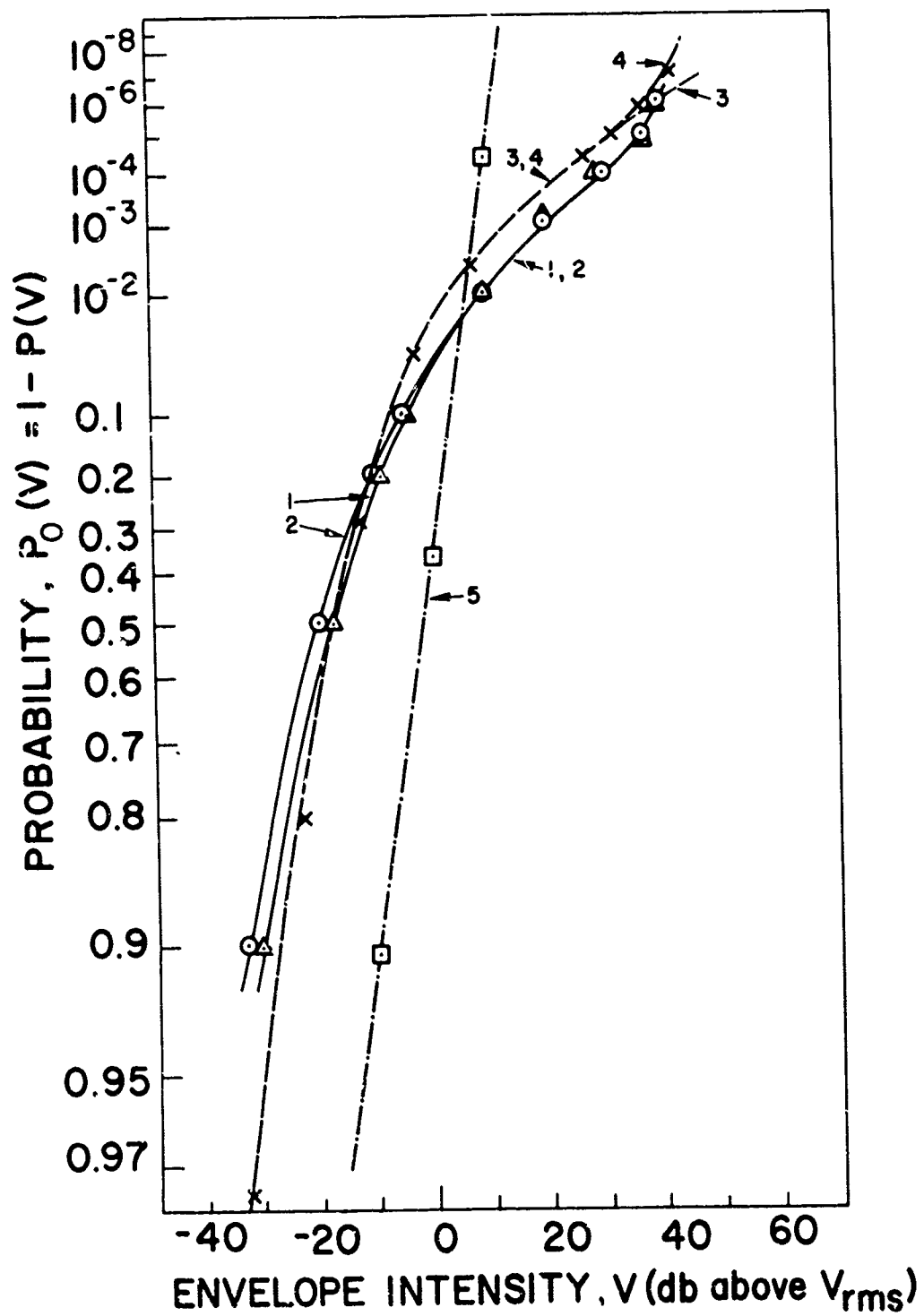


FIG. 10. COMPOSITE PROBABILITY DISTRIBUTION FUNCTION OF THE ENVELOPE OF RECEIVED VLF ATMOSPHERIC NOISE: COMPARISON OF MODEL RESULTS WITH DATA MEASURED AT SLOUGH, ENGLAND AND AT SINGAPORE.

$P_0(V)$  = Probability that envelope intensity  $V$  exceeds abscissa value.

[Note: Vertical scale is  $\log|\log P_0(V)|$ .]

LEGEND:

- 1 Measured data, Slough, England  
 Band center frequency,  $f_0 = 24$  kc  
 Receiver power bandwidth = 425 cps  
 (Clarke, et al, [Ref. 10])
- 2 Measured data, Singapore  
 (Same conditions as above)
- 3 Generalized "t" model  
 $\theta = 3$   
 $\gamma = 0.636 \bar{V}$ ,  $\bar{V} \triangleq E[V] \approx 13$  db below  $V_{rms}$
- 4 Modified generalized "t" model  
 $\theta = 3$   
 $\gamma = 0.636 \bar{V}$   
 $\beta^2 \sigma^2 = 2.5 \times 10^6$
- 5 Rayleigh-distributed envelope  
 $E[V^2] = V_{rms}^2$

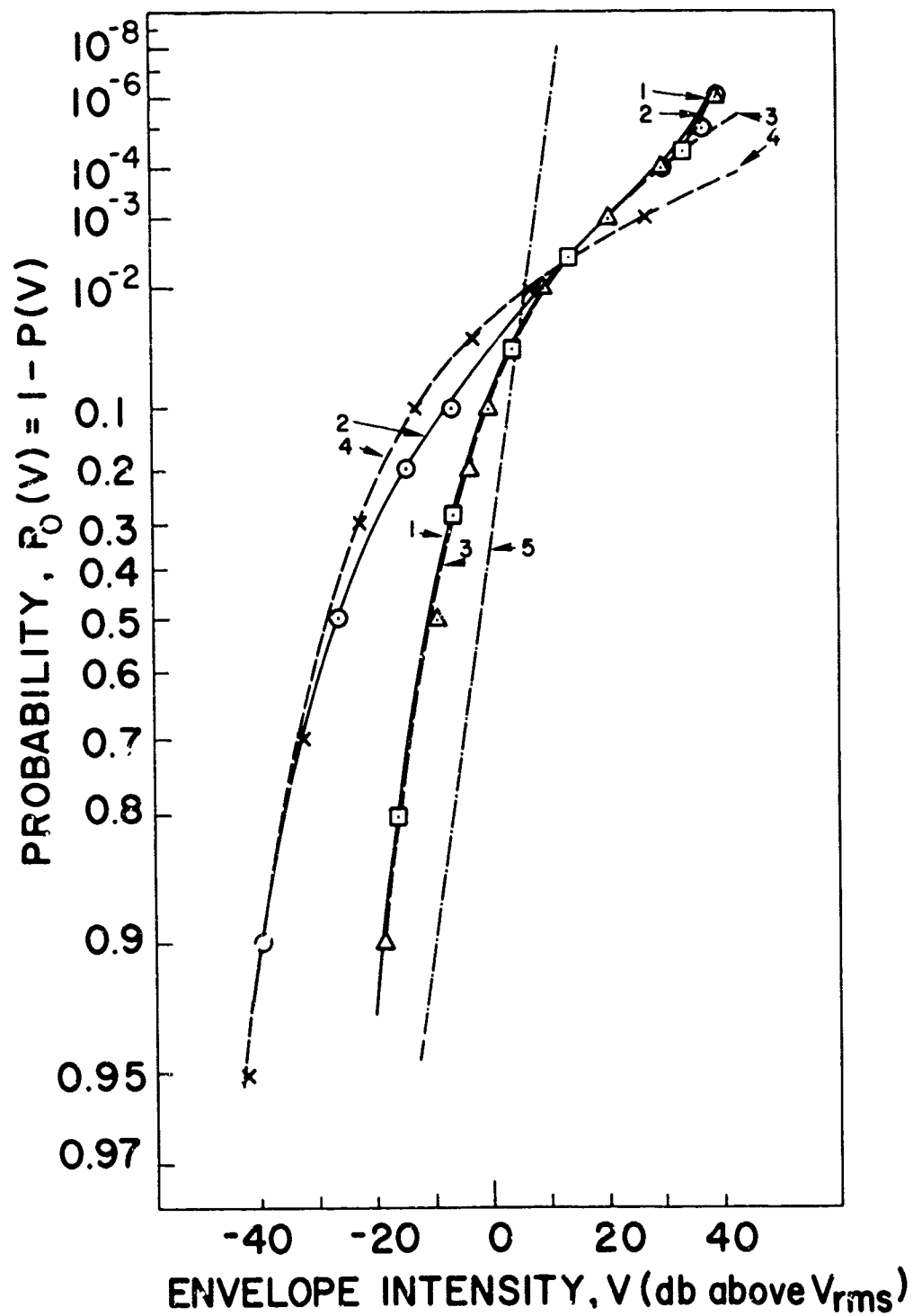


FIG. 11. COMPOSITE PROBABILITY DISTRIBUTION FUNCTION OF THE ENVELOPE OF RECEIVED LF ATMOSPHERIC NOISE: COMPARISON OF MODEL RESULTS WITH DATA MEASURED AT SLOUGH, ENGLAND AND AT SINGAPORE.

$P_0(V)$  = Probability that envelope intensity  $V$  exceeds abscissa value.

[Note: Vertical scale is  $\log|\log P_0(V)|$ .]

LEGEND:

- 1      Measured data, Slough, England  
          Band center frequency,  $f_0 = 135$  kc  
          Receiver power bandwidth = 425 cps  
          (Clarke, et al, [Ref. 10])
- 2      Measured data, Singapore  
          Band center frequency,  $f_0 = 145$  kc  
          Receiver power bandwidth = 425 cps  
          (Clarke, et al, [Ref. 10])
- 3      Generalized "t" model  
           $\theta = 3$   
           $\gamma = 0.636 \bar{V}$ ,       $\bar{V} \triangleq E[V] \approx 6$  db below  $V_{rms}$
- 4      Generalized "t" model  
           $\theta = 2$   
           $\gamma = 33$  db below  $V_{rms}$
- 5      Rayleigh-distributed envelope  
           $E[V^2] = V_{rms}^2$

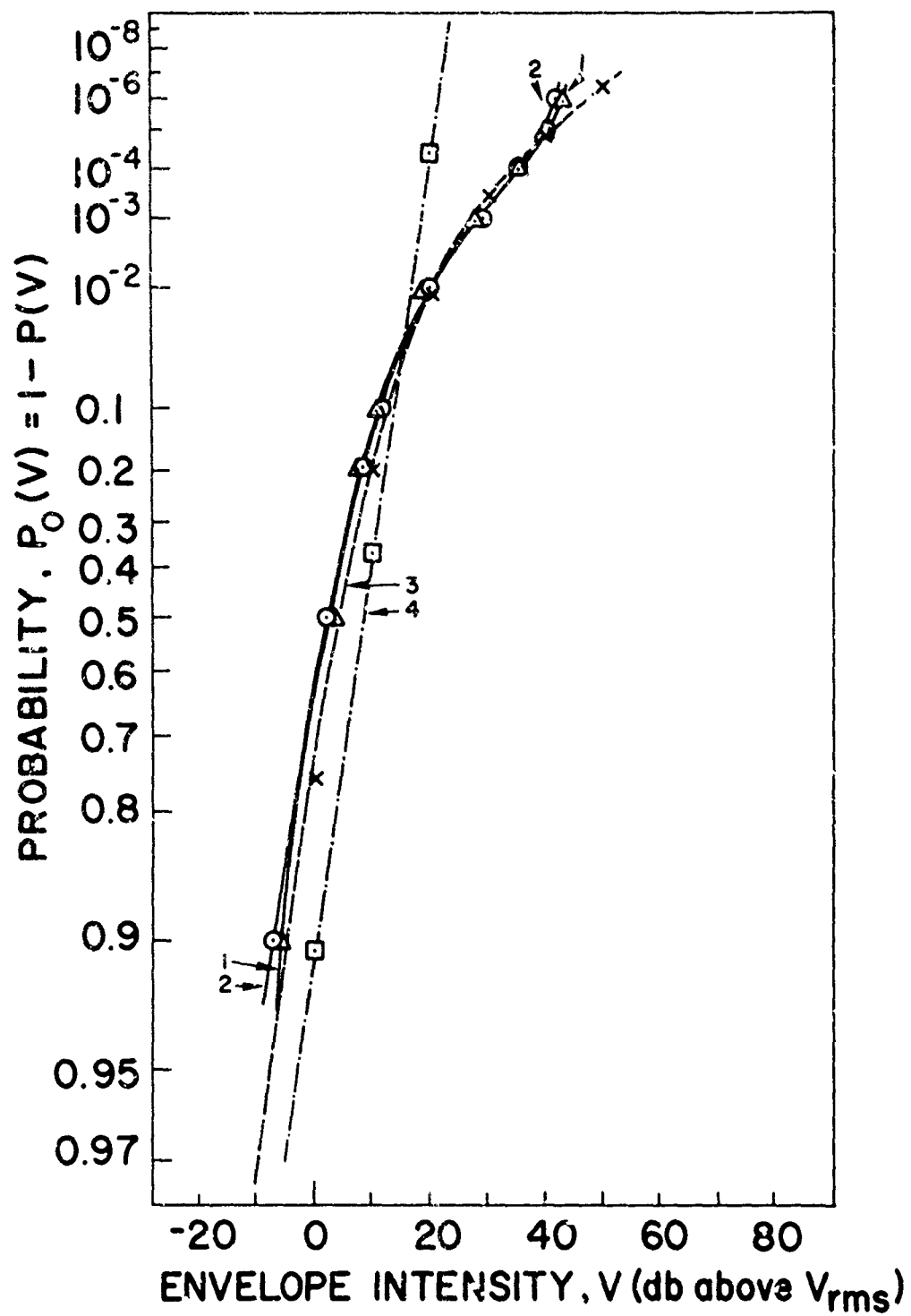


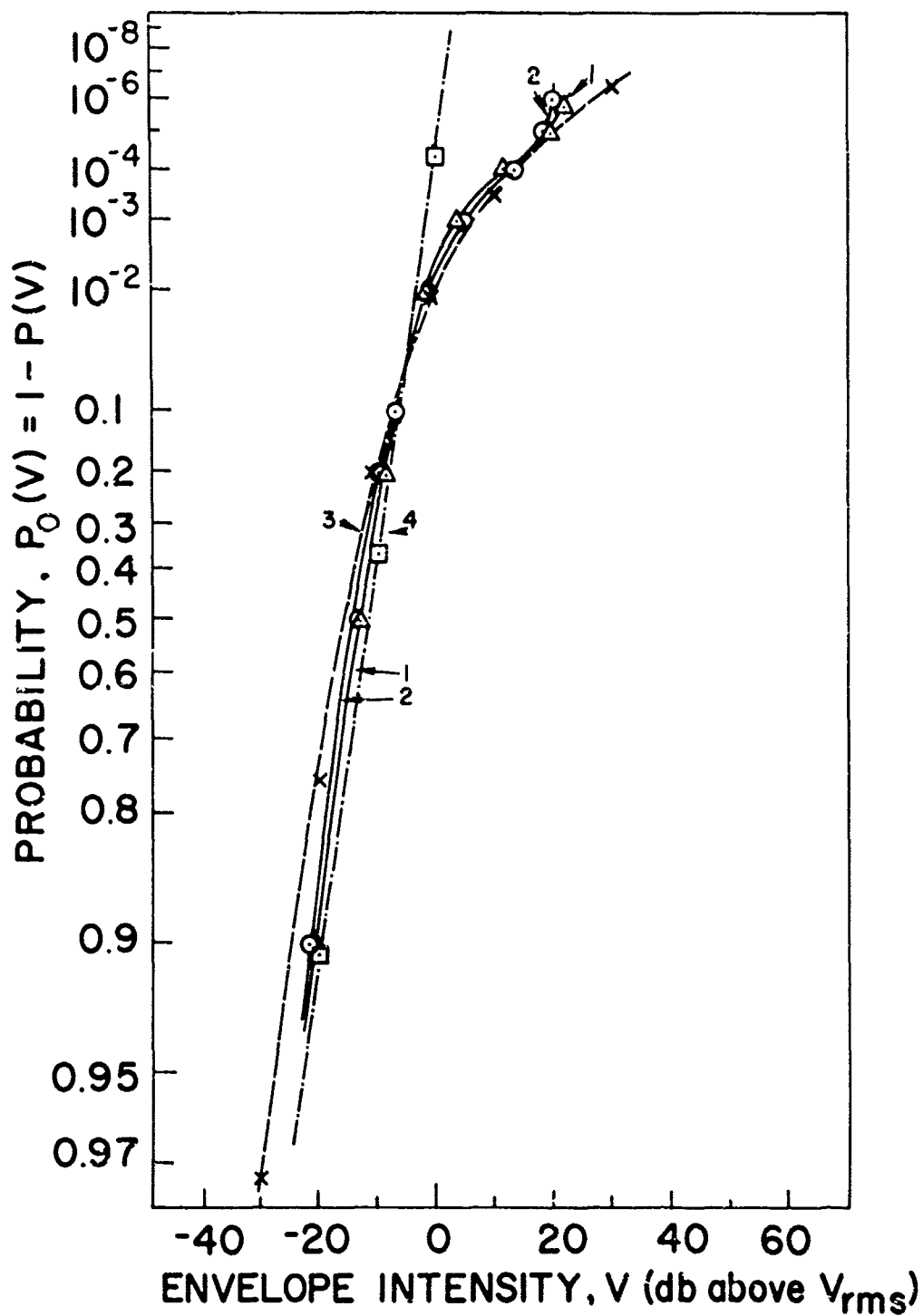
FIG. 12. COMPOSITE PROBABILITY DISTRIBUTION FUNCTION OF THE ENVELOPE OF RECEIVED HF ATMOSPHERIC NOISE: COMPARISON OF MODEL RESULTS WITH DATA MEASURED AT SLOUGH, ENGLAND AND AT SINGAPORE.

$P_0(V)$  = Probability that envelope intensity  $V$  exceeds abscissa value.

[Note: Vertical scale is  $\log|\log P_0(V)|$ .]

LEGEND:

- 1 — Measured data, Slough, England  
Band center frequency,  $f_0 = 11$  Mc  
Receiver power bandwidth = 425 cps  
(Clarke, et al, [Ref. 10])
- 2 — Measured data, Singapore  
(Same conditions as above)
- 3 — Generalized "t" model  
 $\theta = 4$   
 $\gamma = 0.707 \tilde{V}_{rms}$ ,  $\tilde{V}_{rms} \triangleq E[V^2] \approx 10$  db above  $V_{rms}^2$   
(see footnote, page 48)
- 4 — Rayleigh distributed envelope  
 $E[V^2] = \tilde{V}_{rms}^2$



$P_0(V)$  = Probability that envelope intensity  $V$  exceeds abscissa value.

**LEGEND :**

- 1 Measured data, Slough, England  
Band center frequency,  $f_0 = 20 \text{ Mc}$   
Receiver power bandwidth = 425 cps  
(Clarke, et al, [Ref. 10])
- 2 Measured data, Singapore  
(Same conditions as above)
- 3 Generalized "t" model  
 $\theta = 4$   
 $\gamma = 0.07 \tilde{V}_{\text{rms}}$ ,  $\tilde{V}_{\text{rms}}^2 \triangleq E[V^2] \approx 10 \text{ db below } V_{\text{rms}}^2$   
(see footnote, page 48)
- 4 Rayleigh-distributed envelope  
 $E[V^2] = \tilde{V}_{\text{rms}}^2$

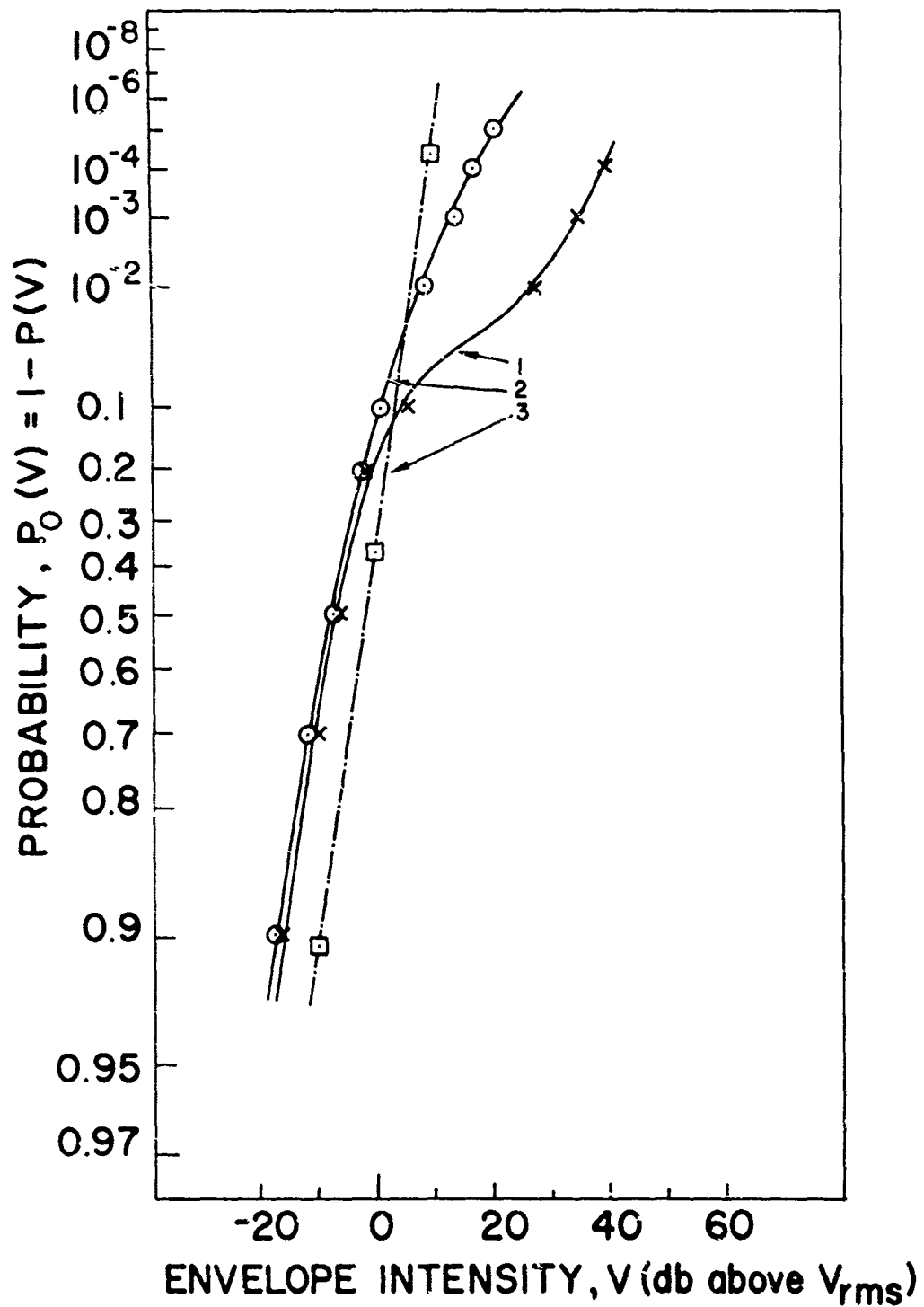


FIG. 14. PROBABILITY DISTRIBUTION FUNCTION OF THE ENVELOPE OF RECEIVED HF ATMOSPHERIC NOISE: DEMONSTRATION OF EFFECT OF A PREDOMINANT LOCAL NOISE SOURCE.

$P_0(V)$  = Probability that envelope intensity  $V$   
exceeds abscissa value

[Note: Vertical scale is  $\log|\log P_0(V)|$ .]

LEGEND:

- 1      Measured data (Furutsu and Ishida [Ref. 6])  
Ohira, Japan, 0218, Feb. 19, 1957  
(Predominant local noise source)  
Band center frequency,  $f_0 = 3.5$  Mc  
Receiver bandwidth = 1.2 kc  
 $\alpha = 5$  db below  $\sigma$  {see [Ref. 6], Fig. 8(a)}
- 2      Measured data (Furutsu and Ishida [Ref. 6])  
Ohira, Japan, 0605, Feb. 19, 1957  
(No predominant local noise source)  
Band center frequency,  $f_0 = 3.5$  Mc  
Receiver bandwidth = 1.2 kc  
 $\alpha = 10$  db above  $a_0$  {see [Ref. 6], Fig. 9(a)}
- 3      Rayleigh-distributed envelope  
 $\alpha = V_{rms}$

where

$$p_V(v) \Big|_{\theta=3} = 2\gamma^2 \frac{v}{(v^2 + \gamma^2)^2}$$

follows from Eq. (2.22). Thus it is found that  $E[V] \Big|_{\theta=3} = \frac{\pi}{2} \gamma$ ; so that, for the case  $\theta = 3$ ,  $\gamma$  was chosen to satisfy

$$\gamma = \frac{2}{\pi} V_{\text{avg}}. \quad (2.29)$$

For the case  $\theta = 4$ , because of the fact that  $V_{\text{rms}}$  and not  $V_{\text{avg}}$  was presented in the measured data where  $\theta = 4$  was appropriate,  $\gamma$  was chosen to make  $(E[V^2])^{1/2} = V_{\text{rms}}^{\dagger}$ . (It is noted that, if available,  $V_{\text{avg}}$  is preferred to  $V_{\text{rms}}$  for calibration, since it is less dependent on large values of  $V$ , at which values the measured data are least reliable because of the tremendous dynamic range and long observation time required to obtain valid results.) Now

$$\begin{aligned} E[V^2] \Big|_{\theta=4} &= \int_0^{\infty} v^2 p_V(v) \Big|_{\theta=4} dv \\ &= \int_0^{\infty} 3\gamma^3 \frac{v^3}{(v^2 + \gamma^2)^{5/2}} dv = 2\gamma^2, \end{aligned} \quad (2.30)$$

so that, for the case  $\theta = 4$ ,  $\gamma$  was chosen to satisfy

$$\gamma = 2^{-1/2} V_{\text{rms}}. \quad (2.31)$$

<sup>†</sup> For Figs. 12 and 13,  $\tilde{V}_{\text{rms}} \neq V_{\text{rms}}$  was chosen to give the best fit, since values of  $V_{\text{rms}}$  presented by Clarke, et al in their Fig. 6, for the cases at 11 Mc and 20 Mc, are not compatible with each other.

Finally, for the case  $\theta = 2$ ,  $\gamma$  was chosen empirically to give the best fit to the measured data, since none of the moments of the envelope of the generalized "t" model are finite in this case. (The nonexistence of these moments is discussed further in the next section.)

#### b. Discussion of Plotted Results

The plotted results are reasonably self-explanatory, but several comments and conclusions of interest are warranted. Because of the extremely impulsive nature of the received atmospheric noise at vlf, it is anticipated that the generalized "t" model for the received noise will be most useful in this portion of the spectrum. Thus the plotted results emphasize the vlf region, the applicable figures being Figs. 4 to 10. Further, because of the fact mentioned in the introduction that the spectral shape of the received noise is determined by the receiver in all cases of available measured data, and since it is desired to model the noise as little affected by the receiver as possible, the plotted data in Figs. 4 to 9 make use of the widest-band measured data known to the author. It is noted, however, that a closely similar form is obtained for the distribution of the envelope for bandwidths in the range from about 100 cps up to at least 2 kc, which is the largest bandwidth for which any experimental results have been reported. Verification of this statement is contained in the experimental results of Watt and Maxwell [Ref. 9] and Harwood [Ref. 27], and it is supported by Fig. 10, where the data were obtained in a 425-cps bandwidth rather than in the 1000-to 1300-cps bandwidths used to obtain Figs. 4 to 9. With this explanation of the choice of vlf experimental data, the conclusions to note are:

1. At vlf the generalized "t" model is obviously a much better fit to the received noise than is a gaussian model (Rayleigh distributed envelope). Quantitatively, it is seen that in most cases the generalized "t" model gives a good fit for cumulative envelope probabilities smaller than about  $1-10^{-5}$  or more, while the gaussian model gives a good fit only for cumulative envelope probabilities smaller than about  $1-10^{-1}$ .
2. It is seen that a good fit to the measured vlf data is attained by the generalized "t" model when the parameter  $\theta$  is assigned an appropriate value in the range  $2 < \theta < 4$ , and the parameter  $\gamma$  is chosen according to an appropriate moment of the envelope given  $\theta$  as discussed above. It is interesting to note that the choice of  $\theta$  is dependent on the location, number, and intensity of noise sources, since in general, the smaller values of  $\theta$  are required to

fit the Canal Zone data (Figs. 8 and 9) characterized by strong local thunderstorm activity, while the larger values of  $\theta$  are appropriate for the Alaskan data (Figs. 4 and 5) characterized by much less local thunderstorm activity.

In addition to the fit of the generalized "t" model at vlf, it is of interest to consider the applicability of the model as the band center frequency  $f_0$  is increased. This subject is considered in Figs. 10 to 14 and leads to the following conclusions:

1. Although the improvement shown by the generalized "t" model as compared with a gaussian model is most dramatic at vlf (Fig. 10) and at lf (Fig. 11) it is seen that the generalized "t" model may have application at frequencies up to and including the hf band (Figs. 12 and 13). The fact that the importance of individual noise source components decreases with increasing band center frequency is evident in the plotted data however, and Fig. 14 is presented to emphasize that the choice between the gaussian model and the generalized "t" model is not as clear at hf as it is at vlf, i.e., Fig. 14 shows that the statistics of hf atmospheric noise are strongly a function of local thunderstorm activity.
2. It is seen, consistent with the fact that the dynamic range of the received noise decreases with increasing band center frequency, that the value of  $\theta$  required to fit the measured data increases with band center frequency with  $\theta \geq 4$  being appropriate at hf (Figs. 12 and 13).

In summary of the above discussion, it is concluded that the first-order statistics of the generalized "t" model are in good agreement with a usefully wide range of measured data on received atmospheric noise. The fit of the generalized "t" model is seen to be especially good at vlf and lf in those situations characterized by low-to-moderate local thunderstorm activity.

With this result in mind, it is of interest to consider modifications to the generalized "t" model that will improve its fit when either the measured data is characterized by strong local thunderstorm activity or the band center frequency of interest is increased to hf. The plotted results discussed above are useful in suggesting the appropriate modifications when the following observations are made:

1. It is noted above that the generalized "t" model produces a probability distribution for the envelope that diverges from some experimental results for cumulative probabilities above about  $1-10^{-5}$  (see, for example, Figs. 10 to 13). It is emphasized that this divergence is somewhat questionable at vlf because of the tremendous dynamic range required for the receiver to observe these probabilities without

distortion, so that it may be receiver nonlinearity that causes this apparent divergence. In fact, it is seen that the relatively wideband data in Figs. 4 to 9 adapted from Watt and Maxwell do not exhibit this divergence, whereas it is evident in the relatively narrowband data in Fig. 10 adapted from Clarke, et al as well as in relatively narrowband data presented by Watt and Maxwell [Ref. 9]. Thus, despite the questionable existence of the divergence between measured and generalized "t" model curves for bandwidths greater than about 1000 cps at vlf, the fact that such a divergence is seen in narrower bandwidths for cumulative probabilities greater than about  $1-10^{-5}$ , plus the fact that the divergence may become more evident as the band center frequency of interest is increased (see Fig. 14) indicate the desirability of modifying the generalized "t" model to accommodate this behavior.

2. It is pointed out above that the fit of the generalized "t" model to measured vlf data is optimized if  $\theta$  is chosen appropriately in the range  $2 < \theta < 4$ . Now, as mentioned in Section B1,  $\theta$  in the range  $2 < \theta \leq 3$  means that  $E[y^2] = \infty$ , so that the generalized "t" model with  $\theta$  in this range does not correspond to a physical noise. This is not disturbing, since it is expected [Refs. 18 and 21] that models for "impulsive" phenomena will be characterized by barely convergent or divergent second moments because of the large dynamic range which these models must possess. Despite this argument, it is desirable to consider modifications to the generalized "t" model which satisfy the condition that every physical noise has finite average power.

#### c. Development of the Modified Generalized "t" Model

With the above observations in mind, the modification proposed here is merely that the ensemble of values that the modulating process  $a(t)$  can assume be truncated as follows:

$$p_a(a) = \frac{k}{|a|^{m+1}} \exp\left(-\frac{m}{2\sigma^2} \frac{1}{a^2}\right), \quad -\beta \leq a \leq \beta, \quad (2.32)$$

where  $k$  is chosen to satisfy

$$\int_{-\beta}^{\beta} p_a(a) da = 1.$$

The physical justification for this modification is simply that since each lightning stroke must emit finite energy the measured data must diverge at

some level from the generalized "t" model with  $\theta \leq 3$ . The above truncation of the range of  $a(t)$  is perhaps the simplest way to introduce into the generalized "t" model a change in trend that will follow the change in trend of the measured data for cumulative probabilities above about  $1-10^{-5}$  (see Figs. 10 to 14). Furthermore, it is clear in agreement with the measured data that this trend change will occur at lower noise levels if either the receiver bandwidth is reduced or the band center frequency is increased, since either procedure results in reducing the importance of any single lightning stroke to the received noise. Now, applying the same procedure used in conjunction with the generalized "t" model in order to calculate the distribution of the envelope for the modified generalized "t" model, it is found that

$$p_V(V) = \int_{1/\beta^2}^{\infty} \frac{kV}{\sigma^2} \exp \left[ - \left( \frac{m}{2\sigma^2} + \frac{V^2}{2\sigma_1^2} \right) \tau \right] d\tau. \quad (2.33)$$

This integral is easily evaluated in closed form for  $m$  even, and we will proceed by considering  $m = 2$ , which corresponds to the important case  $\theta = 3$ . (See Appendix A for evaluation of Eq. (2.33) with  $m$  odd.) Thus, taking  $m = 2$  and substituting the proper value for the normalizing constant  $k$ , it is found using Dwight, item 567.9, that

$$p_V(V) \Big|_{\theta=3} = 2V \exp \left( - \frac{V^2}{2\beta^2 \sigma_1^2} \right) \left[ \frac{\gamma^2}{(V^2 + \gamma^2)^2} + \frac{1}{\beta^2 \sigma^2 (V^2 + \gamma^2)} \right],$$

$$0 \leq V < \infty, \quad (2.34)$$

where

$$\gamma \triangleq 2^{1/2} \frac{\sigma_1}{\sigma}.$$

Now, calculating the complement of the probability distribution function for comparison with the measured data,

$$P_0(V) \Big|_{\theta=3} = \frac{\gamma^2}{V^2 + \gamma^2} \exp\left(-\frac{V^2}{\beta^2 \sigma^2 \gamma^2}\right). \quad (2.35)$$

This result is plotted in Fig. 10, where it is seen that the modification has the desired effect of improving the fit of the model to measured data at cumulative probabilities above about  $1-10^{-6}$  without significantly altering the fit at lower cumulative probabilities. Thus it is concluded that the modified generalized "t" model has flexibility not possessed by the generalized "t" model. This flexibility may be of practical significance when the dynamic range of the received noise becomes sufficiently limited because of either increasing band center frequency or decreasing receiver bandwidth.

Finally, it is conjectured that the model can be further improved with regard to its ability to fit measured data characterized by strong local thunderstorm activity by taking the first-order statistics of  $a(t)$  to be given by

$$p_a(a) = \begin{cases} \frac{k_1}{|a|^{m_1+1}} \exp\left(-\frac{m_1}{2\sigma_0^2} \frac{1}{a^2}\right), & |a| \leq \beta_1 \\ \frac{k_2}{|a|^{m_2+1}} \exp\left(-\frac{m_2}{2\sigma_2^2} \frac{1}{a^2}\right), & \beta_1 < |a| \leq \beta_2. \end{cases} \quad (2.35)$$

This second modification will not be further considered here, because it does not fundamentally change the form of the model although it substantially complicates the calculations of interest.

## 2. Average Intensity of Envelope Level Crossings

As discussed earlier, it is of interest to calculate the average number of crossings of a fixed level by the envelope of the noise per unit

time, both as a further check on the first-order statistics of the generalized "t" model and as a demonstration of the analytical usefulness of this model. Letting  $\overline{N_V(V_0)}$  denote the average number of crossings of the level  $V_0$  by the envelope per second, it is well known [Ref. 24] that for an ergodic random process  $V(t)$

$$\overline{N_V(V_0)} = \int_{-\infty}^{\infty} |\dot{V}| p_{V, \dot{V}}(V, \dot{V}) \Big|_{V=V_0} d\dot{V}, \quad (2.37)$$

where  $\dot{V}(t) \triangleq d/dt V(t)$ . Now, it was shown in Section C1 that with the assumption of negligible spectral overlap of  $a(t)$  and  $n(t)$ ,

$$V(t) \approx |a(t)| E(t), \quad (2.4)$$

where  $E(t)$  is the envelope of the narrowband gaussian process  $n(t)$ . Thus

$$\dot{V}(t) \approx |a(t)| \dot{E}(t) + |\dot{a}(t)| E(t). \quad (2.38)$$

However, noting that the available experimental measurements of  $\overline{N_V(V_0)}$ , which are presented in Fig. 15, were obtained in a bandwidth of 1100 cps, it is interesting to consider the assumption that the modulating function  $a(t)$  is sufficiently slowly varying so that with high probability

$$|a(t)| \dot{E}(t) \gg |\dot{a}(t)| E(t). \quad (2.39)$$

This assumption is of interest since it means that with high probability

$$\dot{V}(t) \approx |a(t)| \dot{E}(t), \quad (2.40)$$

so that one can write

$$\begin{aligned}
p_{V, \dot{V}}(V, \dot{V}) &\approx p_{|a|E, |a|\dot{E}}(V, \dot{V}) \\
&= \int_0^\infty dx \frac{1}{x^2} p_{|a|}(x) p_{E, \dot{E}}\left(\frac{V}{x}, \frac{\dot{V}}{x}\right), \quad (2.41)
\end{aligned}$$

where

$$p_{|a|}(x) = \frac{2\left(\frac{m}{2}\right)^{m/2}}{\sigma^m \Gamma\left(\frac{m}{2}\right)} \frac{1}{|x|^{m+1}} \exp\left(-\frac{m}{2\sigma^2} \frac{1}{x^2}\right), \quad 0 \leq x < \infty$$

follows from Eq. (2.8) and where  $p_{E, \dot{E}}(V/x, \dot{V}/x)$  is calculated as follows: Since  $E(t)$  is the envelope of a stationary gaussian process  $n(t)$  with covariance function  $R_n(\tau)$ , it can be shown [Ref. 26], making the reasonable assumption that  $\dot{n}(t)$  has finite second moment, that

$$\begin{aligned}
p_{E, \dot{E}}(E, \dot{E}) &= \frac{E}{R_n(0) \left[ 2\pi \left( -\ddot{R}_n(0) - \frac{1}{R_n(0)} \tilde{R}_n^2(0) \right) \right]^{1/2}} \\
&\quad \cdot \exp \left\{ -\frac{1}{2} \left[ \frac{E^2}{R_n(0)} + \frac{\dot{E}^2}{\left( -\ddot{R}_n(0) - \frac{1}{R_n(0)} \tilde{R}_n^2(0) \right)} \right] \right\} \\
&= p_E(E) p_{\dot{E}}(\dot{E}), \quad (2.42)
\end{aligned}$$

where  $R_n(0) = \sigma_1^2$  in the previous notation, and  $\tilde{R}_n(\tau)$  is the Hilbert transform of  $R_n(\tau)$ . Now, it is interesting to note that if

$$R_n(\tau) = R_c(\tau) \cos \omega_0 \tau \quad (2.43)$$

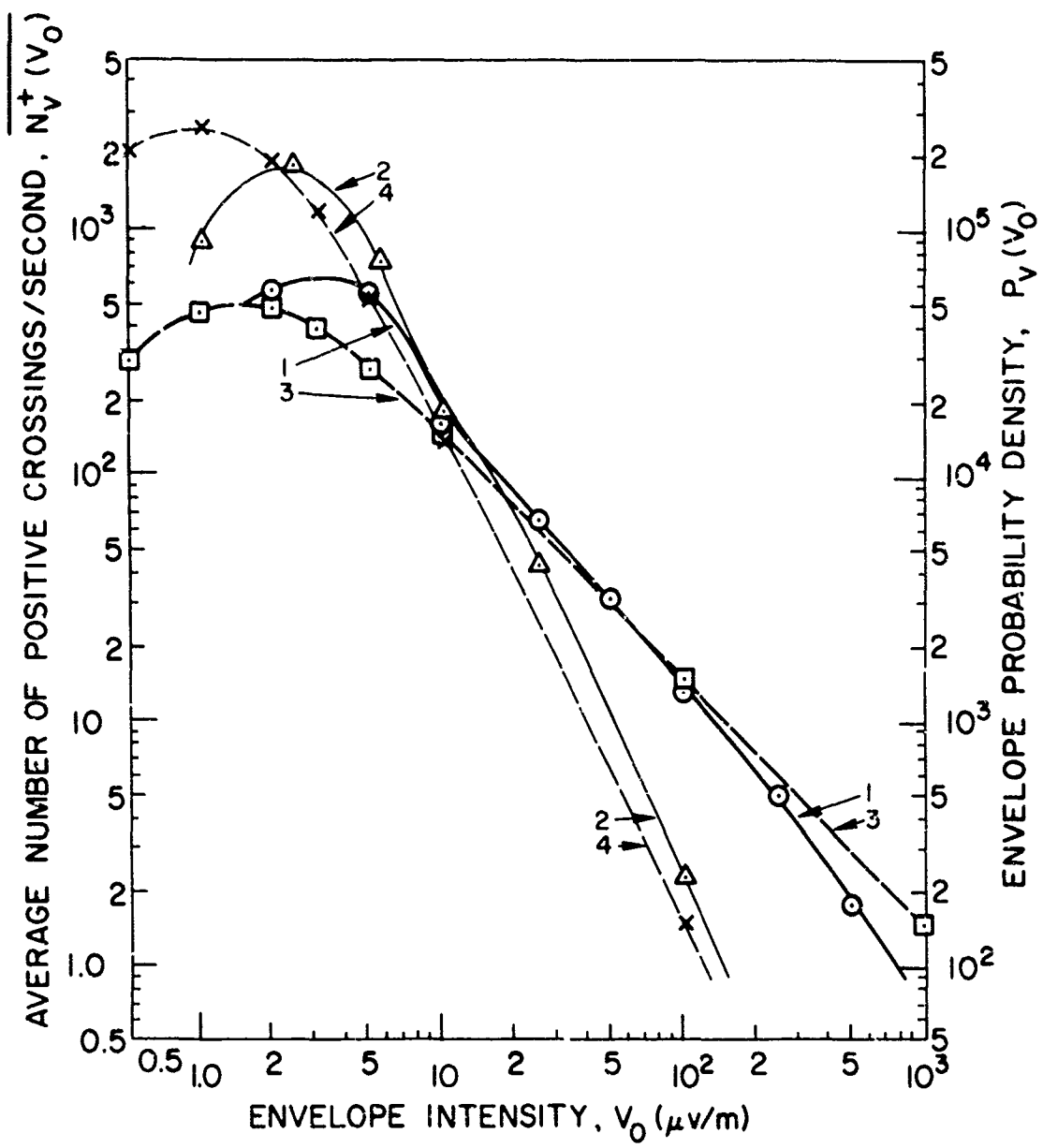


FIG. 15. AVERAGE RATE OF ENVELOPE LEVEL CROSSINGS: COMPARISON OF MODEL RESULTS WITH MEASURED VLF DATA.

LEGEND:

- 1 Measured data: Average rate of envelope level crossings. (Watt and Maxwell [Ref. 9])  
 Point Barrow, Alaska, 1450 A.S.T., Sept. 27, 1956  
 Band center frequency,  $\nu_0 = 2$  ...  
 Receiver 6-db bandwidth = 1100 cps  
 6' antenna, N.E.-S.W. plane
- 2 Measured data: Envelope probability density function.  
 (Watt and Maxwell [Ref. 9])  
 (Same conditions as above)
- 3 Generalized "t" model: Average rate of envelope level crossings.  
 $\theta = 2$   
 $\gamma = 1.5 \times 10^{-6}$   
 rms bandwidth,  $B_c = 500$  cps
- 4 Generalized "t" model: Envelope probability density function.  
 (Same conditions as above)

where  $S_c(f)$ , the Fourier transform of  $R_c(\tau)$ , is zero for  $|f| \geq f_0$  (which is in fact the case of interest in this development), then

$$-\ddot{R}_n(0) - \frac{1}{R_n(0)} \ddot{R}_n^2(0) = -\ddot{R}_c(0) . \quad (2.44)$$

Also, it is easily shown that in this situation

$$-\ddot{R}_c(0) = (2\pi)^2 R_c(0) B_c^2 = (2\pi)^2 R_n(0) B_c^2 , \quad (2.45)$$

where

$$B_c = \left( \int_{-\infty}^{\infty} f^2 \frac{S_c(f)}{R_c(0)} df \right)^{1/2}$$

is defined to be the rms bandwidth of  $n(t)$ . Thus, substituting these results into Eq. (2.42):

$$p_{E,\dot{E}}(E,\dot{E}) = \frac{E}{(2\pi)^{3/2} B_c \sigma_1^3} \exp \left\{ -\frac{1}{2\sigma_1^2} \left[ E^2 + \frac{\dot{E}^2}{(2\pi)^2 B_c^2} \right] \right\} . \quad (2.46)$$

Now, substituting this result into Eq. (2.41), making a change of variable, and using Dwight, item 860.17, it is found that

$$p_{V,\dot{V}}(V,\dot{V}) = \frac{\Gamma(\frac{\theta+2}{2})}{\Gamma(\frac{\theta-1}{2})} \frac{\gamma^{\theta-1}}{\pi^{3/2} B_c} \frac{V}{\left[ V^2 + \frac{\dot{V}^2}{(2\pi)^2 B_c^2} + \gamma^2 \right]^{(\theta+2)/2}} , \quad \theta > 1 . \quad (2.47)$$

Finally, substituting Eq. (2.47) into Eq. (2.37), there is obtained the desired result

$$\overline{N_V(V_0)} = \frac{\Gamma(\frac{\theta+2}{2})}{\Gamma(\frac{\theta-1}{2})} \frac{8\pi^{1/2} \gamma^{\theta-1} B_c}{\theta} \frac{V_0}{(V_0^2 + \gamma^2)^{\theta/2}}, \quad 0 \leq V_0 < \infty, \theta > 1. \quad (2.48)$$

Now, the measured data presented by Watt and Maxwell [Ref. 9] and reproduced in Fig. 15 are for crossings of the level  $V_0$  in the positive direction only, and are seen to correspond to the case  $\theta = 2$ , for which formula (2.48) becomes

$$\overline{N_V^+(V_0)} \Big|_{\theta=2} = 2\gamma B_c \frac{V_0}{V_0^2 + \gamma^2}. \quad (2.49)$$

#### a. Discussion of Plotted Results

Although the basic agreement of the results derived using the generalized "t" model with the measured level-crossing results is clear from inspection of Fig. 15, the following comments and conclusions are in order: Recalling the result due to Rice [Ref. 24] that if the noise were gaussian the average number of level crossings by the envelope per second would be equal to an appropriate bandwidth factor multiplied by the envelope probability density function, it is once again clear that the generalized "t" model is far more appropriate than a gaussian model for vlf atmospheric noise. In fact, it is seen that the generalized "t" model gives the asymptotic result

$$\lim_{V_0 \rightarrow \infty} p_V(V_0) = (\theta-1) \frac{\gamma^{\theta-1}}{V_0^\theta}, \quad \theta > 1, \quad (2.50)$$

whereas

$$\lim_{V_0 \rightarrow \infty} \overline{N_V(V_0)} = 8\pi^{1/2} \frac{\Gamma(\frac{\theta+2}{2})}{\Gamma(\frac{\theta-1}{2})} \frac{B_c}{\theta} \frac{\gamma^{\theta-1}}{V_0^{\theta-1}} . \quad (2.51)$$

In addition to being in good agreement with the experimental data from Watt and Maxwell [Ref. 9], the asymptotic result given by Eq. (2.51) is also in good agreement with the vlf level-crossing rate measurements made by Clarke, et al [Ref. 10], who find for thresholds in excess of the average value of the noise envelope that  $\overline{N_V(V_0)}$  is given by

$$\overline{N_V(V_0)} \approx (V_0/A)^{-C} , \quad (2.52)$$

where A and C are constants such that

$$A \approx V_{avg} + 30 \text{ db} , \quad 1.3 \leq C \leq 2 .$$

Taking now a closer look at the results plotted in Fig. 15, it is noted that, although the measured data correspond well with the generalized "t" model with  $\theta = 2$ , the experimental determination of  $p_V(V_0)$  contains no data points for envelope values larger than that corresponding to 2.4 crossings per second. Now, consistent with the arguments presented earlier in the discussion of the distribution of the envelope, it is seen that the slope of  $p_V(V_0)$  must change at high values of  $V_0$ , since the noise has finite average power. Thus it is conjectured, although it will not be considered further here, that the fit of the generalized "t" model to the measured level-crossing data can be further improved by employing the modified generalized "t" model proposed in subsection 1c. In support of this conjecture, it is noted that the measured data presented by Clarke, et al also shows a departure from the power law  $(V_0/A)^{-C}$  at crossing rates below 1 per second, with this departure becoming less apparent as the value of C increases. This behavior is consistent with the result found from envelope distribution considerations--namely that

the generalized "t" model provides a better fit to the received noise at vlf as the required value of  $\theta$  increases corresponding to the situation of low-to-moderate local thunderstorm activity.

Finally, in summary, it is concluded that the data plotted from Watt and Maxwell in Fig. 15, as well as comparisons with the experimental results of Clarke, et al indicate good agreement between the average number of level crossings of the envelope given by the generalized "t" model and by the measured vlf data. The significance of this agreement is, of course, that it is further verification of the applicability of the generalized "t" model as far as the first-order statistics of the noise are concerned. From a physical point of view, this agreement increases confidence in the generalized "t" model, since it indicates that on the average the envelope of the model varies with time at the same rate (at least at vlf) as the envelope of the received noise. To complete verification of the applicability of the generalized "t" model as a model for vlf atmospheric noise, it remains to investigate the manner in which these variations with time occur. This is, of course, a function of the second- and higher-order statistics of the noise, which will be the next topic of discussion. Before leaving the present discussion of the average level-crossing rate, however, it is noted that the fit of the model to the measured data in Fig. 15 was achieved by taking the rms bandwidth  $B_c$  to be 500 cps. On the other hand, the measured data were taken in a 6-db bandwidth of 1100 cps, which corresponds to an rms bandwidth of the order of 400 cps. This discrepancy is not large, but may be a result of the assumption that the term  $|\dot{a}(t)|E(t)$  is negligible in Eq. (2.38). Thus it is conjectured that the fit of the calculated level-crossing rate to the experimental results may be improved by relaxing the above assumption, which is equivalent to the assumption that the modulating process  $a(t)$  has a much smaller bandwidth than the envelope  $E(t)$  of the narrowband gaussian process  $n(t)$ . Finally, it is pointed out that the bandwidth factor is absorbed into the constant  $A$  in the work of Clarke, et al where all of the measurements of level-crossing rate were made in a fixed power bandwidth of 425 cps.

### 3. The Distribution of Envelope Level Crossings

Having demonstrated that the first-order statistics of the generalized "t" model are in good agreement with measured data on received atmospheric noise over an interesting range of receiver bandwidth and band center frequency, completion of the verification of the applicability of the model to received atmospheric noise requires investigation into the higher-order statistics of the noise. Physically, this means that although the consideration of the average rate of level crossings shows that the envelope of the generalized "t" model fluctuates at the same average rate as the envelope of observed atmospheric noise, it remains to investigate the fashion in which these fluctuations occur. That is, it remains to verify that the higher-order statistics of the generalized "t" model can be chosen so that the relationship between the process at various distinct instants in time, as predicted by the model, is consistent with measured results on this relationship. As mentioned earlier, the available experimental data [Ref. 9] dependent on the higher-order statistics of the noise consist of measurements of the probability distribution function of the interval between successive crossings of a fixed level by the envelope of the noise. Inspection of these data indicates that at vlf the noise pulses do not in general occur in a Poisson fashion, but rather that received noise pulses are usually statistically dependent on preceding ones. Now, the calculation of the probability distribution of the inter-level-crossing interval is difficult, requiring numerical techniques to obtain even an approximate solution [Refs. 24, 28, 29]. This is true even for the special case of gaussian processes, which is the only case that has been treated in any detail in the literature [Refs. 28, 29]. Thus we will not attempt to find an exact solution for the nongaussian situation of interest here, but will resort to simplifying assumptions, based on an understanding of the generalized "t" model, in order to obtain an approximate solution. Noting, as discussed in the introduction, that the received atmospheric noise of interest can be considered to be a narrowband random process, it follows that its envelope can at least be assumed to be bandlimited. Thus it is proposed that a useful representation of the envelope in an interval of observation  $-\Delta t \leq t \leq T$  is given by

$$v(t) \approx \sum_{i=0}^N v(t_i) (\Delta t_i)^{1/2} q_i(t), \quad (2.53)$$

where  $q_i(t)$ ,  $i=0, \dots, N$ , is defined in Fig. 16 and where the value of  $N$  required to make this representation reasonable depends upon the bandwidth through which the signal of duration  $T + \Delta t$  is observed.

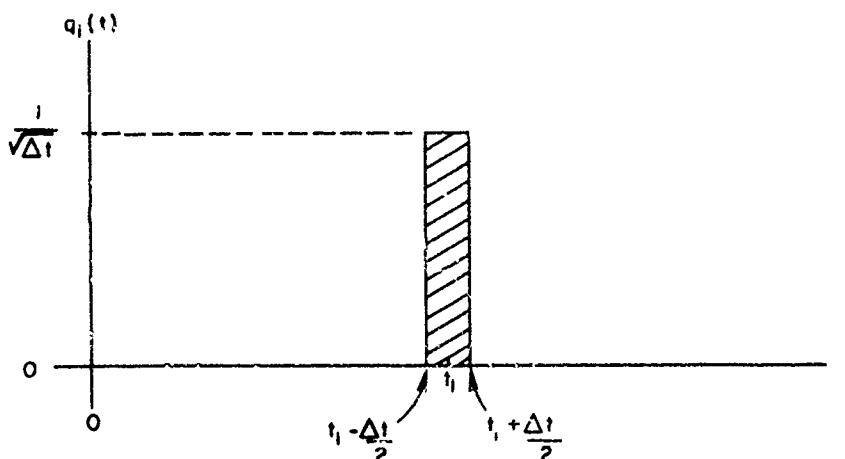


FIG. 16. DEFINITION OF  $q_i(t)$ ,  $i = 0, \dots, N$ , WHERE  $t_i \triangleq \left(1 - \frac{1}{2}\right) \Delta t$ .

Now, recalling that with the reasonable assumption of negligible spectral overlap of  $a(t)$  and  $n(t)$  that

$$v(t) \approx |a(t)| E(t), \quad (2.4)$$

where  $E(t)$  is the envelope of the narrowband gaussian process  $n(t)$ , the representation in Eq. (2.53) becomes

$$v(t) \approx \sum_{i=0}^N |a(t_i)| E(t_i) (\Delta t_i)^{1/2} q_i(t). \quad (2.54)$$

Let  $T$  now be defined as the interval between a down-crossing of the level  $V_0$  by the envelope of the received noise, and the next up-crossing of the

same level. (This is the quantity whose statistics have been measured by Watt and Maxwell [Ref. 9].) Applying the representation of  $V(t)$  proposed in Eq. (2.53), it is seen that the probability distribution actually measured by Watt and Maxwell is given by

$$\begin{aligned}
 P_0(T_0) &\triangleq \text{Probability that } T \text{ exceeds } T_0 \\
 &\triangleq \Pr \{T > T_0\} \\
 &= \Pr \{\text{no up-crossings of } V_0 \text{ in } [t, t+T_0] \mid \text{down-crossing of } V_0 \text{ at } t\} \\
 &= \frac{\Pr \{\text{no up-crossings of } V_0 \text{ in } [0, T_0], \text{ down-crossing of } V_0 \text{ at } t = 0\}}{\Pr \{\text{down-crossing of } V_0 \text{ at } t = 0\}} \\
 &= \frac{\Pr \{V(t_0) > V_0, V(t_1) < V_0, \dots, V(t_{N_0}) < V_0\}}{\Pr \{V(t_0) > V_0, V(t_1) < V_0\}} \quad (2.55)
 \end{aligned}$$

where  $N_0 = \text{smallest integer } \geq T_0/\Delta t$ .

With this simplified formulation of the solution for  $P_0(T_0)$ , one can now proceed to investigate the possibility of specifying the higher-order statistics of  $a(t)$  and  $n(t)$  in such a way as to reproduce the distribution of the inter-level-crossing interval observed experimentally. Two special cases will be considered, as follows.

#### a. Case of Independent Samples

In this special case, which is the simplest case of interest, it is assumed that the values taken on by the envelope at the  $(N_0+1)$  sampling instants are statistically independent. It is obvious that this assumption of independence greatly simplifies the evaluation of  $P_0(T_0)$  given by Eq. (2.55); but it remains to verify that the representation of  $V(t)$  given by Eq. (2.53) is reasonable in the light of the independence assumption. Assuming that the observed atmospheric noise is bandlimited by the receiver to an rf bandwidth  $2B$ , it follows that the envelope of the received noise is bandlimited to a frequency band of width  $2B$  centered about zero frequency [Ref. 30]. Thus it can be shown [Ref. 31] that this

bandlimited envelope  $V(t)$  is approximately described in the time interval  $[0, T_0]$  by its samples at  $N_0$  equidistant instants, where  $N_0 \approx 2T_0 B$  is required if the samples are to be reasonably assumed both independent and sufficient in number to yield a good approximation. Such a representation is given by:

$$v(t) \approx \sum_{i=1}^{2T_0 B} v(t_i) \varphi_i(t), \quad (2.56)$$

where the  $t_i$  are defined as in Fig. 16 and where the best approximation to  $V(t)$  comes from taking the  $\varphi_i(t)$  to be the prolate spheroidal wave functions [Ref. 31]. However, because the spectral shape of the received atmospheric noise is determined by the filter through which it is observed in the situations of practical interest, it is proposed that the representation in Eq. (2.53) in terms of the pulse "basis" functions  $q_i(t)$ ,  $i=0, \dots, 2T_0 B$ , is in fact a reasonable approximation to the envelope of this filtered "white" noise.

Now, making use of the assumption that the  $(2T_0 B+1)$  samples in Eq. (2.55) are statistically independent, it is found directly that

$$P_0(T_0) = \left[ \Pr \{V(t) < v_0\} \right]^{(2T_0 B+1)}, \quad (2.57)$$

where, from Eq. (2.27),

$$\Pr \{V(t) < v_0\} = 1 - \frac{\gamma^{\theta-1}}{(v_0^2 + \gamma^2)^{(\theta-1)/2}}. \quad (2.58)$$

Thus, for the case of independent samples,

$$P_0(T_0) = \left\{ 1 - \frac{\left(\frac{\gamma}{V_0}\right)^{\theta-1}}{\left[1 + \left(\frac{\gamma}{V_0}\right)^2\right]^{(\theta-1)/2}} \right\}^{(2T_0B-1)} \quad (2.59)$$

Special cases of this result corresponding to  $\theta = 2$  and  $\theta = 3$  are plotted in Fig. 17 along with data taken from Watt and Maxwell [Ref. 9], and the special case corresponding to  $\theta = 2$  is also plotted in Fig. 18 along with data taken from Watt and Maxwell and along with data from the constant  $a(t)$  case considered below. It is seen that the assumption of independent samples, like the assumption that noise pulses occur in a Poisson fashion (exponentially distributed intervals, Fig. 17), neglects certain dependencies between adjacent level crossings.<sup>†</sup> In fact, it is seen that for the high levels of most interest, i.e., for  $V_0 \gg \gamma$ ,

$$\lim_{\frac{V_0}{\gamma} \rightarrow \infty} P_0(T_0) = \exp \left[ - 2B \left( \frac{\gamma}{V_0} \right)^{\theta-1} T_0 \right], \quad (2.60)$$

so that the assumption of independent samples produces exponentially distributed inter-level-crossing intervals at high levels. It is noted that the value of  $P_0(T_0)$  given by Eq. (2.59) and plotted in Figs. 17 and 18 is actually consistent with Eq. (2.55) only for those values of  $T_0$  such that  $2T_0B$  is an integer. A smooth curve is fitted through these points in preference to the step function specified by Eq. (2.55) because the probability distribution function of the interval is of course continuous in nature. In any case, the discrepancy between the smooth curve and the associated step function is negligible at large values of  $2T_0B$ , the situation of most interest. Now, the goal of the calculation of the probability distribution of the inter-level-crossing interval here is to investigate

<sup>†</sup> It is noted that the discrepancy between the calculated and measured results at low values of  $T_0$  is due in part to the breakdown of the assumption that  $N_0 \approx 2T_0B$  is sufficient at low values of the  $T_0B$  product.

our ability to specify the higher-order statistics of the generalized "t" model in order to reproduce the distribution of inter-level-crossing intervals observed experimentally. The assumption of independent samples is seen to give a distribution which agrees with some experimental data but which, in general, neglects some observed dependence between adjacent level crossings. A second special case will now be considered in an attempt to introduce this observed dependence into the calculated results.

b. Constant  $a(t)$  Case

In this special case the slowly varying modulating function  $a(t)$  is in fact assumed to be constant for the duration of observation, so that  $V(t)$  as represented by Eq. (2.54) takes the form

$$V(t) \approx \sum_{i=0}^N |a| E(t_i) (\Delta t_i)^{1/2} q_i(t) . \quad (2.61)$$

In order to complete the specification of  $V(t)$  in the interval  $[-\Delta t, T_0]$ , which is the interval of interest in Eq. (2.55), it is assumed that the  $(N_0+1)$  samples of  $E(t)$  are statistically independent [recalling that  $E(t)$  is the envelope of the narrowband gaussian process  $n(t)$ ]. Thus it follows from the development of the independent-samples case that  $N_0 \approx 2T_0 B$  is required, so that the representation of  $V(t)$  in the interval  $[-\Delta t, T_0]$  takes in this case the form

$$V(t) \approx |a| \sum_{i=0}^{2T_0 B} E(t_i) (\Delta t_i)^{1/2} q_i(t) . \quad (2.62)$$

Now, turning to the calculation of  $P_0(T_0)$  as given by Eq. (2.55), it is seen that the solution requires evaluation of the joint probability distribution

$$\Pr \left\{ V(t_0) > v_0, V(t_1) < v_0, \dots, V(t_N) < v_0 \right\} \triangleq \hat{P}_N(v_0) . \quad (2.63)$$

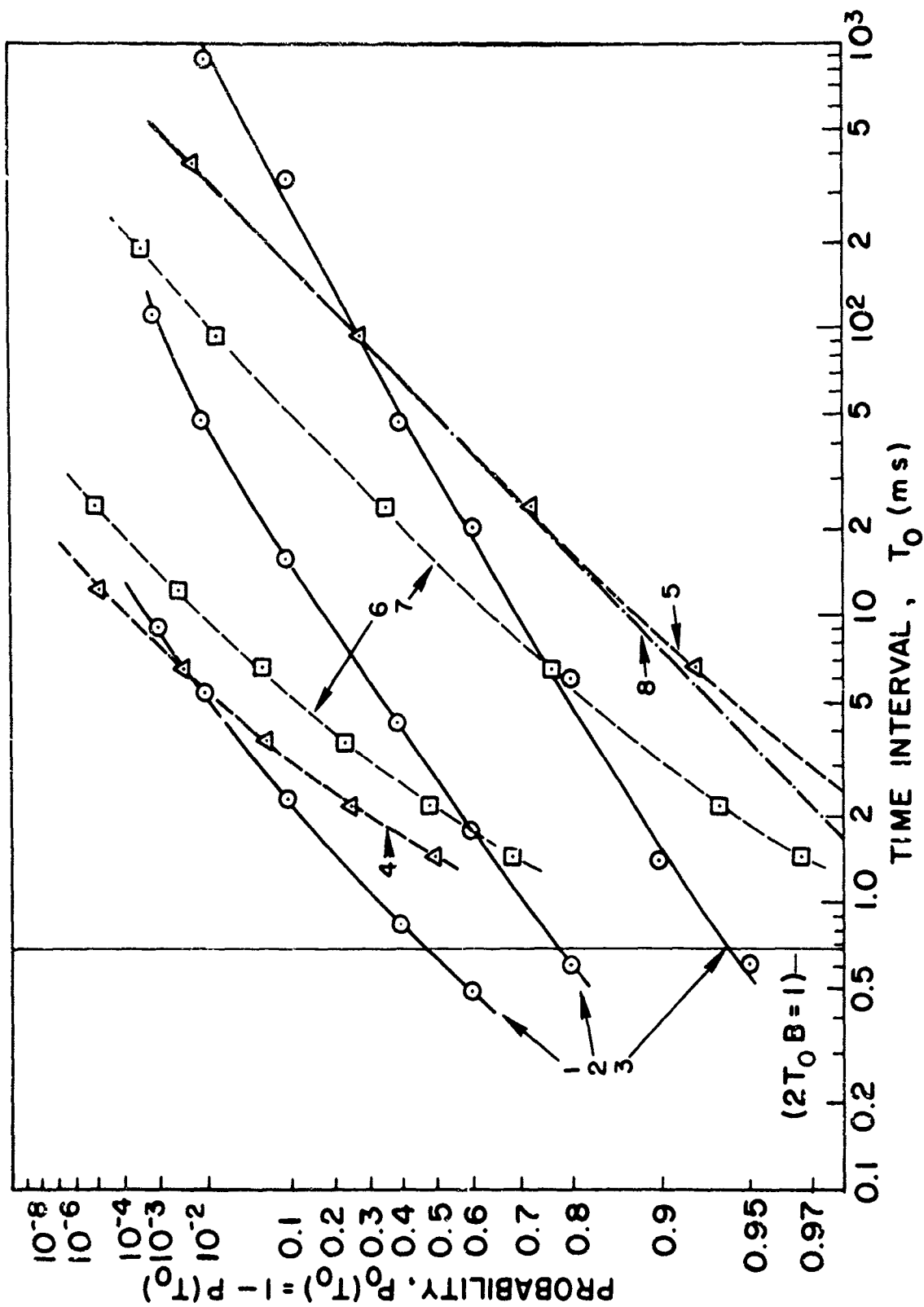


FIG. 17. PROBABILITY DISTRIBUTION OF THE TIME INTERVAL BETWEEN ENVELOPE LEVEL CROSSINGS: COMPARISON OF MODEL RESULTS WITH MEASURED VLF DATA.

$P_0(T_0)$  = Probability that time interval  $T_0$  between a down-crossing and the next up-crossing of a fixed level by the noise envelope exceeds abscissa value.

[Note: Vertical scale is  $\log|P_0(T_0)|$ .]

LEGEND:

Measured data (Watt and Maxwell [Ref. 9])  
Farfan, C.Z., Oct.-Nov., 1955  
Band center frequency,  $f_0 = 22$  kc  
Receiver 6-db bandwidth = 1350 cps

1 ———  
2 ———  
3 ———

$V_0 = 10 \mu\text{v/m}$   
 $V_0 = 100 \mu\text{v/m}$   
 $V_0 = 1000 \mu\text{v/m}$

Generalized "t" model (Independent-samples case)

$\theta = 3$

4 ———  
5 ———

$V_0 = \gamma$   
 $V_0 = 10 \gamma$

Generalized "t" model (Independent-samples case)

$q = 2$

6 ———  
7 ———

$V_0 = (10)^{1/2} \gamma$   
 $V_0 = (1000)^{1/2} \gamma$

8 ———

Exponentially distributed interval

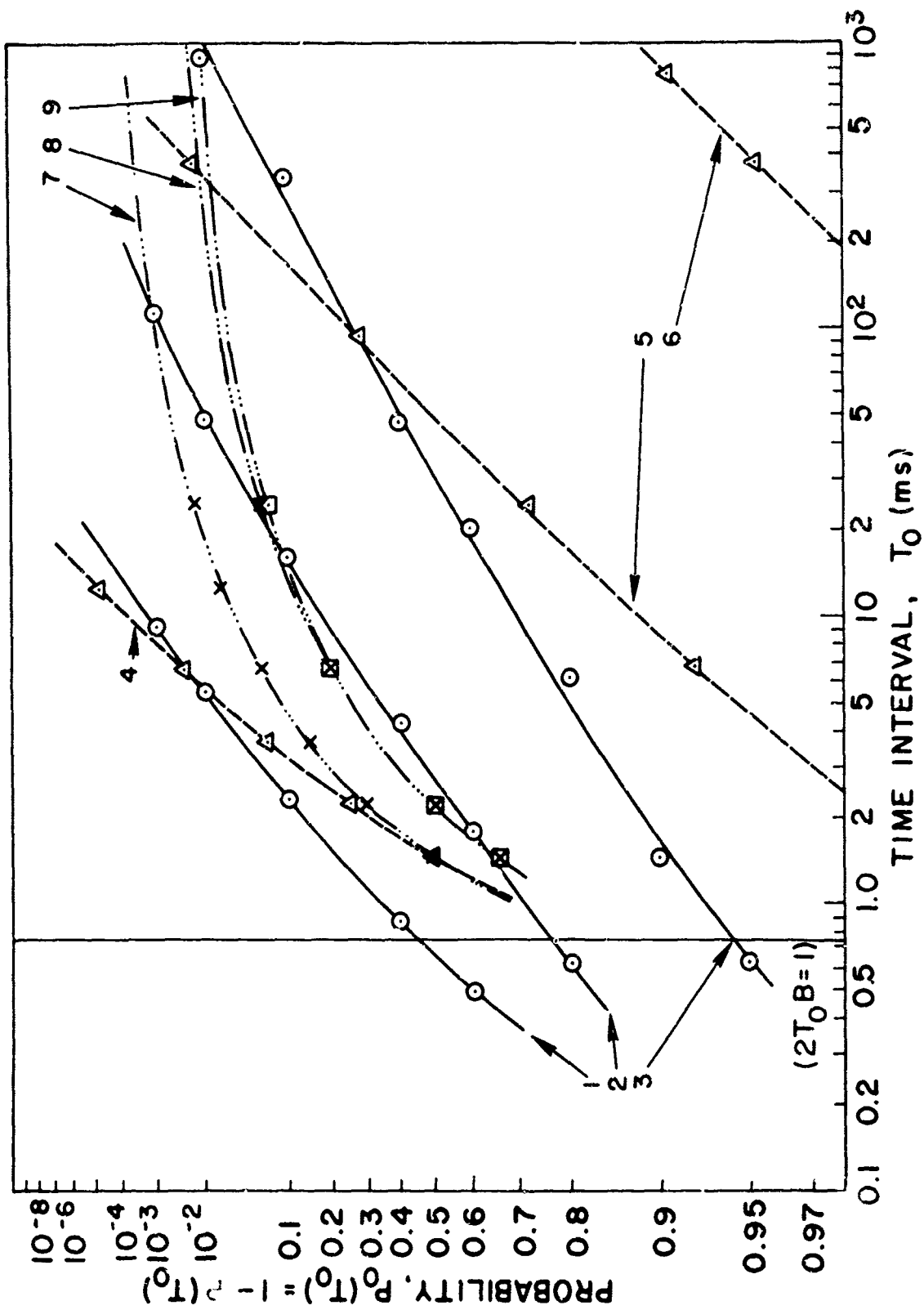


FIG. 18. PROBABILITY DISTRIBUTION OF THE TIME INTERVAL BETWEEN ENVELOPE LEVEL CROSSINGS: COMPARISON OF MODEL RESULTS WITH MEASURED VLF DATA.

$P_0(T_0)$  = Probability that time interval  $T_0$  between a down-crossing and the next up-crossing of a fixed level by the noise envelope exceeds abscissa value.

[Note: Vertical scale is  $\log | \log P_0(T_0) |$ .]

LEGEND:

Measured data (Watt and Maxwell [Ref. 9])

Farfan, C.Z., Oct.-Nov., 1955

Band center frequency,  $f_0 = 22$  kc

Receiver 6-db bandwidth = 1350 cps

$V_0 = 10 \mu\text{v/m}$

$V_0 = 100 \mu\text{v/m}$

$V_0 = 1000 \mu\text{v/m}$

Generalized "t" model (Independent-samples case)

$\theta = 3$

$V_0 = \gamma$

$V_0 = 10 \gamma$

$V_0 = 100 \gamma$

Generalized "t" model [Constant  $a(t)$  case]

$\theta = 3$

$V_0 = \gamma$

$V_0 = 10 \gamma$

$V_0 = 100 \gamma$

Now, in this constant  $a(t)$  case

$$\hat{P}_N(v_0) = \int_{v_0}^{\infty} dv_0 \int_0^{v_0} dv_1 \dots \int_0^{v_0} dv_N p_{\underline{V}}(\underline{v}), \quad (2.64)$$

where

$$p_{\underline{V}}(\underline{v}) \triangleq p_{v_0, \dots, v_N}(v_0, \dots, v_N) = p_{|a| E_0, \dots, |a| E_N}(v_0, \dots, v_N)$$

in which

$$\left\{ \begin{matrix} v(t_i) \\ E(t_i) \end{matrix} \right\} \triangleq \left\{ \begin{matrix} v_i \\ E_i \end{matrix} \right\}, \quad i=0, \dots, N.$$

Thus

$$p_{\underline{V}}(\underline{v}) = \int_0^{\infty} dx \frac{1}{x^{N+1}} p_{|a|}(x) p_{\underline{E}}\left(\frac{\underline{v}}{x}\right), \quad (2.65)$$

where

$$p_{\underline{E}}(\underline{E}) \triangleq p_{E_0, \dots, E_N}(E_0, \dots, E_N) = \prod_{i=0}^N \left[ \frac{E_i}{\sigma_1^2} \exp\left(-\frac{E_i^2}{2\sigma_1^2}\right) \right]$$

follows from Eq. (2.10), since  $E(t)$  is the envelope of  $n(t)$ , and where  $p_{|a|}(x)$  is given by Eq. (2.41). Evaluating Eq. (2.65) by making a change of variable so that Dwight, item 860.17, is appropriate:

$$p_{\underline{V}}(\underline{V}) = 2^{N+1} \frac{\Gamma\left(\frac{2N+m+2}{2}\right)}{\Gamma\left(\frac{m}{2}\right)} \gamma^m \frac{\prod_{i=0}^N (v_i)}{\left[\sum_{i=0}^N (v_i^2) + \gamma^2\right]^{(2N+m+2)/2}} \quad (2.66)$$

Substituting this result into Eq. (2.64),

$$\hat{P}_N(v_0) = 2^N \frac{\Gamma\left(\frac{2N+m+2}{2}\right)}{\Gamma\left(\frac{m}{2}\right)} \gamma^m \cdot \int_{v_0}^{\infty} v_0 \, dv_0 \int_0^{v_0} v_1 \, dv_1 \dots \int_0^{v_0} v_N \, dv_N \frac{1}{\left[\sum_{i=0}^N (v_i^2) + \gamma^2\right]^{(2N+m+2)/2}} \quad (2.67)$$

Now, Eq. (2.67) can be evaluated by recursively applying Dwight, item 201.9, which gives the result

$$\hat{P}_N(v_0) = 2^{N+1} \frac{\Gamma\left(\frac{2N+m+2}{2}\right)}{\Gamma\left(\frac{m}{2}\right)} \gamma^m \frac{1}{(2N+m)(2N+m-2)\dots(m)} \cdot \sum_{k=0}^N \frac{(-1)^k \binom{N}{k}}{\left[(k+1)v_0^2 + \gamma^2\right]^{m/2}} \quad (2.68)$$

where  $\binom{N}{k}$  is the binomial coefficient.

Finally, substituting Eq. (2.68) with the appropriate value for  $N$  into the numerator and denominator respectively of Eq. (2.55) gives the desired result

$$P_0(T_0) = 2^{N_0-1} \frac{\Gamma\left(\frac{2N_0 + m + 2}{2}\right)}{\Gamma\left(\frac{m+4}{2}\right)} \frac{(m+2)(m)}{(2N_0 + m)(2N_0 + m - 2) \dots (m)}$$

$$\frac{\sum_{k=0}^{N_0} \frac{(-1)^k \binom{N_0}{k}}{[(k+1)V_0^2 + \gamma^2]^{m/2}}}{\sum_{k=0}^1 \frac{(-1)^k}{[(k+1)V_0^2 + \gamma^2]^{m/2}}}, \quad (2.69)$$

where  $N_0 = 2T_0B$ . In the interesting special case  $\theta = 3$  ( $m = 2$ ), this gives

$$P_0(T_0) \Big|_{\theta=3} = \frac{\sum_{k=0}^{2T_0B} \frac{(-1)^k \binom{2T_0B}{k}}{k+1 + \left(\frac{\gamma}{V_0}\right)^2}}{\sum_{k=0}^1 \frac{(-1)^k}{k+1 + \left(\frac{\gamma}{V_0}\right)^2}}. \quad (2.70)$$

This result is plotted in Fig. 18 for various values of  $\gamma/V_0$ , along with results from the independent-samples case and experimental data taken from Watt and Maxwell. These plotted results indicate that the constant  $a(t)$  case is characterized by the fact that very short<sup>†</sup> and very long inter-level-crossing intervals occur with a higher probability at high levels

<sup>†</sup> This conclusion follows when we neglect  $T_0$  corresponding to  $2T_0B \lesssim 1$ , where the  $N_0 = 2T_0B$  assumption breaks down.

than is actually observed experimentally. This means that the constant  $a(t)$  case predicts more "clustering" of noise pulses than is consistent with measured data, as contrasted to the independent-samples case, which predicts less "clustering" than is actually observed. The usefulness of this result is that it indicates the versatility of the generalized "t" model, and it is conjectured that the observed distribution of inter-level-crossing intervals can be obtained with the generalized "t" model with the proper specification of the higher-order statistics of the modulating process  $a(t)$ . Although it will not be further considered here, it is suggested that a reasonable approach to this problem follows from considering the special case  $\theta = 2$  for which the generalized "t" model takes the form

$$y(t) = \frac{1}{b(t)} n(t) , \quad (2.71)$$

where  $n(t)$  is a zero-mean narrowband gaussian process with covariance function  $R_n(\tau)$ , and  $b(t)$  is a zero-mean, slowly varying gaussian process, independent of  $n(t)$ , with covariance function  $R_b(\tau)$ . Thus in this case the higher-order statistics of the modulating process are completely specified by the covariance function  $R_b(\tau)$ , so that investigation of the proper choice of these statistics appears to be analytically feasible.

#### D. SUMMARY AND CONCLUSIONS

The work in this chapter has been concerned with the development of an analytical model for "impulsive" phenomena and with verification of the applicability of this model as a description of received atmospheric noise. The generalized "t" model proposed here takes the received atmospheric noise  $y(t)$  to be given by

$$y(t) = a(t) n(t) , \quad (2.3)$$

where  $n(t)$  is a zero-mean, narrowband gaussian process with covariance function  $R_n(\tau)$ , and  $a(t)$  is a stationary slowly varying random process,

independent of  $n(t)$ , which modulates  $n(t)$ . This modulating process is further described as

$$a(t) = \frac{1}{b(t)}, \quad (2.72)$$

where the first-order statistics of  $b(t)$  are specified by the "two-sided" chi distribution with parameters  $m$  and  $\sigma$  given by Eq. (2.8).

The applicability of the generalized "t" model as a model for received atmospheric noise has been investigated in some detail in this chapter, and the pertinent results can be summarized as follows: The first-order statistics of the generalized "t" model are in good agreement with experimental results, with this agreement being particularly good at vlf and lf in those situations characterized by low-to-moderate local thunderstorm activity. This conclusion follows from results obtained in Section C1 and C2, where it is shown that:

1. The probability distribution of the envelope of the generalized "t" model is in good agreement with a large amount of measured data on received atmospheric noise. This is demonstrated in Figs. 4 to 13. It is noted that the agreement with measured data achieved by the generalized "t" model compares favorably with that achievable by either the filtered impulse or the empirical models discussed in Section A2.
2. The phase of the generalized "t" model is distributed uniformly in the interval  $[0, 2\pi]$  in agreement with intuition.
3. The average rate of crossings of a fixed level by the envelope of the generalized "t" model is in good agreement with the available measured data. This is demonstrated in Fig. 15, and means physically that the envelope of the generalized "t" model fluctuates at the same average rate as does the envelope of received atmospheric noise. It is noted that no calculation of this average rate of level crossings has been reported for any of the empirical models, although Nakai [Ref. 25] has obtained numerical results in agreement with the measured data, using a filtered-impulse model.

The higher-order statistics of the generalized "t" model can be specified to give good agreement with experimental results. This conclusion follows from the calculation in Section C3 of the probability distribution of the interval between successive crossings of a fixed level by the envelope of the model. This is demonstrated in Fig. 18, where the plotted data indicate that the higher-order statistics of the modulating process  $a(t)$

[it is to be noted that these statistics are not yet specified in Eq. (2.72) above] can be specified to produce the observed dependence between adjacent level crossings. Physically this means that the generalized "t" model can be specified to imitate the tendency of received atmospheric noise to consist of clusters of noise pulses. This is an advantage of the generalized "t" model over any of the empirical models or any of the filtered-impulse models which assume the noise pulses to occur in a Poisson fashion.

Finally, it is concluded that the generalized "t" model is an appropriate model for received atmospheric noise that may be useful in the study of signal detection and estimation problems in the presence of additive atmospheric noise. This will be demonstrated in Chapter III, where the detection problem is examined in detail.

### III. APPLICATION OF THE GENERALIZED "t" MODEL

#### A. INTRODUCTION

In Chapter II a new model for impulsive phenomena was developed and was demonstrated to be applicable to the representation of received atmospheric noise. The work in this chapter is concerned with the application of this model to the signal detection problem in the presence of additive atmospheric noise. Thus, the communication channel to be considered here is the additive-noise channel shown in Fig. 19, where  $m(t)$  is the transmitted signal,  $y(t)$  is the additive atmospheric noise, and  $x(t)$  is the received sum of signal plus noise. Now, the goal of the analysis is the determination of the receiver form which detects the transmitted signal in the presence of additive atmospheric noise in an optimal manner with respect to a performance criterion to be specified. Thus, while the additive noise  $y(t)$  is given by the generalized "t" model, completion of the statement of the statistical detection problem requires specification of both the character of the transmitted signal and the performance criterion to be used.

#### 1. Summary of Known Results

Before proceeding with this specification, however, a brief summary of known results on the detection problem in the presence of additive atmospheric noise is presented. To the author's knowledge, no analytical result specifying an optimal receiver form for use in the presence of additive

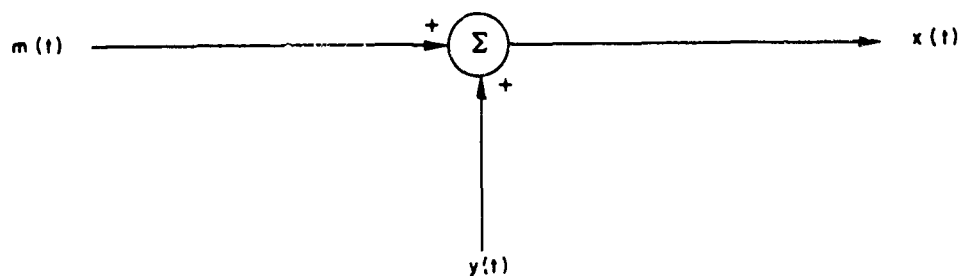


FIG. 19. DESCRIPTION OF ADDITIVE-ATMOSPHERIC-NOISE COMMUNICATION CHANNEL.

atmospheric noise is available in the literature. Rather, the receiving techniques that have been proposed stem from observation of the distinctive impulsive nature of the noise and can be conveniently classified in two categories:

1. Linear receivers. At least two linear receiving techniques have been proposed [Refs. 17, 32] for use in the presence of atmospheric noise. One of these is the "smear-desmear" technique proposed by several workers and discussed by Lerner [Ref. 17]. This technique consists of linearly smearing the received noise pulses in time, so that the smeared noise can be modeled as a gaussian process. Having done this, the optimal receiver in the presence of the smeared noise is just the well-known matched-filter receiver which must, of course, be matched to the smeared signal. It is clear that this technique is suboptimal in the presence of atmospheric noise. This can be seen quantitatively by comparing the error curve resulting from its use with the optimal error curve, if known. In fact, for the known signal situation considered in this chapter, it will be seen that use of the smear-desmear technique corresponds to a loss of 12-15 db in input SNR.
2. Nonlinear receivers. Most proposed techniques [Refs. 17, 33, 34], and in fact the techniques generally used in practice, employ nonlinear processing of the received signal. The purpose of this nonlinear processing is to reduce the effects of noise pulses on the receiver decision by amplifying the received signal nonlinearly prior to the performance of any linear filtering. (This of course refers to matched filtering, and not to the bandpass filtering discussed in Section IIB, which is required in practice in the front end of the receiver to suppress adjacent channel interference.) It will be shown that this procedure is supported by the "logarithmic-correlator" receiver shown to be optimum in the known signal situation analyzed in this chapter. It is noted that the log-correlator receiver is compared in detail with specific nonlinear receivers used in practice in Chapter IV.

Although no analytical determination of optimal receiver forms is available in the literature, there are several analytical results of interest on the performance of specific receiving techniques. Several workers [Refs. 35, 36, 37, 38] have computed the probability of error resulting from the use of a matched filter receiver in the presence of additive atmospheric noise. Bello [Ref. 37] and Conda [Ref. 38] have, in addition, included the effects of fading on these error curves. It will be seen in Section D4 below that the results obtained by these investigators in the absence of fading, using various models for the atmospheric noise, are in good agreement with the results obtained using the generalized "t" model. These results lead to the conclusion that the matched filter is a poor receiver choice in the

presence of additive atmospheric noise. Finally, we note the work of Bowen [Ref. 7] who uses an SNR criterion to investigate the use of hard limiting in the presence of atmospheric noise. He shows that the use of a hard limiter followed by a zonal filter produces a much greater improvement in the ratio of output SNR to input SNR when the additive noise is impulsive, than is obtained when the additive noise is a gaussian process. This result supports the use of nonlinear processing of the received signal as mentioned above.

With this brief summary of available results in mind, the specification of the detection problem to be considered here will now be completed. There are, of course, several possible specifications of the transmitted signal of practical importance. Consideration will be focused here on the simple hypothesis-testing situation, wherein the transmitted signal is one or the other of two a priori equally probable known signals. This situation is described in Fig. 20, where  $m^{(1)}(t)$  and  $m^{(2)}(t)$  are known signals described by

$$\begin{aligned} m^{(1)}(t) &= m(t), & 0 \leq t \leq T, \\ m^{(2)}(t) &= 0, \end{aligned} \quad (3.1)$$

with

$$\int_0^T m^2(t) dt = E$$

and where  $y(t)$  is the additive atmospheric noise described by the generalized "t" model. The performance criterion to be used here is the probability-of-error criterion, so that the statistical detection problem at the receiver becomes that of choosing between the a priori equally probable hypotheses

$$\left. \begin{aligned} h^{(1)}: & x(t) = m(t) + y(t) \\ h^{(2)}: & x(t) = y(t) \end{aligned} \right\}, \quad 0 \leq t \leq T \quad (3.2)$$

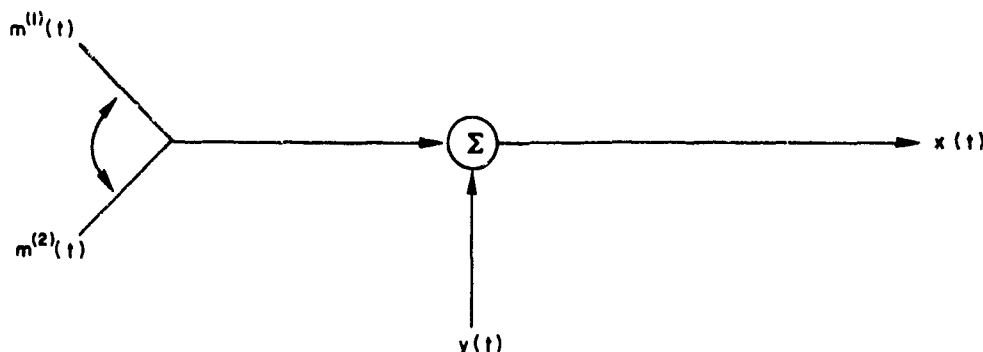


FIG. 20. DESCRIPTION OF "KNOWN"-SIGNALS DETECTION PROBLEM.  
 $m^{(1)}(t)$  and  $m^{(2)}(t)$  are equally probable, a priori.

with the smallest probability of error. Now, it is well known [Refs. 5, 39, 40, 41] that the decision rule which minimizes the probability of error in this situation is the Bayes rule given by

Choose  $h^{(1)}$  iff

$$L[x(t)] \triangleq \frac{w[x(t)|h^{(1)}]}{w[x(t)|h^{(2)}]} \geq 1, \quad (3.3)$$

where  $w[x(t)|h^{(i)}]$ ,  $i=1, 2$ , is the probability density of  $x(t)$ ,  $0 \leq t \leq T$ , under hypothesis (i), and where  $L[x(t)]$  is the likelihood ratio. Thus the solution of the detection problem requires the calculation of  $w[x(t)|h^{(i)}]$ ,  $i=1, 2$ , which will be done here by expressing  $x(t)$ ,  $0 \leq t \leq T$ , in vector notation with respect to a suitable set of orthonormal basis functions. In order to express  $x(t)$  in this manner, however, it is necessary to specify the temporal behavior of the additive atmospheric noise; i.e., it is necessary to specify the higher-order statistics of the generalized "t" model.

It is recalled that the generalized "t" model takes the received atmospheric noise to be given by

$$y(t) = a(t) n(t) , \quad (2.3)$$

where  $n(t)$  is a zero-mean narrowband gaussian process with covariance  $R_n(\tau)$ , and  $a(t)$  is a stationary slowly varying random process, independent of  $n(t)$ , whose first-order statistics are given by Eq. (2.72). Thus, as in Section IIC3, it is convenient to distinguish two cases, depending on the temporal behavior of the modulating process  $a(t)$ .

**B. CASE I: SHORT-DURATION SIGNALS,  $a(t) = a$ ,  $0 \leq t \leq T$**

This case is similar to the constant  $a(t)$  case considered in Section IIC3, in that it assumes the slowly varying modulating process  $a(t)$  to remain constant for the signal duration  $T$ . Physically, this corresponds to the situation in which the signal duration is sufficiently short that, with high probability, the modulating process  $a(t)$  can be assumed constant in the signaling interval. (The practical applicability of this assumption will be discussed further in Section B5.) In this case the decision problem reduces to choosing between the two hypotheses

$$\left. \begin{array}{l} h^{(1)}: x(t) = m(t) + a n(t) \\ h^{(2)}: x(t) = a n(t) \end{array} \right\} , \quad 0 \leq t \leq T . \quad (3.4)$$

An often-used procedure for developing the desired vector formulation, which is applicable to this problem, is to expand the gaussian process  $n(t)$  in terms of a Karhunen-Loève expansion. Assuming that  $R_n(\tau)$  is continuous in  $\tau$ , it is possible to write [Refs. 30, 41]

$$n(t) = \text{l.i.m.}_{N \rightarrow \infty} \sum_{i=1}^N n_i \phi_i(t) , \quad 0 \leq t \leq T , \quad (3.5)$$

where l.i.m. denotes "limit in the mean,"

$$n_i = \int_0^T n(t) \phi_i(t) dt , \quad (3.6)$$

and the  $\varphi_i(t)$  are the eigenfunctions of  $R_n(t,s)$ , i.e., they are the solutions to

$$\int_0^T R_n(t,s) \varphi_i(s) ds = \lambda_i \varphi_i(t), \quad 0 \leq t \leq T. \quad (3.7)$$

This expansion has the desirable properties:

1. The  $\varphi_i(t)$  are orthogonal, i.e., they can be normalized to satisfy

$$\int_0^T \varphi_i(t) \varphi_j(t) dt = \delta_{ij}, \quad (3.8)$$

where  $\delta_{ij}$  is the Kronecker delta.

2. The  $n_i$  are uncorrelated, i.e.,

$$E[n_i n_j] = \lambda_i \delta_{ij}. \quad (3.9)$$

If  $R_n(t,s)$  is strictly positive definite,<sup>†</sup> the  $\varphi_i(t)$ ,  $i=1, \dots, \infty$ , will span  $L_2(T)$  the (Hilbert) space of square integrable functions on  $[0,T]$ . Then the signal  $m(t)$  can be expressed in terms of the  $\varphi_i(t)$  as

$$m(t) = \text{l.i.m.}_{N \rightarrow \infty} \sum_{i=1}^N m_i \varphi_i(t), \quad 0 \leq t \leq T, \quad (3.10)$$

<sup>†</sup>If  $R_n(t,s)$  is not strictly positive definite, it suffices to assume that  $m(t)$  lies in the space spanned by the eigenfunctions of  $R_n(t,s)$ . If this is not true, error-free detection can obviously be obtained.

where

$$m_1 = \int_0^T m(t) p_1(t) dt . \quad (3.11)$$

Having expressed  $n(t)$  and  $m(t)$  in terms of the orthonormal functions  $\phi_i(t)$ ,  $i=1, \dots, N$ , in Eqs. (3.5) and (3.10), the problem can now be formulated in vector notation as follows:

$$\begin{aligned} h^{(1)}: \underline{x} &= \underline{m} + a \underline{n} , \\ h^{(2)}: \underline{x} &= a \underline{n} , \end{aligned} \quad (3.12)$$

where, for example,  $\underline{n}_t = n_1, \dots, n_N$  is an element of Euclidean  $N$ -space  $E_N$ . It is noted that this formulation is written in terms of  $N$  dimensions, so that  $N \rightarrow \infty$  will be taken at the conclusion of the problem. For a rigorous justification of this procedure, see Grenander [Ref. 42].

#### i. Calculation of the Likelihood Ratio

One can write

$$w(\underline{x} | h^{(1)}) = \int_{-\infty}^{\infty} w(\underline{x} | h^{(1)}, b) p_b(b) db , \quad (3.13)$$

where  $p_b(b)$  is given by Eq. (2.7), and where Eq. (3.12) plus the fact that  $a(t) \triangleq 1/b(t)$  gives

$$w(\underline{x} | h^{(1)}, b) = |b|^N p_{\underline{n}}[b(\underline{x} - \underline{m})] , \quad (3.14)$$

---

$\underline{n}_t^{\dagger}$  denotes the transpose of the column vector  $\underline{n}$ .

where

$$p_{\underline{n}}(\underline{n}) = \frac{1}{(2\pi)^{N/2} |\Lambda|^{1/2}} \exp \left[ -\frac{1}{2} \underline{n}_t \Lambda^{-1} \underline{n} \right], \quad (3.15)$$

with

$$\Lambda = \left\{ \lambda_i \delta_{ij} \right\}.$$

Therefore

$$w(\underline{x}|h^{(1)}, b) = \frac{|b|^N}{(2\pi)^{N/2} |\Lambda|^{1/2}} \exp \left[ -\frac{1}{2} b^2 (\underline{x} - \underline{m})_t \Lambda^{-1} (\underline{x} - \underline{m}) \right]; \quad (3.16)$$

so that, substituting into Eq. (3.13),

$$w(\underline{x}|h^{(1)}) = \int_{-\infty}^{\infty} \frac{\left(\frac{m}{2}\right)^{m/2} |b|^{m+N-1}}{(2\pi)^{N/2} \sigma^m \Gamma\left(\frac{m}{2}\right) |\Lambda|^{1/2}} \cdot \exp \left[ -\frac{1}{2} \left( \|\underline{x} - \underline{m}\|_{\Lambda^{-1}}^2 + \frac{m}{\sigma^2} \right) b^2 \right] db, \quad (3.17)$$

where  $\|\underline{x} - \underline{m}\|_{\Lambda^{-1}}^2 \triangleq (\underline{x} - \underline{m})_t \Lambda^{-1} (\underline{x} - \underline{m})$ . This integral can be evaluated using Dwight, item 860.17, which gives

$$w(\underline{x}|h^{(1)}) = \frac{\Gamma\left(\frac{m+N}{2}\right)}{\Gamma\left(\frac{m}{2}\right)} \frac{\left(\frac{m}{\sigma^2}\right)^{m/2}}{\pi^{N/2} |\Lambda|^{1/2}} \frac{1}{\left[ \|\underline{x} - \underline{m}\|_{\Lambda^{-1}}^2 + \frac{m}{\sigma^2} \right]^{(m+N)/2}}, \quad m > 0. \quad (3.18)$$

Similarly,

$$w(\underline{x}|h^{(2)}) = \frac{\Gamma\left(\frac{m+N}{2}\right)}{\Gamma\left(\frac{m}{2}\right)} \frac{\left(\frac{m}{\sigma^2}\right)^{m/2}}{\pi^{N/2} |\Lambda|^{1/2}} \frac{1}{\left[\|\underline{x}\|_{\Lambda^{-1}}^2 + \frac{m}{\sigma^2}\right]^{(m+N)/2}}, \quad m > 0. \quad (3.19)$$

Now, substituting Eqs. (3.18) and (3.19) into the vector formulation of Eq. (3.3), there results

$$L(\underline{x}) = \frac{\left[\|\underline{x}\|_{\Lambda^{-1}}^2 + \frac{m}{\sigma^2}\right]^{(m+N)/2}}{\left[\|\underline{x}-\underline{m}\|_{\Lambda^{-1}}^2 + \frac{m}{\sigma^2}\right]^{(m+N)/2}}. \quad (3.20)$$

Thus, the optimal decision rule is given by:

Choose  $h^{(1)}$  iff

$$\|\underline{x}\|_{\Lambda^{-1}}^2 + \frac{m}{\sigma^2} \geq \|\underline{x}-\underline{m}\|_{\Lambda^{-1}}^2 + \frac{m}{\sigma^2}, \quad (3.21)$$

which reduces to the familiar rule for the detection of known signals in additive gaussian noise:

Choose  $h^{(1)}$  iff

$$\langle \underline{x}, \underline{m} \rangle_{\Lambda^{-1}} \geq \frac{1}{2} \|\underline{m}\|_{\Lambda^{-1}}^2, \quad (3.22)$$

where

$$\langle \underline{x}, \underline{m} \rangle_{\Lambda^{-1}} \triangleq \underline{x}_t \Lambda^{-1} \underline{m}.$$

Now, letting  $N \rightarrow \infty$ , it is seen that in terms of the time functions available to the receiver, rule Eq. (3.22) goes over into

Choose  $h^{(1)}$  iff

$$\int_0^T x(t) c(t) dt \geq \frac{1}{2} \int_0^T m(t) c(t) dt, \quad (3.23)$$

where  $c(t)$  is the solution to the Fredholm integral equation

$$\int_0^T R_n(t,s) c(s) ds = m(t), \quad 0 \leq t \leq T. \quad (3.24)$$

## 2. Discussion of the Optimal Receiver Rule

It is seen from Eq. (3.23) that the receiver that minimizes the probability of error for the additive generalized "t" noise channel in the case where  $a(t) = a$  is constant for the duration of the signal is the well-known correlator or matched-filter receiver. Before proceeding to the calculation of the probability of error resulting from the use of this optimal receiver, there are several points of interest to note. First, the decision rule is independent of the parameters  $m$  and  $\sigma$  of the generalized "t" model; i.e., the same receiver is applicable in the presence of additive generalized "t" noise regardless of the value of the parameter  $\theta > 1$ . (It will be shown in Section B3 that similar statements are also true for additive modified generalized "t" noise.) Also, it is worthwhile to note that the receiver rule Eq. (3.23) could have been deduced directly by inspection of  $p_y(y)$ , the probability density of the additive noise vector. This deduction proceeds as follows: Noting that  $w(\underline{x}|h^{(2)})$  given by Eq. (3.19) is just  $p_y(\underline{x})$ , there results

$$p_y(y) = \frac{\Gamma\left(\frac{m+N}{2}\right)}{\Gamma\left(\frac{m}{2}\right)} \frac{\left(\frac{m}{2}\right)^{m/2}}{\pi^{N/2} |\Lambda|^{1/2}} \frac{1}{\left[\|\underline{y}\|_{\Lambda^{-1}}^2 + \frac{m}{2}\right]^{(m+N)/2}}, \quad m > 0 \quad (3.25)$$

where  $\underline{y}_t = \underline{y}_1, \dots, \underline{y}_N$ . However, assuming  $R_n(t,s)$  to be strictly positive definite, there exists a nonsingular "whitening" transformation  $W$  such that

$$p_{\underline{y}_w}(\underline{y}_w) = \frac{\Gamma\left(\frac{m+N}{2}\right)}{\Gamma\left(\frac{m}{2}\right)} \frac{\left(\frac{m}{2}\right)^{m/2}}{\pi^{N/2}} \frac{1}{\left[\|\underline{y}_w\|^2 + \frac{m}{2}\right]^{(m+N)/2}}, \quad m > 0, \quad (3.26)$$

where  $\underline{y}_w = W\underline{y}$ . In fact, in this case it is easily seen that

$$W = \left\{ (\lambda_i)^{-1/2} \delta_{ij} \right\}. \quad (3.27)$$

Now, in terms of the whitened noise vector  $\underline{y}_w$ , the detection problem becomes that of choosing between the a priori equally probable hypotheses

$$\begin{aligned} h^{(1)}: \underline{x}_w &= \underline{m}_w + \underline{y}_w, \\ h^{(2)}: \underline{x}_w &= \underline{y}_w. \end{aligned} \quad (3.28)$$

It can easily be shown that the correlator receiver given by Eq. (3.23) is indeed the optimal receiver in this case, and in fact this result can be generalized as specified in the following well-known proposition:

**Proposition 3.1.** Given an additive noise channel where the two hypotheses can be written in the form of Eq. (3.28), and given that the probability density function of the additive noise can be written as a monotonically decreasing function of the norm of the noise vector, then the receiver that minimizes the probability of error is a correlator receiver.

Proof of Proposition 3.1.

The proof of this proposition is so short that it will be given here. The likelihood ratio is given by

$$L(\underline{x}_w) = \frac{w(\underline{x}_w | h^{(1)})}{w(\underline{x}_w | h^{(2)})} = \frac{p_{\underline{y}_w}(\underline{x}_w - \underline{m}_w)}{p_{\underline{y}_w}(\underline{x}_w)} = \frac{f(\|\underline{x}_w - \underline{m}_w\|)}{f(\|\underline{x}_w\|)}, \quad (3.29)$$

where  $f(\|\underline{x}\|)$  is a monotonically decreasing function of  $\|\underline{x}\|$ . Therefore, from Eq. (3.3), the optimal decision rule is given by:

Choose  $h^{(1)}$  iff

$$f(\|\underline{x}_w - \underline{m}_w\|) \geq f(\|\underline{x}_w\|); \quad (3.30)$$

$\Leftrightarrow$  Choose  $h^{(1)}$  iff

$$\|\underline{x}_w - \underline{m}_w\| \leq \|\underline{x}_w\|, \quad (3.31)$$

since  $f(\|\underline{x}\|)$  is a monotonically decreasing function of  $\|\underline{x}\|$ .

$\Leftrightarrow$  Choose  $h^{(1)}$  iff

$$\langle \underline{x}_w, \underline{m}_w \rangle \geq \frac{1}{2} \|\underline{m}_w\|^2. \quad (3.32)$$

This completes the Proof of Proposition 3.1.

3. Case I<sub>m</sub>: Modified Generalized "t" Noise

As an application of Proposition 3.1, the results of Case I will now be extended to the case of additive modified generalized "t" noise. In this situation the additive noise is given in the vector notation of Eq. (3.12) by

$$\underline{y} = \underline{a} \underline{n}, \quad (3.33)$$

where  $p_{\underline{n}}(\underline{n})$  is given by Eq. (3.15) and  $p_a(a)$  is given by Eq. (2.32).  
Thus

$$\begin{aligned}
 p_{\underline{y}}(\underline{y}) &= \int_{-\infty}^{\infty} \frac{1}{|x|^N} p_a(x) p_{\underline{n}}\left(\frac{\underline{y}}{x}\right) dx \\
 &= \int_{1/\beta^2}^{\infty} \frac{K}{(2\pi)^{N/2} |\Lambda|^{1/2}} \tau^{(m+N-2)/2} \exp\left[-\frac{1}{2}\left(\|\underline{y}\|_{\Lambda^{-1}}^2 + \frac{m}{2}\right)\tau\right] d\tau,
 \end{aligned}
 \tag{3.34}$$

where it is recalled that  $K$  is a constant chosen to satisfy

$$\int_{-\beta}^{\beta} p_a(a) da = 1.
 \tag{2.32}$$

For  $m+N-2 \geq 0$  and even, the integral in Eq. (3.34) can be evaluated using Dwight, item 860.17, which gives

$$\begin{aligned}
 p_{\underline{y}}(\underline{y}) &= \frac{K}{(2\pi)^{N/2} |\Lambda|^{1/2}} \exp\left[-\frac{1}{2\beta^2} f\left(\|\underline{y}\|_{\Lambda^{-1}}^2\right)\right] \\
 &\cdot \left\{ \frac{2}{\beta^{m+N-2} f\left(\|\underline{y}\|_{\Lambda^{-1}}^2\right)} + \frac{4 \frac{(m+N-2)}{2}}{\beta^{m+N-4} f^2\left(\|\underline{y}\|_{\Lambda^{-1}}^2\right)} + \dots \right. \\
 &\left. + \frac{2^{(m+N-2)/2} \frac{(m+N-2)!}{2}}{\beta^2 \left[f\left(\|\underline{y}\|_{\Lambda^{-1}}^2\right)\right]^{(m+N-2)/2}} + \frac{2^{(m+N)/2} \frac{(m+N-2)!}{2}}{\left[f\left(\|\underline{y}\|_{\Lambda^{-1}}^2\right)\right]^{(m+N)/2}} \right\},
 \end{aligned}
 \tag{3.35}$$

where

$$f\left(\|y\|_{\Lambda}^2\right) \triangleq \left(\|y\|_{\Lambda}^2 + \frac{m}{2}\right). \quad (3.36)$$

For  $m+N-2 > 0$  and odd, Eq. (3.34) is evaluated in Appendix A, where it is shown that

$$p_y(y) = \frac{K}{(2\pi)^{N/2} |\Lambda|^{1/2}} \left\{ \exp\left(-\frac{1}{2\beta^2} f\left(\|y\|_{\Lambda}^2\right)\right) \right. \\ \cdot \left[ \frac{2}{\beta^{m+N-2} f\left(\|y\|_{\Lambda}^2\right)} + \frac{4}{\beta^{m+N-4} f^2\left(\|y\|_{\Lambda}^2\right)} + \dots \right. \\ \left. + \frac{2^{(m+N-3)/2} \frac{(m+N-2)}{2} \frac{(m+N-4)}{2} \dots \left(\frac{5}{2}\right)(1)}{\beta^3 \left[f\left(\|y\|_{\Lambda}^2\right)\right]^{(m+N-3)/2}} \right. \\ \left. + \frac{2^{(m+N-1)/2} \frac{(m+N-2)}{2} \frac{(m+N-4)}{2} \dots \left(\frac{3}{2}\right)(1)}{\left[f\left(\|y\|_{\Lambda}^2\right)\right]^{(m+N-1)/2}} \right. \\ \left. \cdot \left[ \frac{1}{\beta} \exp\left(-\frac{1}{2\beta^2} f\left(\|y\|_{\Lambda}^2\right)\right) + \left(\frac{2\pi}{f\left(\|y\|_{\Lambda}^2\right)}\right)^{1/2} \operatorname{erfc}\left(\frac{f^{1/2}\left(\|y\|_{\Lambda}^2\right)}{\beta}\right) \right] \right\}. \quad (3.37)$$

Now, assuming that  $R_n(t,s)$  is strictly positive definite, the whitening transformation  $W$  given by Eq. (3.27) can be applied to the modified generalized "t" noise vector  $y$  to produce the whitened noise vector

$y_w = Wy$ . Furthermore, inspection of  $p_y(y)$  given by Eq. (3.35) or Eq. (3.37) shows that the probability density  $p_{y_w}(y_w)$  of the whitened noise vector will be a monotonically decreasing function of  $\|y_w\|$ . Thus, applying Proposition 3.1, the receiver that minimizes the probability of error in the presence of Case I<sub>m</sub> modified generalized "t" noise is a correlator receiver. In fact, inspection of the proof of Proposition 3.1 shows that this optimal receiver is the same correlator receiver, specified by Eq. (3.23), that is optimal in the presence of Case I generalized "t" noise.

#### 4. Calculation of the Probability of Error for Case I and Case I<sub>m</sub>

As given by Eq. (3.22), the receiver that minimizes the probability of error in Case I (and also in Case I<sub>m</sub>) is the one that implements the rule

Choose  $h^{(1)}$  iff

$$\langle x, m \rangle_{\Lambda^{-1}} \geq \frac{1}{2} \|m\|_{\Lambda^{-1}}^2. \quad (3.22)$$

Since the hypotheses are a priori equally probable, the probability of error  $P_e$  is given by

$$\begin{aligned} P_e &= \Pr \left\{ \langle x, m \rangle_{\Lambda^{-1}} \geq \frac{1}{2} \|m\|_{\Lambda^{-1}}^2 \mid h^{(2)} \text{ is true} \right\} \\ &= \Pr \left\{ \langle y, m \rangle_{\Lambda^{-1}} \geq \frac{1}{2} \|m\|_{\Lambda^{-1}}^2 \right\}. \end{aligned} \quad (3.38)$$

However, this expression is identical to

$$P_e = \Pr \left\{ \langle y_w, m_w \rangle \geq \frac{1}{2} \|m_w\|^2 \right\}, \quad (3.39)$$

where  $y_w = Wy$  and  $m_w = Wm$ , since as mentioned above, the nonsingular transformation  $W$  is known to exist when  $R_n(t,s)$  is strictly positive

definite, and in fact is given by Eq. (3.27). Now, it is seen from Eqs. (3.36), (3.35), and (3.37) that  $p_{\underline{y}_w}(\underline{y}_w)$  for both generalized "t" noise and modified generalized "t" noise is a function only of the length of the noise vector; i.e.,

$$p_{\underline{y}_w}(\underline{y}_w) = f(\|\underline{y}_w\|^2). \quad (2.40)$$

Thus, because of the spherical symmetry of this probability distribution, it follows, as shown geometrically in Fig. 21, that the calculation of  $P_e$  reduces to the one-dimensional calculation independent of direction:

$$P_e = \Pr\left\{\underline{y}_w \cdot \underline{m}_w \geq \frac{1}{2}\|\underline{m}_w\|^2\right\}. \quad (3.41)$$

That is, the spherical symmetry of  $p_{\underline{y}_w}(\underline{y}_w)$  means that the probability that the component of the noise vector in the direction of  $\underline{m}_w$  is greater than or equal to  $(1/2)\|\underline{m}_w\|^2$  is independent of the direction of  $\underline{m}_w$ .

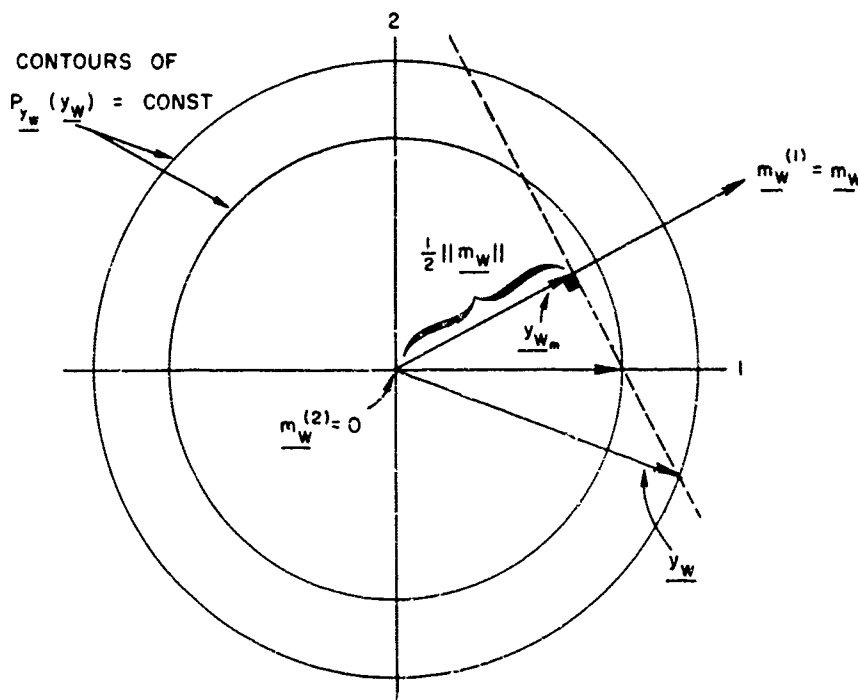


FIG. 21. GEOMETRICAL PICTURE OF SPHERICAL SYMMETRY OF THE PROBABILITY DISTRIBUTION OF THE CASE 1 ADDITIVE-NOISE VECTOR.

### 5. Generalized "t" Noise

Applying the above results to the case of generalized "t" noise, it is found by setting  $N = 1$  in  $p_{y_w}(y_w)$  given by Eq. (3.26) that

$$p_{y_w m}(x) = \frac{\Gamma(\frac{\theta}{2})}{\Gamma(\frac{\theta-1}{2})} \frac{\gamma_w^{\theta-1}}{\pi^{1/2}} \frac{1}{[x^2 + \gamma_w^2]^{\theta/2}}, \quad -\infty < x < \infty, \quad (3.42)$$

where  $\theta \triangleq m + 1 > 1$  and  $\gamma_w \triangleq m^{1/2} 1/\sigma$ . Thus, using this probability density to evaluate Eq. (3.41), there results:

$$P_e = \int_{\frac{1}{2}\|m_w\|}^{\infty} \frac{\Gamma(\frac{\theta}{2})}{\Gamma(\frac{\theta-1}{2})} \frac{\gamma_w^{\theta-1}}{\pi^{1/2}} \frac{1}{[x^2 + \gamma_w^2]^{\theta/2}} dx. \quad (3.43)$$

Now, it is necessary to specify  $\theta$  in order to evaluate this integral in closed form. Initially, consider the important case  $\theta = 3$  (see Section IIC1) which gives

$$P_e \Big|_{\theta=3} = \frac{1}{2} \left\{ 1 - \left[ 1 + 4(\gamma_w / \|m_w\|)^2 \right]^{-1/2} \right\}. \quad (3.44)$$

In order to evaluate the significance of this result, it is convenient to consider two subcases of interest, corresponding to high and low average SNR:

a. High SNR; i.e.,  $\|m_w\| \gg \gamma_w$

In this case there is found the asymptotic result

$$\lim_{\frac{\|m_w\|}{\gamma_w} \rightarrow \infty} P_e \Big|_{\theta=3} = \left[ \frac{\gamma_w}{\|m_w\|} \right]^2. \quad (3.45)$$

b. Low SNR; i.e.,  $\|\underline{m}_w\| \ll \gamma_w$

In this case there is found the asymptotic result

$$\lim_{\frac{\|\underline{m}_w\|}{\gamma_w} \rightarrow 0} P_{e_{\theta=3}} = \frac{1}{2} \left[ 1 - \frac{1}{2} \frac{\|\underline{m}_w\|}{\gamma_w} \right]$$

$$= \lim_{\frac{\|\underline{m}_w\|}{\gamma_w} \rightarrow 0} \text{erfc} \left( \sqrt{\frac{\pi}{8}} \frac{\|\underline{m}_w\|}{\gamma_w} \right) \quad \dagger \quad (3.46)$$

Discussion of these results for the generalized "t" model will be postponed until the associated results for the modified generalized "t" model have been determined. Plots of  $P_e$  vs  $\|\underline{m}_w\|/\gamma_w$  are presented in Fig. 22 for both the generalized "t" and modified generalized "t" models. These error curves are presented to show the effects of various types of noise on the optimal performance achievable using "short duration" signals. For purposes of comparison, the gaussian noise curve is also presented for a noise whose average power is equal to that typically measured in atmospheric noise situations where the generalized "t" model with parameters  $\theta = 3$  and  $\gamma_w$  is appropriate.<sup>‡</sup>

†

$$\text{erfc}(x) = \int_x^\infty \frac{1}{(2\pi)^{1/2}} \exp\left(-\frac{\tau^2}{2}\right) d\tau ;$$

denotes the area under the tail of the normal probability density with zero mean and unity variance.

<sup>‡</sup>This normalization is accomplished by using the fact that for the generalized "t" model

$$E[V] \Big|_{\theta=3} = \frac{\pi}{2} \gamma_w , \quad (2.28)$$

together with the empirical result at temperate latitudes that, typically at vlf and lf,  $V_{\text{rms}}/V_{\text{avg}} \approx 3$  [Refs. 9, 10].

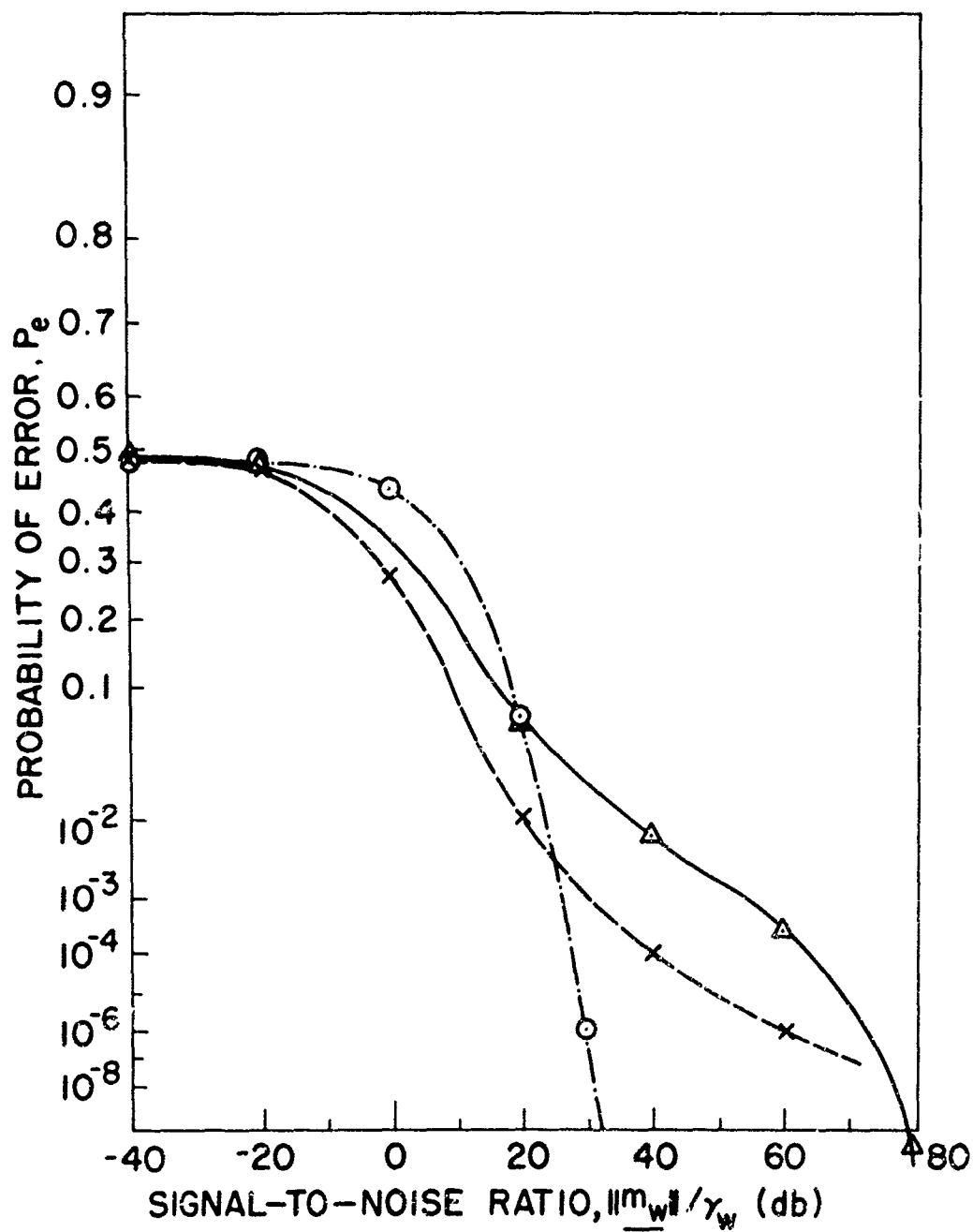


FIG. 22. "SHORT-DURATION" SIGNAL (CASE I) PERFORMANCE: COMPARISON OF ERROR CURVES ACHIEVABLE BY OPTIMAL MATCHED FILTER RECEIVER IN PRESENCE OF VARIOUS ADDITIVE NOISES.

[Note: Vertical scale is  $\log|\log P_e|$ .]

LEGEND:

———— Modified generalized "t" noise model

$$\theta = 2$$

$$\beta = 10^3 \gamma_w$$

----- Generalized "t" noise model

$$\theta = 3$$

..... Gaussian noise model

Same average power as typically  
observed when the generalized  
"t" model with parameters  $\theta = 3$   
and  $\gamma_w$  is appropriate.

## 6. Modified Generalized "t" Noise

Turning attention to modified generalized "t" noise and taking  $\theta = 2$ , since this is the simplest case of interest, it is found by setting  $N = 1$  in  $p_y(y)$  given by Eq. (3.35) that

$$p_{y_w m} (x) \Big|_{\theta=2} = \frac{K}{(2\pi)^{1/2}} \frac{2}{x^2 + \gamma_w^2} \exp \left[ -\frac{1}{2\beta^2} (x^2 + \gamma_w^2) \right], \quad -\infty < x < \infty, \quad (3.47)$$

where  $\gamma_w \triangleq 1/\sigma$  and

$$K = \left\{ \int_{-\beta}^{\beta} \frac{1}{a} \exp \left[ -\frac{1}{2} \frac{\gamma_w^2}{a^2} \right] da \right\}^{-1}. \quad (3.48)$$

Thus, evaluating Eq. (3.41) in this case,

$$P_{e \Big|_{\theta=2}} = \int_{\frac{1}{2} \frac{\|m_w\|^2}{\gamma_w}}^{\infty} \left( \frac{2}{\pi} \right)^{1/2} \frac{K}{x^2 + \gamma_w^2} \exp \left[ -\frac{1}{2\beta^2} (x^2 + \gamma_w^2) \right] dx. \quad (3.49)$$

Now, this integral cannot be evaluated in closed form as it stands; but it can be approximated in two subcases of interest, corresponding to high and low SNR:

a. High SNR; i.e.,  $\|m_w\|^2 \gg \gamma_w$

In this case is found the approximate result

$$\begin{aligned} P_{e \Big|_{\theta=2}} &\approx \int_{\frac{1}{2} \frac{\|m_w\|^2}{\gamma_w}}^{\infty} \left( \frac{2}{\pi} \right)^{1/2} \frac{K}{\gamma_w y} \exp \left[ -\frac{\gamma_w^2}{2\beta^2} y^2 \right] dy \\ &= \left( \frac{2}{\pi} \right)^{1/2} K \left\{ \frac{2}{\frac{\|m_w\|^2}{\gamma_w}} \exp \left[ -\frac{\frac{\|m_w\|^2}{\gamma_w}}{8\beta^2} \right] - \frac{2\pi}{\beta} \operatorname{erfc} \left( \frac{\frac{\|m_w\|}{2\beta}}{\gamma_w} \right) \right\}. \end{aligned} \quad (3.50)$$

In order to complete this evaluation,  $K$  must be determined from Eq. (3.48), which gives

$$K = \frac{\gamma_w}{2(2\pi)^{1/2} \operatorname{erfc}\left(\frac{\gamma_w}{\beta}\right)} \quad (3.51)$$

However, this expression can be simplified by using the fact that  $\beta \gg \gamma_w$  is satisfied in the application of the modified generalized "t" model to atmospheric noise.<sup>†</sup> Now

$$\begin{aligned} \lim_{\frac{\gamma_w}{\beta} \rightarrow 0} K &= \frac{\gamma_w}{(2\pi)^{1/2} - 2\left(\frac{\gamma_w}{\beta}\right)} \\ &\approx \frac{\gamma_w}{(2\pi)^{1/2}} \end{aligned} \quad (3.52)$$

Therefore, substituting this result into Eq. (3.50),

$$P_{e_{\theta=2}} \approx \frac{\gamma_w}{\pi} \left\{ \frac{2}{\|m_w\|} \exp\left[-\frac{\|m_w\|^2}{8\beta^2}\right] - \frac{(2\pi)^{1/2}}{\beta} \operatorname{erfc}\left(\frac{\|m_w\|}{2\beta}\right) \right\} \quad (3.53)$$

<sup>†</sup>This follows from the results of Section II C1. From their definitions

$$\frac{\gamma_w}{\beta} = \frac{\gamma}{\sigma_1 \beta} = \frac{m^{1/2}}{\sigma \beta} = \frac{1}{\beta \sigma},$$

since  $m = 1$  here. However, in the application of the modified generalized "t" model in Fig. 10 it is seen that  $\beta \sigma = 5 \times 10^2$  is required to fit the measured data. Thus, for this case, which is typical of results at vlf and lf,

$$\frac{\gamma_w}{\beta} = 2 \times 10^{-3} \ll 1.$$

In order more easily to compare the form of this high SNR result with that given by Eq. (3.45) for the generalized "t" model, it is illuminating to consider two further subcases as follows:

$$(1) \frac{\|m_w\|}{\beta} \ll 1:$$

In this case there results

$$P_{e|\theta=2} \approx \frac{2}{\pi} \frac{\gamma_w}{\|m_w\|} \quad (3.54)$$

$$(2) \frac{\|m_w\|}{\beta} \gg 1:$$

In this case there results

$$P_{e|\theta=2} \approx \frac{8}{\pi} \frac{\beta^2 \gamma_w}{\|m_w\|^3} \exp\left[-\frac{\|m_w\|^2}{8\beta^2}\right] = \lim_{\frac{\|m_w\|}{\beta} \rightarrow \infty} \left(\frac{2}{\pi}\right)^{1/2} \frac{4\beta \gamma_w}{\|m_w\|^2} \operatorname{erfc}\left(\frac{\|m_w\|}{2\beta}\right). \quad (3.55)$$

b. Low SNR; i.e.,  $\|m_w\| \ll \gamma_w$

Rewriting  $P_{e|\theta=2}$  given by Eq. (3.49) in the form

$$P_{e|\theta=2} = \frac{1}{2} - \int_0^{\frac{1}{2} \frac{\|m_w\|}{\gamma_w}} \left(\frac{2}{\pi}\right)^{1/2} \frac{K}{\gamma_w} \frac{1}{y^2 + 1} \exp\left[-\frac{\gamma_w^2}{2\beta^2} (y^2 + 1)\right] dy, \quad (3.56)$$

it is seen, using the fact  $\gamma_w/\beta \ll 1$  in conjunction with the low SNR condition  $\|m_w\|/\gamma_w \ll 1$ , that

$$P_{e|\theta=2} \approx \frac{1}{2} - \int_0^{\frac{1}{2} \frac{\|m_w\|}{\gamma_w}} \frac{1}{\pi} \frac{1}{y^2 + 1} dy. \quad (3.57)$$

Thus, for the low SNR case:

$$\begin{aligned}
 P_{e|_{\theta=2}} &\approx \frac{1}{2} - \frac{1}{\pi} \tan^{-1} \left( \frac{\|m_w\|}{2\gamma_w} \right) \\
 &\approx \frac{1}{2} \left\{ 1 - \frac{1}{\pi} \frac{\|m_w\|}{\gamma_w} \right\} \\
 &= \lim_{\frac{\|m_w\|}{\gamma_w} \rightarrow 0} \operatorname{erfc} \left( (2\pi)^{1/2} \frac{\|m_w\|}{\gamma_w} \right). \quad (3.58)
 \end{aligned}$$

## 7. Discussion of Probability-of-Error Results

Before proceeding to the discussion of the  $P_e$  results calculated above, it is recalled that these Case I results apply to the situation where the additive atmospheric noise is given by  $y(t) = a n(t)$ ,  $0 \leq t \leq T$ ; i.e., they apply when the transmitted signal duration  $T$  is short enough that  $a(t) = a$  can be assumed constant for the duration of the signal. With this in mind, the  $P_e$  results for Case I lead to the following conclusions:

### a. Generalized "t" Noise

The description of the lightning discharge presented in Section IIA indicates that the  $P_e$  results for Case I apply at vlf when the duration of the transmitted signal is less than about 0.1 msec. In addition, inspection of the plotted results in Chapter II indicates that these results apply practically to any situation at vlf or lf where the duration of the transmitted signal is less than or equal to the inverse of the receiver bandwidth<sup>†</sup> for bandwidths greater than a few hundred cycles per second.

<sup>†</sup>This follows as an engineering approximation from the fact that the rise time of a signal passed through a bandpass filter of bandwidth  $2B$  is about  $1/2B$  seconds; i.e.,  $2TB \leq 1$  in these situations. This is consistent with the short-duration signal idea, since receiver bandwidth is restricted in practice at both vlf and lf because of the lack of spectrum availability (see Section IIA).

To the author's knowledge, there are no vlf communication systems in operation with either of these characteristics. There is good reason for this (in addition to the difficulty of obtaining transmitting antenna bandwidths of this size at vlf), as indicated by the  $P_e$  results. In particular, the high SNR result given by Eq. (3.45) indicates that, even when using the optimal receiver, the improvement in  $P_e$  with increased signal energy at low error rates is very small compared to the improvement achieved in the case of additive gaussian noise (see Fig. 22). This indicates that short-duration signals are not an optimal choice for use in the presence of vlf or lf atmospheric noise if it is desired to achieve economically a low probability of error; this is physically reasonable because of the distinctly impulsive nature of atmospheric noise.

#### b. Modified Generalized "t" Noise

Inspection of the plotted results in Chapter II indicates that the  $P_e$  results for Case I<sub>m</sub> apply practically in two situations: those situations at mf or hf in which the duration of the transmitted signal is less than or equal to the inverse of the receiver bandwidth, and those situations at vlf or lf in which the duration of the transmitted signal is less than or equal to the inverse of the receiver bandwidth for bandwidths less than a few hundred cycles per second. Once again, the most interesting results are those pertaining to the high SNR case, given by Eqs. (3.54) and (3.55). These results are demonstrated in Fig. 22, where it is seen that the improvement in  $P_e$  with increasing  $\|m_w\|$  is greatly enhanced when the inequality  $\|m_w\|/\beta \gg 1$  is satisfied.

In regard to the practical applicability of these results for the modified generalized "t" model, the plotted data in Chapter II indicate that, for a fixed receiver bandwidth, the value of  $\beta/\gamma_w$  decreases as the operating frequency is increased. Thus the use of short-duration signals is more attractive at hf than at lower operating frequencies.

#### C. CASE II: LONG-DURATION SIGNALS; THE GENERAL CASE

The probability-of-error results obtained in Case I indicate that short-duration signals are not an optimal choice in the presence of additive atmospheric noise. This follows from the fact that, particularly at vlf and

If where the generalized "t" model is appropriate, the  $P_e$  resulting from the use of short-duration signals behaves in a much less desirable fashion than would the  $P_e$  if the additive noise were gaussian. Thus it is desirable to investigate the use of long-duration signals, where "long duration" means that the Case I assumption that  $a(t) = a$  is constant for the duration of the signal must now be relaxed. This consideration of long-duration signals is well motivated physically, since we would like to be able to disregard the received signal when it is largely the result of a pulse of noise, and base our decision on the relatively noise free signal received between these noise pulses. This, in fact, is the procedure typically employed in practice, where long-duration signals are used in conjunction with nonlinear receiving techniques.

In this case, the decision problem at the receiver becomes that of choosing between the two a priori equally probable hypotheses

$$\left. \begin{array}{l} h^{(1)}: x(t) = m(t) + a(t) n(t) \\ h^{(2)}: x(t) = a(t) n(t) \end{array} \right\}, \quad 0 \leq t \leq T. \quad (3.59)$$

The desired vector formulation in this case is developed as follows: Defining  $q_i(t)$ ,  $i=1, \dots, N$ , as shown in Fig. 16, and assuming the additive noise  $y(t) = a(t) n(t)$  to have a continuous covariance function, it is possible to write [Ref. 41]

$$y(t) = \text{l.i.m.}_{N \rightarrow \infty} \sum_{i=1}^N y(t_i) (\Delta t_i)^{1/2} q_i(t), \quad 0 \leq t \leq T. \quad (3.60)$$

Since it is also possible to write

$$m(t) = \text{l.i.m.}_{N \rightarrow \infty} \sum_{i=1}^N m(t_i) (\Delta t_i)^{1/2} q_i(t), \quad 0 \leq t \leq T \quad (3.61)$$

for all square-integrable signals  $m(t)$ , it is seen that the vector formulation of the decision problem can be written as follows with respect to the orthonormal basis functions  $q_i(t)$ ,  $i = 1, \dots, N$ : (As in Case I,  $N$  will be taken to infinity at the conclusion of the problem.)

$$\begin{aligned} h^{(1)}: \underline{x} &= \underline{m} + \underline{y}, \\ h^{(2)}: \underline{x} &= \underline{y}, \end{aligned} \quad (3.62)$$

where, e.g.,  $\underline{y}_t = \underline{y}_1, \dots, \underline{y}_N$  with  $y_i = y(t_i) (\Delta t_i)^{1/2}$ .

#### 1. Calculation of the Likelihood Ratio

Now

$$w(\underline{x}|h^{(1)}) = p_{\underline{y}}(\underline{x} - \underline{m}), \quad (3.63)$$

where the probability density function  $p_{\underline{y}}(\underline{y})$  of the additive-noise vector is specified as follows: Recalling that  $a(t)$  is now allowed to vary "slowly" on the interval  $[0, T]$  one can write

$$\begin{aligned} y_i &= y(t_i) (\Delta t_i)^{1/2} = a(t_i) n(t_i) (\Delta t_i)^{1/2} \\ &= a_i n_i, \quad i = 1, \dots, N, \end{aligned} \quad (3.64)$$

where  $n_i \triangleq n(t_i) (\Delta t_i)^{1/2}$  and  $a_i \triangleq a(t_i)$ . (It is noted that this is consistent with the interpretation in Chapter II of  $a(t)$  as a dimensionless weighting factor.) Since, as in Case I,  $n(t)$  is a zero-mean gaussian process with covariance function  $R_n(t, s)$ , the distribution  $p_{\underline{n}}(\underline{n})$  of the vector  $\underline{n}_t = \underline{n}_1, \dots, \underline{n}_N$  is given by

$$p_{\underline{n}}(\underline{n}) = \frac{1}{(2\pi)^{N/2} |R_n|^{1/2}} \exp \left[ -\frac{1}{2} \underline{n}_t R_n^{-1} \underline{n} \right], \quad (3.65)$$

where

$$R_n = \left\{ R_n(t_i, t_j) (\Delta t_i \Delta t_j)^{1/2} \right\}. \quad (3.66)$$

In order to complete the specification of the problem, the distribution of the vector  $\underline{a}$  of coefficients must be specified. However, recalling that  $a(t) \triangleq 1/b(t)$ , the distribution  $p_{\underline{b}}(\underline{b})$  of the vector  $\underline{b}_t = b_1, \dots, b_N$  can be equivalently specified. Now, the first-order statistics of  $b(t)$  are given by the two-sided chi distribution  $x_2(m, \sigma)$ . However, in the special case  $\theta = 2$  ( $m = 1$ ) this reduces to the normal distribution  $N(0, \sigma^2)$ , so that  $b(t)$  is a gaussian process in this special case. Thus, initially considering the case  $\theta = 2$ ,

$$p_{\underline{b}}(\underline{b}) = \frac{1}{(2\pi)^{N/2} |R_b|^{1/2}} \exp \left[ -\frac{1}{2} \underline{b}_t R_b^{-1} \underline{b} \right], \quad (3.67)$$

where

$$R_b = \left\{ R_b(t_i, t_j) \right\}, \quad (3.68)$$

in which it is noted that  $R_b(t_i, t_j) = \sigma^2$  in the notation previously used. Now

$$p_{\underline{y}}(\underline{y}) = \int_{-\infty}^{\infty} p_{\underline{y}}(\underline{y}|\underline{b}) p_{\underline{b}}(\underline{b}) d\underline{b}, \quad (3.69)$$

where setting  $y_i = n_i/b_i$ ,  $i = 1, \dots, N$ , gives

$$\begin{aligned} p_{\underline{y}}(\underline{y}|\underline{b}) &= \left| \prod_{i=1}^N b_i \right| p_{\underline{n}}(n_i = b_i y_i, i = 1, \dots, N) \\ &= \left( \prod_{i=1}^N |b_i| \right) \frac{1}{(2\pi)^{N/2} |R_n|^{1/2}} \exp \left( -\frac{1}{2} \underline{b}_i y_i R_n^{-1} b_i y_i \right), \end{aligned} \quad (3.70)$$

in which  $\underline{b_i y_i} \triangleq b_1 y_1, \dots, b_N y_N$ .<sup>†</sup> Thus, substituting into Eq. (3.69),

$$p_{\underline{y}}(\underline{y}) = \frac{1}{(2\pi)^N |\underline{R_n}|^{1/2} |\underline{R_b}|^{1/2}} \int_{-\infty}^{\infty} db_1, \dots, \int_{-\infty}^{\infty} db_N \left( \prod_{i=1}^N |b_i| \right) \cdot \exp \left[ -\frac{1}{2} \left( \underline{b_i y_i} \underline{R_n}^{-1} \underline{b_i y_i} + \underline{b_t} \underline{R_b}^{-1} \underline{b} \right) \right]. \quad (3.71)$$

In order to evaluate this N-fold integral, it seems reasonable to diagonalize simultaneously the two quadratic forms in the exponent. This can be done [Ref. 43], but requires the use of linear transformations dependent in an unknown way on the vector  $\underline{y}$ . As a result, it does not appear feasible to pursue this general formulation without specification of one or the other (or both) of  $\underline{R_n}(t,s)$  and  $\underline{R_b}(t,s)$ . Actually, it is easily shown that both  $\underline{R_n}(t,s)$  and  $\underline{R_b}(t,s)$  must be specified if  $p_{\underline{y}}(\underline{y})$  is to be evaluated as a known function of  $\underline{y}$ ; hence we will proceed to consider special cases of interest as follows:

The special case that first comes to mind is a "white" noise case:

$$\underline{R_n}(t,s) = N_0/2 \delta(t-s), \quad (3.72a)$$

$$\underline{R_b}(t,s) = B_0/2 \delta(t-s), \quad (3.72b)$$

but this case will not be further considered here since it is not applicable to the communication channels of interest. This follows from the results of Chapter II, where it is shown that the generalized "t" model is in practice an appropriate model for received atmospheric noise when  $n(t)$  is a narrowband random process and  $a(t) = 1/b(t)$  is a slowly-varying random process. While these results discourage the "whiteness" assumption, they do suggest alternate ways of specifying the higher-order statistics of  $a(t)$  and  $n(t)$ . One such specification which is of

<sup>†</sup> Note that  $\underline{b_i y_i}$  is the transpose of the column vector  $b_i y_i$ .

particular interest, since it provides a formulation retaining much of the simplicity of the white noise case, is considered below as Case IIa.

#### D. CASE IIa: COMPLEX ENVELOPE REPRESENTATION

Recalling from the discussion in Section IIB that in practice attention can be restricted to the situation in which the receiver bandwidth is substantially less than the band center frequency, the Case II hypotheses can be further described by noting that  $x(t)$ ,  $m(t)$ , and  $y(t) = a(t)n(t)$  can be considered to be narrowband functions of time. Thus it follows that the Case II decision problem can be written directly in terms of the slowly varying complex envelopes [Ref. 40] of  $x(t)$ ,  $m(t)$ , and  $y(t)$ . In terms of these complex envelopes, the decision problem becomes that of choosing between the hypotheses

$$\left. \begin{aligned} h^{(1)}: x(t) &= \mu(t) + \eta(t) \\ h^{(2)}: x(t) &= \eta_1(t) \end{aligned} \right\}, \quad 0 \leq t \leq T, \quad (3.73)$$

where, e.g.,

$$\begin{aligned} x(t) &= x_c(t) \cos 2\pi f_0 t - x_s(t) \sin 2\pi f_0 t \\ &= \operatorname{Re} \left\{ x(t) e^{i2\pi f_0 t} \right\} \end{aligned} \quad (3.74)$$

and  $x(t) = x_c(t) + ix_s(t)$  is the slowly varying complex envelope of  $x(t)$ . Proceeding as in the Case II development, one can write

$$x(t) = \lim_{N \rightarrow \infty} \sum_{i=1}^N x(t_i) (\Delta t_i)^{1/2} q_i(t), \quad 0 \leq t \leq T. \quad (3.75)$$

Furthermore, it is proposed that a practically useful model results from assuming that the slowly varying complex envelope is given by

$$x(t) \approx \sum_{i=1}^N x(t_i) (\Delta t_i)^{1/2} q_i(t), \quad 0 \leq t \leq T, \quad (3.76)$$

where the value of  $N$  required will be discussed further below and is dependent on the bandwidth in which the signal of duration  $T$  is observed. Proceeding again as in Case II, the vector formulation of this problem with respect to the orthonormal basis functions  $q_i(t)$ ,  $i = 1, \dots, N$ , can be written as

$$\begin{aligned} h^{(1)}: \underline{x} &= \underline{\mu} + \underline{\eta} \\ h^{(2)}: \underline{x} &= \underline{\eta} \end{aligned} \quad (3.77)$$

where, e.g.,  $\underline{\eta}_t = \underline{\eta}_1, \dots, \eta_N$  with  $\eta_i = \eta(t_i) (\Delta t_i)^{1/2}$ .

#### 1. Calculation of the Likelihood Ratio for Case IIa

Now

$$w(\underline{x} | h^{(1)}) = p_{\underline{\eta}}(\underline{x} - \underline{\mu}), \quad (3.78)$$

where the probability density function  $p_{\underline{\eta}}(\underline{\eta})$  of the complex additive noise vector is specified as follows: Recalling that  $a(t)$  is itself a slowly varying random process, one can write

$$\eta_i = \eta(t_i) (\Delta t_i)^{1/2} = a(t_i) v(t_i) (\Delta t_i)^{1/2} = a_i v_i \quad (3.79)$$

where  $a_i \triangleq a(t_i)$  and  $v_i \triangleq v(t_i) (\Delta t_i)^{1/2}$ , in which  $v(t)$  is the complex envelope of  $n(t)$ . Since  $v(t)$  is the complex envelope of a gaussian process, it follows that it is a complex gaussian process. Thus the probability density function  $p_{\underline{v}}(\underline{v})$  of the vector  $\underline{v}_t = \underline{v}_1, \dots, v_N$  can be written (assuming the power spectral density of the narrowband process

$n(t)$  to be symmetric about the band center frequency) [Refs. 40, 41] in the form:

$$p_{\underline{v}}(\underline{v}) = \frac{1}{\pi^N |\Phi_{\underline{v}}|} \exp \left[ -\frac{\underline{v}_t^* \Phi_{\underline{v}}^{-1} \underline{v}}{1} \right], \quad (3.80)$$

where

$$\Phi_{\underline{v}} = E[\underline{v}_t \underline{v}_t^*], \quad (3.81)$$

with

$$E[v_i v_j^*] = E[v(t_i) v^*(t_j)] (\Delta t_i \Delta t_j)^{1/2}. \quad (3.82)$$

Motivated by the difficulties encountered in the Case II calculations, it is proposed that an interesting case for initial consideration is given by

$$E[v(t_i) v^*(t_j)] = N_0 \delta_{ij}, \quad i, j = 1, \dots, N. \quad (3.83)$$

Substituting this specification into Eq. (3.80),

$$p_{\underline{v}}(\underline{v}) = \frac{1}{\pi^N (N_0 \Delta t)^N} \exp \left[ -\frac{1}{N_0 \Delta t} \underline{v}_t^* \underline{v} \right], \quad (3.84)$$

where the fact that  $\Delta t_i = \Delta t$  for all  $i = 1, \dots, N$  has been used.

It now remains to specify the probability density function of the vector  $\underline{a}_t = \underline{a}_1, \dots, \underline{a}_N$  of coefficients. Following Case II above, the equivalent specification of  $p_{\underline{b}}(\underline{b})$  will again be made where  $\vartheta = 2$  is assumed so that  $b(t)$  is a gaussian process. Thus  $p_{\underline{b}}(\underline{b})$  is given by Eq. (3.67). However, again motivated by the Case II results, it is proposed that a case of interest follows from the assumption

$$E[b(t_i) b(t_j)] = \frac{B_0}{2} \delta_{ij}, \quad i, j = 1, \dots, N. \quad (3.85)$$

Although the representation for the received signal given by Eq. (3.76) is particularly convenient in the detection problem being considered here, it remains to verify the validity of this representation in the light of the assumption on  $\phi_v$  and  $R_b$  made in Eqs. (3. ) and (3.85), respectively. In order to do this, it will be recalled that the received signal  $x(t)$  has one of the forms

$$\left. \begin{array}{l} h^{(1)}: x(t) = m(t) + y(t) \\ h^{(2)}: x(t) = y(t) \end{array} \right\}, \quad 0 \leq t \leq T, \quad (3.59)$$

where  $y(t) = [1/b(t)] n(t)$ . Then the following observations can be made:

1. As far as the observed noise  $y(t)$  is concerned, the representation proposed by Eq. (3.76) with  $\phi_v$  and  $R_b$  given by Eqs. (3.83) and (3.85) is identical in form to the representation considered in the case of independent samples in Section IIC3. It follows, from the results shown there, that this representation is a reasonable first approximation to the complex envelope  $\eta(t)$  when  $N \approx 2TB$ , where  $2B$  is the rf bandwidth in which the received signal of duration  $T$  is observed.
2. As far as the known signal  $m(t)$  is concerned, it will be found that in practice this signal of duration  $T$  has a bandwidth significantly less than the receiver bandwidth  $2B$ . Thus the representation proposed by Eq. (3.76) with  $N \approx 2TB$  gives a good approximation to the complex envelope  $\mu(t)$ .

Therefore, combining observations (1) and (2), it is concluded that the representation given by Eq. (3.76) with  $N = 2TB$  is a reasonable representation for the received signals of interest in Case IIa when  $\phi_v$  and  $R_b$  are given by Eqs. (3.83) and (3.85). Now, substituting Eq. (3.85) into Eq. (3.67),

$$p_{\underline{b}}(\underline{b}) = \frac{1}{\pi^{N/2} B_0^{N/2}} \exp \left[ -\frac{1}{B_0} \underline{b}_t \underline{b} \right]. \quad (3.86)$$

Now

$$p_{\underline{1}}(\underline{1} | \underline{b}) = \left( \prod_{i=1}^N b_i^2 \right) p_{\underline{v}}(v_i = b_i \eta_i, i = 1, \dots, N), \quad (3.87)$$

where use has been made of the fact that in terms of real variables

$$p_{v_i}(v_i) = p_{n_{ic}, n_{is}}(n_{ic}, n_{is}) = p_{n_{ic}}(n_{ic}) p_{n_{is}}(n_{is}), \quad (3.88)$$

so that the Jacobian of the transformation is

$$J(v_i \rightarrow r_i) = b_i^2. \quad (3.89)$$

Therefore,

$$p_{\underline{r}}(\underline{r}|\underline{b}) = \left( \prod_{i=1}^N b_i^2 \right) \frac{1}{\pi^N (N_0 \Delta t)^N} \exp \left[ - \frac{1}{N_0 \Delta t} \sum_{i=1}^N (b_i^2 |r_i|^2) \right], \quad (3.90)$$

so that

$$\begin{aligned} p_{\underline{r}}(\underline{r}) &= \frac{1}{\pi^{3N/2} (N_0 \Delta t)^N B_0^{N/2}} \int_{-\infty}^{\infty} db_1, \dots, \int_{-\infty}^{\infty} db_N \left( \prod_{i=1}^N b_i^2 \right) \\ &\cdot \exp \left[ - \sum_{i=1}^N \left( \frac{|r_i|^2}{N_0 \Delta t} + \frac{1}{B_0} \right) b_i^2 \right] \\ &= \frac{1}{(2\pi)^N} \left( \frac{N_0 \Delta t}{B_0} \right)^{N/2} \prod_{i=1}^N \frac{1}{\left[ |r_i|^2 + \frac{N_0 \Delta t}{B_0} \right]^{3/2}}. \end{aligned} \quad (3.91)$$

Now, using Eq. (3.78) and the similar expression for  $h^{(2)}$ , the likelihood ratio can be written directly as follows:

$$L(\underline{x}) = \frac{w(\underline{x}|h^{(1)})}{w(\underline{x}|h^{(2)})} = \prod_{i=1}^N \frac{\left[|x_i|^2 + \frac{N_0 \Delta t}{B_0}\right]^{3/2}}{\left[|x_i - \mu_i|^2 + \frac{N_0 \Delta t}{B_0}\right]^{3/2}}. \quad (3.92)$$

Thus the Bayes rule in this case is given by:

Choose  $h^{(1)}$  iff

$$\prod_{i=1}^N \left[|x_i|^2 + \frac{N_0 \Delta t}{B_0}\right] \geq \prod_{i=1}^N \left[|x_i - \mu_i|^2 + \frac{N_0 \Delta t}{B_0}\right]. \quad (3.93)$$

However, this is equivalent to the rule

Choose  $h^{(1)}$  iff

$$\sum_{i=1}^N \ln \left[|x(t_i)|^2 + \frac{N_0}{B_0}\right] \geq \sum_{i=1}^N \ln \left[|x(t_i) - \mu(t_i)|^2 + \frac{N_0}{B_0}\right]. \quad (3.94)$$

Therefore, noting that it has been assumed

$$x(t) = x(t_i) \quad \forall t \in \Delta t_i, \quad (3.95a)$$

$$\mu(t) = \mu(t_i) \quad \forall t \in \Delta t_i, \quad (3.95b)$$

it follows that, in terms of the time functions available to the receiver, the Bayes rule is given by

Choose  $h^{(1)}$  iff

$$\int_0^T \ln \left[|x(t)|^2 + \frac{N_0}{B_0}\right] dt \geq \int_0^T \ln \left[|x(t) - \mu(t)|^2 + \frac{N_0}{B_0}\right] dt. \quad (3.96)$$

Noting that  $|x(t)|$  is the envelope of  $x(t)$ , and  $|x(t) - m(t)|$  is the envelope of  $x(t) - m(t)$ , it is seen that one receiver structure which implements this rule is that shown in Fig. 23.

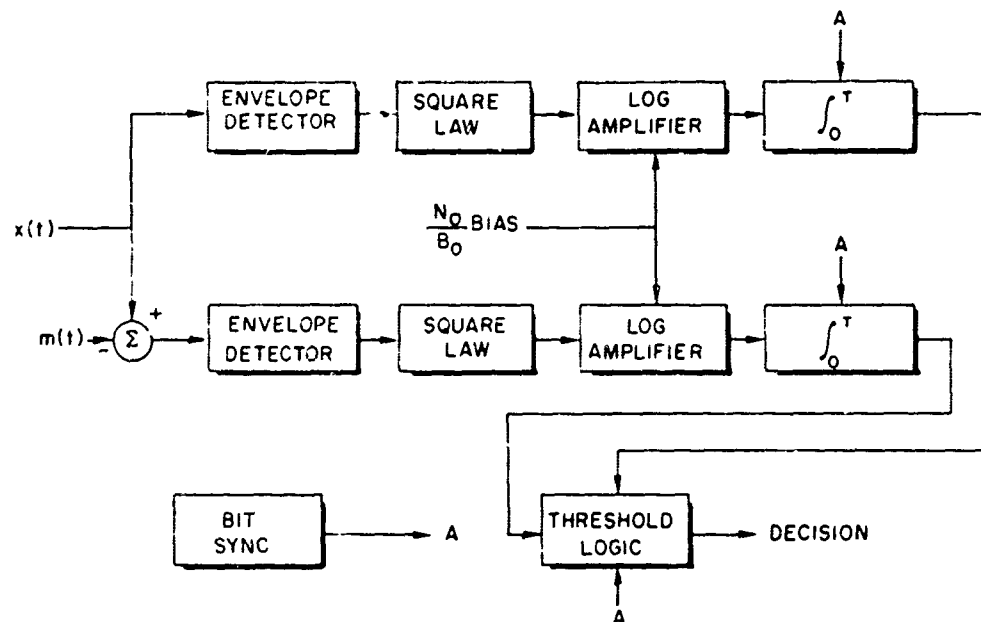


FIG. 23. BLOCK DIAGRAM OF OPTIMAL LOGARITHMIC-CORRELATOR RECEIVER.

## 2. Discussion of Optimal Receiver Rule (Case IIa)

In this case, which is proposed as perhaps the simplest formulation of the long-duration signal problem of practical interest, several comments are warranted. First, it is interesting to compare the receiver rule given by Eq. (3.96), and its implementation shown in Fig. 23, with intuitive notions concerning receiver operation in the presence of additive atmospheric noise. It is seen from Eq. (3.96) that this nonlinear receiver, which will be called here the "logarithmic-correlator" receiver, does indeed agree with intuition, since it suppresses consideration of the received signal at those times when the quantities  $|x(t)|^2$  and  $|x(t) - \mu(t)|^2$  are both large, i.e., those times when the received signal is predominantly due to a pulse of noise, and bases its decision strongly on the received signal at those times when one of the quantities  $|x(t)|^2$  or  $|x(t) - \mu(t)|^2$  is

small. Thus, heuristically, the log-correlator receiver ignores the received signal when it is largely the result of a pulse of noise and bases its decision on the relatively quiet periods between the occurrence of these noise pulses. Furthermore, it is noted that the receiver becomes increasingly nonlinear as the average SNR increases, which (again in agreement with intuition) means that the receiver has increasing confidence in the received signal at those times when either  $|x(t)|^2$  or  $|x(t) - \mu(t)|^2$  is small as the average SNR increases.

Although the calculation of the receiver rule Eq. (3.96) was carried out for the special case  $\theta = 2$ , it is seen that the Case IIa calculations could have equally easily been carried out without specification of  $\theta$ , by making the assumption that the received noise is statistically independent at the instants  $t_i$  and  $t_j$  for all  $i, j = 1, \dots, N$ . When the calculation of the likelihood ratio is carried out with this assumption, it is seen that the decision rule becomes:

Choose  $h^{(1)}$  iff

$$\int_0^T \ln \left[ |x(t)|^2 + m \frac{N_0}{B_0} \right] dt \geq \int_0^T \ln \left[ |x(t) - \mu(t)|^2 + m \frac{N_0}{B_0} \right] dt, \quad (3.97)$$

where it is recalled that  $\theta = m + 1 > 1$ . Thus it is seen that the form of the optimal decision rule is not changed as  $m$  is varied, the only effect on the realization shown in Fig. 23 being a change of the bias on the logarithmic amplifier. It is noted that such a modification is reasonable, since the average noise power is proportional to  $m(N_0/B_0)$ , with  $m = 1$  leading to Eq. (3.96).

It is clear that the realization of the optimal receiver rule given in Fig. 23 is not the only realization possible. It is desirable to find realizations that are simpler in the sense that the number of zero-memory nonlinear operations required is reduced. Specialization to the high SNR case does not appear to lead to any such simplifications, but specialization to the low SNR case does as follows:

Low SNR case, i.e.,

$$\|\underline{\mu}\|^2 \ll \xi^2,$$

where

$$\xi^2 \triangleq m \frac{N_0}{B_0} \Delta t.$$

In this case it is easily shown that the optimal decision rule is given approximately by

Choose  $h^{(1)}$  iff

$$\operatorname{Re} \left\{ \int_0^T \frac{x(t) \mu^*(t)}{\left[ |x(t)|^2 + m \left( \frac{N_0}{B_0} \right) \right]} dt \right\} \geq \int_0^T \frac{\frac{1}{2} |\mu(t)|^2}{\left[ |x(t)|^2 + m \left( \frac{N_0}{B_0} \right) \right]} dt. \quad (3.98)$$

Thus it is seen that the low SNR assumption gives an interesting rule which is in fact the correlator receiver modified by the weighting of each instantaneous contribution by a factor dependent on the value of the envelope of the received signal at that instant. However, closer examination of the derivation of Eq. (3.98) shows that the low SNR assumption can actually be relaxed, since the condition required to produce Eq. (3.98) is precisely that  $|\mu_i|^2 \ll \xi^2 \forall i = 1, \dots, N$ . Now, this condition does not necessarily imply the low SNR case, and in fact may be compatible with the high SNR case, i.e. with  $\|\underline{\mu}\|^2 \gg \xi^2$ ; so that the receiver rule given by Eq. (3.98) may be of practical interest. This possibility will be examined further in Section E and is of importance because Eq. (3.98) has a realization similar to the matched-filter realization of the correlator-receiver rule.

Finally, it is interesting to apply the Case IIa assumptions to the situation where the additive noise is given by the modified generalized "t" model, rather than by the generalized "t" model considered above. The calculation of the Bayes rule appropriate to this situation can be carried out in the same manner as that demonstrated above for additive

generalized "t" noise. The decision rule for the special case  $\theta = 3$  is found to be:

Choose  $h^{(1)}$  iff

$$\int_0^T \left\{ \ln \left[ \frac{\left[ |x(t)|^2 + 2 \frac{N_0}{B_0} \right]^2}{|x(t)|^2 + N_0 \left( \beta^2 + \frac{2}{B_0} \right)} \right] + \frac{2}{N_0 \beta^2} \operatorname{Re}[x(t) \mu^*(t)] \right\} dt$$

$$\geq \int_0^T \left\{ \ln \left[ \frac{\left[ |x(t) - \mu(t)|^2 + 2 \frac{N_0}{B_0} \right]^2}{|x(t) - \mu(t)|^2 + N_0 \left( \beta^2 + \frac{2}{B_0} \right)} \right] + \frac{1}{N_0 \beta^2} |\mu(t)|^2 \right\} dt. \quad (3.99)$$

This result is interesting, since it allows a quantitative check as to whether or not the log-correlator receiver is appropriate in a given situation. It is clear that the rule given by Eq. (3.99) reduces to the log-correlator receiver rule as  $\beta^2 \rightarrow \infty$ ; and inspection of the experimental data presented in Section IIC1 shows that, in fact, the log-correlator receiver is the receiver of practical interest at vlf and lf frequencies of operation. On the other hand, no such statement can be made when the operating frequency is increased to hf. In this case, Eq. (3.99) must be examined for each particular situation. This follows from the fact noted in Section IIC1 that the nature of the received noise at hf is strongly a function of local thunderstorm activity.

### 3. Calculation of the Probability of Error (Case IIa)

The receiver that minimizes the probability of error in Case IIa is the one that implements the rule given by Eq. (3.93). Thus the probability of error resulting from the use of the optimal receiver is given by

$$\begin{aligned}
P_e &= \Pr \left\{ L(\underline{x}) \geq 1 \mid h^{(2)} \text{ is true} \right\} \\
&= \Pr \left\{ \prod_{i=1}^N \left[ \frac{|\underline{x}_i|^2 + m \frac{N_0}{B_0} \Delta t}{|\underline{x}_i - \underline{\mu}_i|^2 + m \frac{N_0}{B_0} \Delta t} \right] \geq 1 \mid h^{(2)} \text{ is true} \right\} \\
&= \Pr \left\{ \prod_{i=1}^N \left[ \frac{|\eta_i|^2 + m \frac{N_0}{B_0} \Delta t}{|\eta_i - \underline{\mu}_i|^2 + m \frac{N_0}{B_0} \Delta t} \right] \geq 1 \right\}. \tag{3.100}
\end{aligned}$$

However, (3.100) is equivalent to the more manageable formulation

$$P_e = \Pr \left\{ \sum_{i=1}^N \ln \left[ \frac{|\eta_i|^2 + m \frac{N_0}{B_0} \Delta t}{|\eta_i - \underline{\mu}_i|^2 + m \frac{N_0}{B_0} \Delta t} \right] \geq 0 \right\} = \Pr \left\{ \sum_{i=1}^N \ln z_i \geq 0 \right\}, \tag{3.101}$$

where

$$z_i \triangleq \frac{|\eta_i|^2 + m \frac{N_0}{B_0} \Delta t}{|\eta_i - \underline{\mu}_i|^2 + m \frac{N_0}{B_0} \Delta t}. \tag{3.102}$$

Since the  $z_i$  are statistically independent, it follows that the central limit theorem can be invoked to obtain a valid estimate of the probability of error at high values of  $P_e$ , where the range of validity of this estimate is dependent upon the size of  $N$  [Ref. 14]. Therefore, the calculations of initial interest are those of  $E[\ln z_i]$  and  $\text{var}(\ln z_i)$ . However, the difficulties involved in making even these calculations are

clear, so that it is reasonable to consider bounds on the probability of error obtainable in closed form. One such bound of interest, since it tightens with increasing  $P_e$  (i.e., tightens as the SNR decreases), is given as follows: Noting that

$$\ln z_i \geq 1 - \frac{1}{z_i} \quad (3.103)$$

with equality iff  $z_i = 1$ , it follows that

$$P_e \geq \Pr \left\{ \sum_{i=1}^N \left( 1 - \frac{1}{z_i} \right) \geq 0 \right\}. \quad (3.104)$$

Invoking the central limit theorem as discussed above in order to evaluate this lower bound on  $P_e$ , it is found that

$$E \left[ 1 - \frac{1}{z_i} \right] = \int_{-\infty}^{\infty} d\eta_{ic} \int_{-\infty}^{\infty} d\eta_{is} \frac{\frac{m\xi^m}{2\pi} \frac{2\eta_{ic}\mu_{ic} + 2\eta_{is}\mu_{is} - |\mu_i|^2}{[\eta_{ic}^2 + \eta_{is}^2 + \xi^2]^{(m+4)/2}}}{}, \quad (3.105)$$

where use has been made of

$$p_{\eta_i}(\eta_i) = \frac{m\xi^m}{2\pi} \frac{1}{[|\eta_i|^2 + \xi^2]^{(m+2)/2}} = p_{\eta_{ic}, \eta_{is}}(\eta_{ic}, \eta_{is}), \quad (3.106)$$

in which  $\eta_i = \eta_{ic} + i\eta_{is}$ ,  $\mu_i = \mu_{ic} + i\mu_{is}$ , and  $\xi^2 = m N_0/B_0 \Delta t$ . [It is noted that Eq. (3.106) is obtained by setting  $N = 1$  in  $p_{\underline{\eta}}(\underline{\eta})$ , which is given by Eq. (3.91) for the special case  $m = 1$ .] Taking now the special case  $\theta = 3$ , since it is the case of most interest,

$$E \left[ 1 - \frac{1}{z_i} \right] = - \frac{\xi^2}{\pi} \int_{-\infty}^{\infty} d\eta_{ic} \int_{-\infty}^{\infty} d\eta_{is} \frac{|\mu_i|^2}{[\eta_{ic}^2 + \eta_{is}^2 + \xi^2]^3} = - \frac{1}{2} \left( \frac{|\mu_i|}{\xi} \right)^2. \quad (3.107)$$

Thus

$$E \left[ \sum_{i=1}^N \left( 1 - \frac{1}{z_i} \right) \right] = - \frac{1}{2} \sum_{i=1}^N \left( \frac{|\mu_1|}{\xi} \right)^2 . \quad (3.108)$$

Similarly,

$$E \left[ 1 - \frac{1}{z_i} \right]^2 = \frac{1}{3} \left( \frac{|\mu_1|}{\xi} \right)^2 + \frac{1}{3} \left( \frac{|\mu_1|}{\xi} \right)^4 , \quad (3.109)$$

so that

$$\text{var} \left( 1 - \frac{1}{z_i} \right) = \frac{1}{3} \left( \frac{|\mu_1|}{\xi} \right)^2 + \frac{1}{12} \left( \frac{|\mu_1|}{\xi} \right)^4 . \quad (3.110)$$

Therefore, since the  $z_i$  are statistically independent,

$$\text{var} \left[ \sum_{i=1}^N \left( 1 - \frac{1}{z_i} \right) \right] = \frac{1}{12} \sum_{i=1}^N \left[ 4 \left( \frac{|\mu_1|}{\xi} \right)^2 + \left( \frac{|\mu_1|}{\xi} \right)^4 \right] . \quad (3.111)$$

Now, knowing that

$$\sum_{i=1}^N \left( 1 - \frac{1}{z_i} \right)$$

becomes normally distributed as  $N \rightarrow \infty$ , an estimate of the lower bound given by Eq. (3.104) can be obtained as follows:

$$P_{e|\theta=3} \gtrsim \int_0^\infty \frac{1}{(2\pi\sigma_z^2)^{1/2}} \exp \left[ - \frac{(x - \mu_z)^2}{2\sigma_z^2} \right] dx , \quad (3.112)$$

where  $\mu_2$  is given by Eq. (3.108) and  $\sigma_z^2$  is given by Eq. (3.111). Thus

$$P_{e|\theta=3} \gtrsim \operatorname{erfc} \left( \frac{\frac{1}{2} \sum_{i=1}^N \left( \frac{|\mu_i|}{\xi} \right)^2}{\left\{ \frac{1}{12} \sum_{i=1}^N \left[ 4 \left( \frac{|\mu_i|}{\xi} \right)^2 + \left( \frac{|\mu_i|}{\xi} \right)^4 \right] \right\}^{1/2}} \right). \quad (3.113)$$

Since this bound was obtained by applying the central limit theorem to the sum of  $N$  independent random variables, it is well known that the resulting error is small if attention is restricted to those situations where  $P_e$  is sufficiently large--i.e., greater than about  $C/N^{1/2}$ , where  $C$  is a proportionality constant [Ref. 44]. Thus for the finite  $N$  of interest, there is negligible error in the result given by Eq. (3.113) when this result is specialized to the low SNR case; i.e., there is negligible error when

$$\sum_{i=1}^N |\mu_i|^2 \ll \xi^2,$$

and there is obtained the asymptotic result

$$\lim_{\frac{\|\underline{\mu}\|}{\xi} \rightarrow 0} P_{e|\theta=3} \gtrsim \operatorname{erfc} \left[ \left( \frac{3}{4} \right)^{1/2} \frac{\|\underline{\mu}\|}{\xi} \right], \quad (3.114)$$

where use has been made of the fact that

$$\|\underline{\mu}\| = \left[ \sum_{i=1}^N |\mu_i|^2 \right]^{1/2}.$$

However, in addition to the fact that the accuracy of the result obtained using the central limit theorem improves as  $\|\mu\|/\xi \rightarrow 0$  for fixed  $N$ , it is also true that the lower bound on  $\ln z_1$  used to obtain Eq. (3.113) tightens as  $|\mu_1|/\xi \rightarrow 0$ , so that, asymptotically, we have the low SNR result

$$\lim_{\frac{\|\mu\|}{\xi} \rightarrow 0} P_{e|G=3} = \operatorname{erfc} \left[ \left( \frac{3}{4} \right)^{1/2} \frac{\|\mu\|}{\xi} \right]. \quad (3.115)$$

It is interesting to note that, as expected, this low SNR result is dependent only upon a ratio of signal energy to noise energy and is not dependent on signal shape.

Now, if the low SNR condition  $\|\mu\| \ll \xi$  is not satisfied, Eq. (3.115) does not hold and attention must be returned to the bound given by Eq. (3.113). However, as mentioned above, Eq. (3.113) is not a useful bound on the probability of error at low values of  $P_e$  with the finite  $N$  of interest here. Therefore, it is necessary to find a better estimate of  $P_e$  for the high SNR, low  $P_e$  situation. One method for accomplishing this is to apply the technique known as distribution "tilting" [Ref. 45]. Noting that the results found for low  $P_e$  using the central limit theorem are poor because of the fact that it is the tail of the probability distributed that must be evaluated, the tilting procedure will be applied here with the purpose of moving the mean of the tilted distribution to the point at which the cumulative probability is to be calculated. Having accomplished this, the desired cumulative probability can be determined accurately using the central limit theorem; and, in fact, an exponentially correct bound on this probability is given by the appropriate Chernoff bound [Ref. 41]. Now, Eq. (3.101) states that

$$P_e = \Pr \left\{ \sum_{i=1}^N \ln z_i \geq 0 \right\}, \quad (3.101)$$

where

$$z_i \triangleq \frac{|\eta_i|^2 + \xi^2}{|\eta_i - \mu_i|^2 + \xi^2} . \quad (3.102)$$

Also, there is the Chernoff bound given by

$$\Pr \left\{ \sum_{i=1}^N \ln z_i \geq 0 \right\} \leq \exp[\mu_N(s) - s \mu'_N(s)] \Big|_{s=s_0} , \quad (3.116)$$

where

$$\mu_N(s) \triangleq \ln g_N(s) \quad (3.117)$$

and

$$g_N(s) = \prod_{i=1}^N g_i(s) , \quad (3.118)$$

in which the  $g_i(s)$ ,  $i = 1, \dots, N$ , are the moment-generating functions of the independent random variables  $\ln z_i$ ,  $i = 1, \dots, N$ , respectively. Furthermore, the point  $s_0$  at which the right hand side of Eq. (3.116) is to be evaluated specifies the amount of tilt employed. It is given here by the value of  $s > 0$  which satisfies  $\mu'_N(s) = 0$ , where

$$\mu'_N(s) \triangleq \frac{d}{ds} \mu_N(s) . \quad (3.119)$$

Thus for the case of interest here, there is obtained the bound

$$\Pr \left\{ \sum_{i=1}^N \ln z_i \geq 0 \right\} \leq \prod_{i=1}^N g_i(s) \Big|_{s=s_0} . \quad (3.120)$$

Now, although the Chernoff bound given by Eq. (3.120) is an upper bound, it can be shown [Ref. 41] through application of the Berry-Esseen theorem [Ref. 44] that this bound is "exponentially correct", i.e., that

$$\Pr \left\{ \sum_{i=1}^N \ln z_i \geq 0 \right\} \approx f(N^{-1/2}) \prod_{i=1}^N g_i(s) \Big|_{s=s_0}, \quad (3.121)$$

where  $f(N^{-1/2})$  is a polynomial in  $N^{-1/2}$ . Therefore

$$P_e \approx f(N^{-1/2}) \prod_{i=1}^N g_i(s) \Big|_{s=s_0}, \quad (3.122)$$

where  $f(N^{-1/2})$  is a polynomial in  $N^{-1/2}$ , and  $s_0 > 0$  is that value of  $s$  satisfying  $\mu'_N(s) = 0$ . Thus the calculation of  $P_e$  reduces to the determination of  $g_i(s) \Big|_{s=s_0}$ ,  $i = 1, \dots, N$ . This determination is accomplished as follows:

$$\begin{aligned} g_i(s) &= E[\exp(s \ln z_i)] = E[z_i^s] \\ &= \frac{\Gamma(\frac{m+2}{2})}{\Gamma(\frac{m}{2})} \frac{\xi^m}{\pi} \int_{-\infty}^{\infty} d\eta_{ic} \int_{-\infty}^{\infty} d\eta_{is} \frac{[|\eta_i|^2 + \xi^2]^{(2s-m-2)/2}}{[|\eta_i - \mu_i|^2 + \xi^2]^s}. \end{aligned} \quad (3.123)$$

Now, in order to simplify the calculations the following assumptions will be made:

Assumption 1. Let  $\mu_{is} = 0 \forall i = 1, \dots, N$ , so that the known signal  $m(t)$  takes the form  $m(t) = \mu_c(t) \cos \omega_0 t$ . This assumption is not essential but greatly simplifies the resultant integrals.

Assumption 2. Take  $\theta = 3$  ( $m = 2$ ), since this case is easily evaluated and in fact is the case of most interest.

With these assumptions,

$$g_i(s) \Big|_{s=s_0} = \frac{\xi^2}{\pi} \int_{-\infty}^{\infty} dx \int_{-\infty}^{\infty} dy \frac{[x^2 + y^2 + \xi^2]^{s_0-2}}{[(x - \mu_{ic})^2 + y^2 + \xi^2]^{s_0}}, \quad (3.124)$$

where  $s_0 > 0$  must satisfy the equation

$$\sum_{i=1}^N \frac{d}{ds} [\ln g_i(s)] \Big|_{s=s_0} = 0. \quad (3.125)$$

That is,  $s_0 > 0$  must be the solution of

$$\sum_{i=1}^N \frac{\int_{-\infty}^{\infty} dx \int_{-\infty}^{\infty} dy \frac{[x^2 + y^2 + \xi^2]^{s-2}}{[(x - \mu_{ic})^2 + y^2 + \xi^2]^s} \ln \left[ \frac{x^2 + y^2 + \xi^2}{(x - \mu_{ic})^2 + y^2 + \xi^2} \right]}{\int_{-\infty}^{\infty} dx \int_{-\infty}^{\infty} dy \frac{[x^2 + y^2 + \xi^2]^{s-2}}{[(x - \mu_{ic})^2 + y^2 + \xi^2]^s}} = 0. \quad (3.126)$$

Conveniently, it can be shown (see Appendix B) that Eq. (3.126) is in fact uniquely satisfied by  $s = 1$ . Thus, plugging this fortunate result into Eq. (3.124):

$$g_i(s) \Big|_{s=1} = \frac{\xi^2}{\pi} \int_{-\infty}^{\infty} dx \int_{-\infty}^{\infty} dy \frac{1}{[x^2 + y^2 + \xi^2][(x - \mu_{ic})^2 + y^2 + \xi^2]}. \quad (3.127)$$

Now, the integration with respect to  $x$  can easily be done as a contour integral (see Appendix A), and it is found that

$$\begin{aligned}
g_1(s) \Big|_{s=1} &= 2\xi^2 \int_{-\infty}^{\infty} dy \frac{1}{[y^2 + \xi^2]^{1/2} [4y^2 + 4\xi^2 + \mu_{ic}^2]} \\
&= \frac{\xi}{\frac{\mu_{ic}^2}{4} + \xi^2} \int_0^{\infty} dy \frac{1}{\left[1 + \frac{1}{2} y^2\right]^{1/2} \left[1 + \frac{1}{\frac{\mu_{ic}^2}{4} + \xi^2} y^2\right]}. \quad (3.128)
\end{aligned}$$

This integral can be evaluated using Erdelyi [Ref. 46], item 6.2(35), which gives

$$g_1(s) \Big|_{s=1} = {}_2F_1\left(1, \frac{1}{2}; \frac{3}{2}; 1 - \frac{4\xi^2}{\mu_{ic}^2 + 4\xi^2}\right) \frac{4\xi^2}{\mu_{ic}^2 + 4\xi^2}, \quad (3.129)$$

where  ${}_2F_1(a, b; c; x)$  is Gauss' hypergeometric function. Finally, substituting Eq. (3.129) into Eq. (3.122),

$$P_e \Big|_{\theta=3} \approx f(N^{-1/2}) \prod_{i=1}^N \left\{ \frac{4\xi^2}{\mu_{ic}^2 + 4\xi^2} {}_2F_1\left(1, \frac{1}{2}; \frac{3}{2}; 1 - \frac{4\xi^2}{\mu_{ic}^2 + 4\xi^2}\right) \right\}, \quad (3.130)$$

where it is recalled that  $N = 2TB$ .

At this point it should be mentioned that the estimate of  $P_e$  given by Eq. (3.130) can perhaps be further refined by approximating the  $f(N^{-1/2})$  factor. This possibility will not be pursued at this time, however, since Eq. (3.130) gives the essential behavior, particularly at low values of  $P_e$ . Rather, we will consider optimization of the exponentially correct estimate given by Eq. (3.130) with respect to parameters under the control of the design engineer, where it is noted that this estimate is dependent on both signal shape and receiver bandwidth in addition to signal energy and noise energy. In order to proceed with this optimization,

it is necessary to set down the pertinent constraints on the transmitted signal and on the receiver bandwidth. These can be specified as follows:

1. The only constraint to be placed on the transmitted signal in the interval  $[0, T]$  is an average-power constraint, although it is noted that this will lead to the same result as if a peak-power constraint were also imposed.
2. In order to specify the constraint on the receiver bandwidth, it is noted that the dependence of Eq. (3.130) on the receiver bandwidth enters through  $N = 2TB$ . This dependence follows, of course, from the signal representation used in this case (Case IIa), which assumes that the atmospheric noise is observed in an rf bandwidth  $2B$ . This assumption stems from the discussion of limited spectrum availability in Section IIB, and means that the log-correlator receiver shown in Fig. 23 is in practice preceded by a bandpass filter of bandwidth  $2B$ . Therefore, it follows that the pertinent constraint on the receiver bandwidth is that it be small enough to suppress strong adjacent channel signals, and yet large enough to pass the transmitted signal.

Proceeding now with the optimization problem, it is first of all noted that the optimal signal shape must be achieved when the transmitted signal energy is distributed uniformly in a portion, say  $T_k \leq T$ , of the available signaling interval of length  $T$ . This follows directly from the Case IIa representation of the complex envelope of the received signal in terms of the pulse basis functions  $q_i(t)$ ,  $i = 1, \dots, N$ . With this result in mind, it is convenient to rewrite Eq. (3.130) as

$$P_{e|\theta=3} \approx f(1/\sqrt{2T_k B}) \prod_{i=1}^{2T_k B} \left\{ \frac{Y_0 B}{Q_i + Y_0 B} {}_2F_1 \left( 1, \frac{1}{2}; \frac{3}{2}; 1 - \frac{Y_0 B}{Q_i + Y_0 B} \right) \right\}, \quad (3.131)$$

where

$$Q_i \triangleq \mu_{ic}^2 B = \frac{\mu^2(t_i)}{2} \quad (3.132)$$

is the signal power received under  $h^{(1)}$  in the interval  $\Delta t_i$ , and

$$\frac{Y_0}{2} \triangleq 2\xi^2 \quad (3.133)$$

is proportional to the average noise energy received in each interval of length  $\Delta t$ ; so that

$$Y_0 B = 2\gamma^2 = 4 \frac{N_0}{B_0} \quad (3.134)$$

is proportional to the average noise power received in the bandwidth  $2B$ . These identifications are seen to be consistent with the assumption that in practice the atmospheric noise can be considered to be "white" prior to filtering by the receiver.

It is next observed that, in the optimal situation,

$$\frac{Y_0 B}{Q_1 + Y_0 B}$$

must be independent of the value of  $T_k \leq T$ , since both  $Q_1$  and  $B_{\min}$  are directly proportional to  $1/T_k$  when the constraints imposed above are satisfied. Thus it follows directly that the optimal choice of  $T_k$  is given by  $T_k = T$ . Plugging this result into Eq. (3.131) and making use of the fact discussed above that  $Q_i = Q \forall i = 1, \dots, 2T_k B$  is optimal, there results

$$P_{e_{\theta=3}} \approx f\left(1/\sqrt{2TB}\right) \left\{ \frac{Y_0 B}{Q + Y_0 B} {}_2F_1\left(1, \frac{1}{2}; \frac{3}{2}; 1 - \frac{Y_0 B}{Q + Y_0 B}\right) \right\}^{2TB} \quad (3.135)$$

Thus, as far as the signal shape is concerned, it is concluded that the minimum value of  $P_e$  follows from distributing the signal energy uniformly in the signaling interval  $[0, T]$ . Furthermore; as expected,  $P_e$  is minimized by making  $T$  as large as possible.

It now remains to choose the optimal receiver bandwidth  $2B$ . It is shown in Appendix C that, in fact,  $B_{\text{opt}} = \infty$ . This result is disturbing, of course, since the noise model from which it is derived has been demonstrated to be valid only for bandwidths up to a few thousand cycles per second. However, examination of the value of  $P_e$  resulting from large  $B$

shows that the estimate given by Eq. (3.135) is of practical interest, since there is found the result (see Appendix C):

If  $B \gg Q/Y_0$ , then

$$P_{e\theta=3} \approx f\left(1/\sqrt{2TB}\right) (0.51)^{2TQ/Y_0} \quad (3.136)$$

Furthermore, the practical usefulness of this result is demonstrated by the fact that the asymptote is approached quite rapidly with increasing receiver bandwidth, since, e.g.,  $B = 3Q/Y_0$  gives

$$P_{e\theta=3} \Big|_{B=3 \frac{Q}{Y_0}} \approx f\left(1/\sqrt{2TB}\right) (0.56)^{2TQ/Y_0} \quad (3.137)$$

Examination of the error curve given by Eq. (3.137) (see Fig. 24) shows that error rates of the order of  $10^{-5}$  can be achieved in practice using receiver bandwidths of the order of a thousand cycles per second. Thus it is concluded that Eq. (3.136) gives a valid estimate of the error performance achievable in the presence of additive atmospheric noise. This estimate is conveniently written as

$$\lim_{\substack{Y_0 B \\ Q} \rightarrow \infty} P_{e\theta=3} \approx f\left(1/\sqrt{2TB}\right) \exp\left[-\frac{1.35 E}{Y_0}\right], \quad (3.138)$$

where  $E = QT$  is the signal energy under  $h^{(1)}$  distributed uniformly in the signaling interval. This  $P_e$  result is plotted vs SNR in Fig. 24, along with the error curve resulting from the use of a matched-filter receiver in the presence of additive generalized "t" noise. In addition, the error curve achieved by a noncoherent FSK system operating at vlf is also presented using measured data obtained by Watt, et al [Ref. 47].

In Fig. 24, the parameter  $\Delta = V_{\text{rms}}/V_{\text{avg}}$  is introduced and the error curves plotted for  $2 \leq \Delta \leq 4$  because of the fact, discussed in detail in Chapter II, that  $V_{\text{rms}}$  is determined primarily by the tail of the probability distribution, whose observation is made difficult by the large dynamic range exhibited by atmospheric noise. Thus, noting that the noise envelope distributed according to the generalized "t" model actually has a divergent second moment for  $\theta \leq 3$ , the parameter  $2 \leq \Delta \leq 4$  is introduced to show the variation in the error curve due to the range of values of  $\Delta$  actually observed in practice.<sup>†</sup>

#### 4. Discussion of Probability-of-Error Results (Case IIa)

Before proceeding to the discussion of the results calculated above it is recalled that these Case II results apply to long-duration signals, where long duration means that the slowly varying modulating process  $a(t)$  is allowed to vary on the signaling interval. Furthermore, the Case IIa results apply specifically to the Case II situation where the complex envelope of the received signal can be described by Eq. (3.76) in terms of  $N = 2TB$  statistically independent samples. It is proposed that this is the simplest representation of Case II signals of practical interest. It is seen that it essentially includes the Case I signals as a special case. With this in mind, inspection of the error curves plotted in Fig. 24 shows that the performance predicted for the log-correlator receiver in the presence of additive atmospheric noise is significantly better than either that predicted for the matched-filter receiver or that actually achieved by the FSK system. Although the error curves are fairly self explanatory, several comments concerning their derivation are warranted:

<sup>†</sup> Note that the square of the rms carrier-to-noise ratio plotted on the abscissa in Fig. 24 is related by a proportionality constant to the signal-to-noise energy ratio  $E/Y_0$ . This constant is proportional to the ratio of signal bandwidth to receiver bandwidth. For the case in Fig. 24 (using  $\Delta = 3$ ) it is about  $5 \times 10^{-3}$ , although this value may be too small by a factor 1/2. This error would result in the performance of both the matched-filter receiver and the log-correlator receiver being 3 db worse than that shown in Fig. 24. This cannot be resolved due to the fact that  $E_{\text{rms}}$  as given by Watt, et al in their Fig. 18 does not appear to be consistent with the scale on the abscissa.

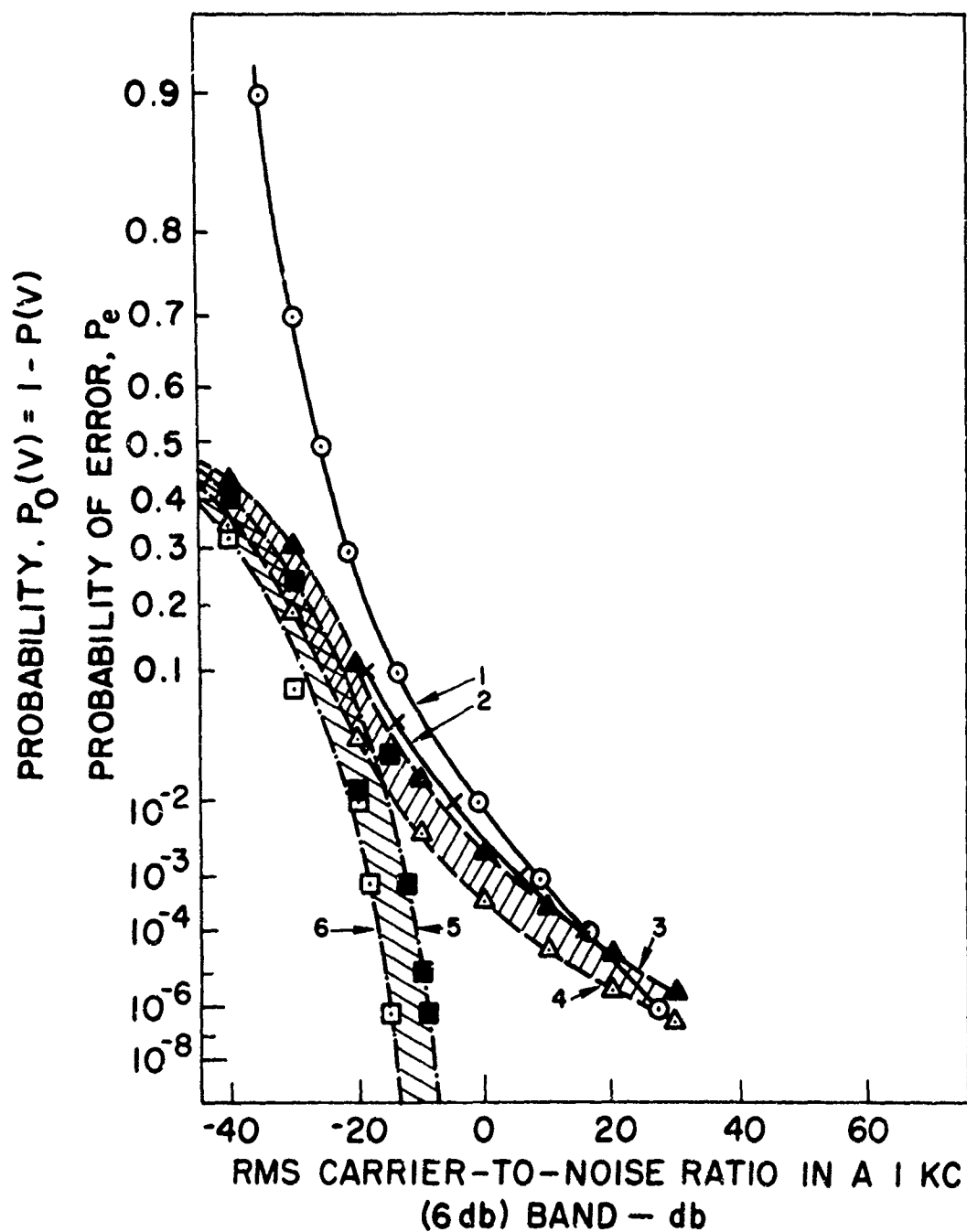


FIG. 24. RECEIVER PERFORMANCE IN PRESENCE OF ADDITIVE ATMOSPHERIC NOISE:  
COMPARISON OF PREDICTED ERROR CURVES WITH MEASURED PERFORMANCE OF AN  
FSK SYSTEM OPERATING AT VLF.

Specification of transmitted signal:  
Frequency shift keyed,  $\pm 25$  cps shift  
60 WPM start-stop teletype

[Note: Vertical scale is  $\log|\log P_e|$  or  $\log|\log P_0(V)|$   
where  $P_0(V)$  is the probability that the envelope  
 $V$  exceeds the value specified by abscissa.]

LEGEND:

- 1 ——— Measured data: Complement of the probability dis-  
tribution function of the envelope of the received  
vlf noise. (Watt, et al, [Ref. 47])  
Receiver 6-db bandwidth = 120 cps
- 2 ——— Measured data: Noncoherent receiver binary error  
curve (derived by Watt, et al from measured character  
error rates).  
Receiver specifications:  
120 cps IF bandwidth  
70 cps base-bandwidth
- Predicted matched-filter receiver error curves  
(matched to mark frequency only).  
Generalized "t" noise model,  $\theta = 3$
- 3 ———  $V_{rms}/V_{avg} = 2$   
4 ———  $V_{rms}/V_{avg} = 4$  } (see page 129)
- Predicted log-correlator receiver error curves (coher-  
ent detection of mark frequency, space frequency re-  
moved)  
Generalized "t" noise model,  $\theta = 3$
- 5 ———  $V_{rms}/V_{avg} = 2$   
6 ———  $V_{rms}/V_{avg} = 4$  } (see page 129)

1. Log-correlator receiver: The error curve presented for the log-correlator receiver was obtained by using the exponentially correct estimate given by Eq. (3.138) in conjunction with the low SNR result given by Eq. (3.115). The low SNR result gives a good estimate of the probability of error at high values of  $P_e$ . This portion of the error curve was obtained by writing Eq. (3.115) in terms of the notation introduced in Eq. (3.131). This gives the convenient form:

$$\lim_{\frac{E}{Y_0} \rightarrow 0} P_{e|_{\theta=3}} = \operatorname{erfc}\left(\sqrt{\frac{6E}{Y_0}}\right) \quad (3.139)$$

Note, as mentioned earlier, that this low SNR, high  $P_e$  result depends only upon a ratio of signal energy to noise energy and is independent of signal shape. In contrast to this, the estimate of  $P_e$  given by Eq. (3.138), which is exponentially correct at all values of  $P_e$ , was shown above to depend crucially on signal shape. Now, it is interesting to investigate the claim that the performance predicted by Eq. (3.138) is, in fact, guaranteed only if the signal energy is distributed uniformly in the signaling interval. Observation of the result that  $B = \infty$  is optimum is actually seen to discount this claim when the only constraint on the transmitted signal is an average power constraint, since a given  $P_e$  performance can be obtained (when the signal energy is not uniformly distributed in the signaling interval) merely by sufficiently increasing the receiver bandwidth  $2B$ . However, it must be remembered that these results are obtained using the Case IIa assumption that the samples of the complex envelope of the received noise are statistically independent--an assumption that certainly breaks down for receiver bandwidths larger than about  $10^4$  cps. Thus it is concluded that, practically speaking, the optimal situation is indeed that where the signal energy is uniformly distributed in the signaling interval, since this achieves a given level of performance with the smallest receiver bandwidth.

2. Matched-filter receiver: The error curve presented for the matched-filter receiver was obtained by noting that if attention is restricted to a class of signals whose matched filter can be assumed to be a narrowband filter of bandwidth  $1/T$ , then the calculation of the probability of error reduces to a one-dimensional calculation [Ref. 37] similar to that required in Case I. It may be noted that this class of signals contains many signals of interest, including the FSK signal used in the system studied by Watt, *et al.*

Now, as in Case I, the high SNR case is the most interesting and gives the result

$$\lim_{\frac{E}{Y_0} \rightarrow \infty} P_{e|_{\theta=3}} = \frac{Y_0}{8E} \quad (3.140)$$

Thus the improvement possible using the log-correlator receiver instead of the matched-filter receiver in the presence of additive generalized "t" noise is clear. This is demonstrated in Fig. 24 where the entire error curve is plotted.

3. Noncoherent FSK system: The error curve presented for the FSK system was derived by Watt, et al from measured character error rates. Once again, the advantage to be gained by using a log-correlator receiver instead of the receiver actually employed is obvious. Although all of the details of operation of this receiver are not presented by Watt, it is one of a class of receivers often used in practice and will be considered in more detail in Chapter IV.

The fact that the predicted performance of the log-correlator receiver is much better than that predicted for the matched-filter receiver indicates the necessity of using nonlinear receiving techniques in the presence of additive atmospheric noise. In fact, this is the procedure used in practice in conjunction with long-duration signals. However, the relatively poor performance of the FSK system studied by Watt, et al indicates that some of the receiving techniques used in practice are far from optimum. For example, for the 60 wpm start-stop teletype system considered in Fig. 24, the plotted error curves indicate that an error rate of 1 error per  $10^4$  bits can be achieved using an appropriate log-correlator receiver with an SNR that is 20 to 30 db less than the SNR required by the FSK system analyzed by Watt, et al. This means that there is an order-of-magnitude difference in the transmitter power required by the two systems in order to reach this particular level of performance; and this, of course, has strong economic overtones. As a result, it is of interest to apply the generalized "t" model in an attempt to predict the probability of error resulting from the use of the various receiving techniques that have been proposed for use in additive atmospheric noise. For example, the "smear-desmear" technique mentioned earlier can be investigated using the generalized "t" model. It appears from cursory examination that this technique leads to considerably poorer error performance than that calculated for the log-correlator receiver. This follows from the fact that the performance predicted by Eq. (3.138) for the log-correlator receiver is significantly superior to the performance of an optimal matched-filter receiver in the presence of additive gaussian noise with the same average noise power. Quantitatively, this superiority is equivalent to 12 to 15 db in input SNR; and the fact of this superiority is consistent with

the notion that the additive-atmospheric-noise channel has a higher capacity than the additive-gaussian-noise channel having the same average noise power.

This investigation of proposed receiving techniques will be pursued further in Chapter IV, where proposed nonlinear receiving techniques will be considered.

#### E. SUMMARY AND CONCLUSIONS

The work in this chapter has been concerned with the detection of known signals in additive atmospheric noise. In particular, detailed consideration has been given to the problem of deciding between the two a priori equiprobable hypotheses

$$\left. \begin{array}{l} h^{(1)}: x(t) = m(t) + y(t) \\ h^{(2)}: x(t) = y(t) \end{array} \right\}, \quad 0 \leq t \leq T \quad (3.2)$$

with the smallest probability of error. The additive atmospheric noise  $y(t)$  is represented in this work by the generalized "t" model developed in Chapter II. Two cases are identified:

1. Case I: Short-duration signals. This case is characterized by the fact that the slowly varying modulating process  $a(t)$  in the generalized "t" model can be assumed constant for the duration of the transmitted signal. The correlator receiver described by Eq. (3.23) is found to be optimum in this case, and the probability of error achieved by this receiver is calculated in Eq. (3.44). The probability of error for high SNR is the result of most interest, and is given by

$$\lim_{\substack{E_w \rightarrow \infty \\ \gamma_w}} P_e \Big|_{\theta=3} = \frac{\gamma_w^2}{E_w}, \quad (3.45)$$

where  $\gamma_w^2$  is proportional to the average received "whitened" noise energy and  $E_w$  is the energy of the known signal  $m(t)$  at the output of the whitening filter. The slow decrease with increasing signal energy of this  $P_e$  result, relative to the exponential decrease

achieved in the presence of additive gaussian noise (see Fig. 22), indicates that short-duration signals are not an optimal choice in the presence of atmospheric noise. This is, of course, physically reasonable because of the distinctive impulsive nature of atmospheric noise. This suggests the use of signals of long duration relative to that of the typical noise pulse.

In addition to these short-duration signal results, the Case I assumption was also applied to the situation (Case I<sub>m</sub>) where the additive noise is described by the modified generalized "t" model. The correlator receiver given by Eq. (3.23) continues to be optimum in this case, but the probability of error is now given approximately in the high SNR case by

$$P_{e|_{\theta=2}} \approx \frac{\gamma_w}{\pi} \left\{ \frac{2}{\sqrt{E_w}} \exp\left[-\frac{E_w}{8\beta^2}\right] - \frac{(2\pi)^{1/2}}{\beta} \operatorname{erfc}\left(\frac{\sqrt{E_w}}{2\beta}\right) \right\}. \quad (3.53)$$

This result reduces in form to that given by Eq. (3.45) above when  $(E_w/\beta^2) \ll 1$  is satisfied, which is the case of practical interest at vlf and lf frequencies of operation. On the other hand, (3.53) predicts an exponential decrease in  $P_e$  with increasing signal energy when  $(E_w/\beta^2) \gg 1$  is satisfied; this condition may be approached in practice at hf. Thus it is concluded that short-duration signals are more attractive for use at hf than at lower frequencies of operation. This is consistent with the fact that the received noise loses its impulsive appearance as the frequency of observation increases.

2. Case II: Long-duration signals, the general case. This case is characterized by the fact that the slowly varying process  $a(t)$  is now allowed to vary on the signaling interval. In particular, Case IIa generalized "t" noise is considered in detail and is specified to be that Case II noise whose complex envelope can be described by Eq. (3.76) in terms of 2TB statistically independent samples. This is proposed as the simplest representation of Case II signals of practical interest, and the optimal receiver in this case is found to be a "logarithmic-correlator" receiver (see Fig. 23) which implements the rule

Choose  $h^{(1)}$  iff

$$\int_0^T \ln[|x(t)|^2 + \gamma^2] dt \geq \int_0^T \ln[|x(t) - \mu(t)|^2 + \gamma^2] dt, \quad (3.97)$$

where  $|x(t)|$  is the envelope of  $x(t)$ ,  $|x(t) - \mu(t)|$  is the envelope of  $x(t) - \mu(t)$  and  $\gamma^2$  is proportional to the average received noise power. An "exponentially correct" estimate of the probability of error achieved by this receiver when the transmitted signal energy is distributed uniformly in the signaling interval is given by

$$\lim_{\substack{Y_0 B \\ Q} \rightarrow \infty} P_e \Big|_{\theta=3} \approx f(1/\sqrt{2TB}) \exp \left[ -\frac{1.35 E}{Y_0} \right], \quad (3.138)$$

where  $f(1/\sqrt{2TB})$  is a polynomial in  $(1/\sqrt{2TB})$ ,  $E = QT$  is the energy of the known signal  $m(t)$ , and  $Y_0 = 2(\gamma^2/B)$  is proportional to the average received noise energy. The exponential behavior of this  $P_e$  result is strikingly superior to that given by Eq. (3.45) for short-duration signals. Furthermore, it is shown (see Fig. 24) that this performance of the log-correlator receiver is significantly better than either that achievable by a matched-filter receiver or that actually achieved by a typical FSK vlf communication system. Also, to demonstrate that the asymptotic performance predicted by Eq. (3.138) can be closely approached in practice, the special case  $Y_0 B/Q = 3$  is noted. It is shown in Section D3 that this special case is reasonably achieved in practice, and that it gives the result

$$P_e \Big|_{\substack{\theta=3 \\ Y_0 B \\ Q = 3}} \approx f(1/\sqrt{2TB}) \exp \left[ -\frac{1.15 E}{Y_0} \right]. \quad (3.141)$$

With the above probability-of-error results in mind, it is interesting to note that there is an alternate realization of the log-correlator receiver given by Eq. (3.98) that is approximately equivalent to Eq. (3.97) when the condition  $(Y_0 B)/(4Q) \gg 1$  is satisfied. This realization takes the form:

Choose  $h^{(1)}$  iff

$$\operatorname{Re} \left\{ \int_0^T \frac{x(t) \mu^*(t)}{[|x(t)|^2 + \gamma^2]} dt \right\} \geq \int_0^T \frac{\frac{1}{2} |\mu(t)|^2}{[|x(t)|^2 + \gamma^2]} dt. \quad (3.98)$$

This receiver rule is of interest, since it may be simpler to implement than Eq. (3.97), and since it has a realization closely related to the matched-filter realization of the correlator receiver rule. However, it is important to note that the condition  $(Y_0 B)/(4Q) \gg 1$  is a low signal-to-noise power ratio condition whose satisfaction in practice may introduce more system complexity than it removes, given a desired level of system performance.

Finally, it is concluded that the error performance predicted by Eq. (3.138) for the log-correlator receiver in the presence of additive atmospheric noise is of particular interest, since it is the only theoretical estimate known to the author of the performance achievable in the presence of additive atmospheric noise. Furthermore, the simplicity of the log-correlator receiver indicates that this level of performance can be approached by practically realizable receivers.

#### IV. RELATED TOPICS

##### A. COMPARISON OF THE LOG-CORRELATOR WITH ANOTHER RECEIVER FORM

In the Case II "known signal" considerations in Chapter III, it was shown that the receiver which is optimal in the presence of additive atmospheric noise, in the sense that its use minimizes the probability of error, is the log-correlator receiver. During the discussion of this Case II result, the desirability of comparing the performance predicted for the log-correlator receiver with that obtainable using other receiving techniques was mentioned. In particular, it is desired to compare its performance with that of receivers commonly used in practice. Inspection of the log-correlator receiver (Fig. 23) leads to several qualitative conclusions on this comparison. It is seen that the log-correlator receiver performs essentially four operations as it processes the received signal. In the order of their performance, these operations can be described as follows:

1. The receiver makes use of the "known" nature of the transmitted signal, i.e., the received signal is compared with each of the possible transmitted signals, each of which is known.
2. The results of the comparisons in (1) are nonlinearly processed in a fashion which suppresses the effect on the resultant decision of the comparisons at those times when the received signal is largely the result of a pulse of noise.
3. The results of the zero-memory nonlinear processing of step (2) are summed over the signaling interval.
4. The resultant sums in step (3) are compared against one another and a decision made on the basis of this comparison.

It is important to note that the Case II considerations of Chapter III make the assumption that the received signal has been appropriately bandpass-filtered prior to step (1) above. Several factors enter into the choice of this predetection bandwidth, which is discussed in detail in Chapter III; but in practice the selection procedure can be summarized as follows: At operating frequencies where atmospheric noise is important, the predetection bandwidth should be chosen as large as possible consistent with the exclusion of strong interfering narrowband signals. This means that the limited spectrum availability in the frequency range

of interest is typically the factor that determines the predetection receiver bandwidth.

The receiver form whose performance will be compared here with the performance of the log-correlator receiver is that shown in Fig. 25. This receiver is of interest because of its simplicity of construction, which makes it perhaps the most commonly used receiver form in the presence of additive atmospheric noise. Typical zero-memory nonlinear devices used in the configuration shown in Fig. 25, depending upon the type of modulation employed at the transmitter, are:

1. The wideband "clipper" which operates to limit the amplitude of the received signal when this signal amplitude exceeds a specified level indicating that it is predominantly the result of a pulse of noise.
2. The wideband "limiter", often used with angle modulation schemes, which provides an output signal whose amplitude is fixed independent of the amplitude of the input signal, and whose sign is the same as that of the input signal.

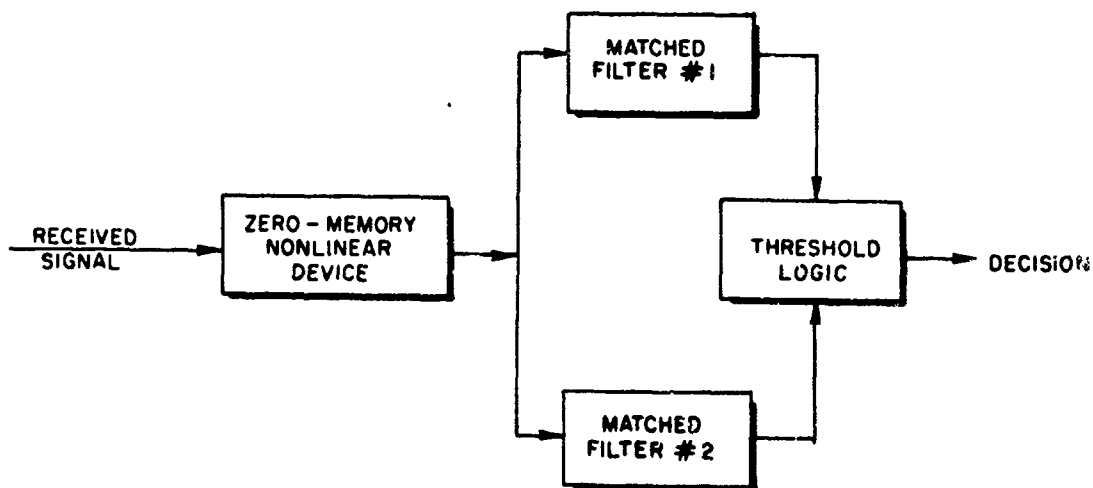


FIG. 25. BLOCK DIAGRAM OF RECEIVER COMMONLY USED IN PRESENCE OF ADDITIVE ATMOSPHERIC NOISE.

Comparison of the performance of the receiver form described in Fig. 25 with the performance previously outlined for the log-correlator receiver proceeds qualitatively as follows: Noting that the predetection filtering required in conjunction with the log-correlator receiver is also required in practice by the receiver described by Fig. 25, it is seen that the two receivers perform similar operations on the received signal, with the exception that the order in which operations (1) and (2) are performed is interchanged. In addition to the fact that the two receivers employ different zero-memory nonlinear devices, it is clear that the receiver described by Fig. 25 must be inferior to the log-correlator receiver because of this interchange of operations. This conclusion follows from the fact that the receiver described by Fig. 25 destroys part of the information known about the possible transmitted signals before it makes use of this information, and thus must perform less well than the optimal log-correlator receiver in the "known signal" situation being considered here. Experimental support for this conclusion was given in Fig. 24, where the performance predicted for the log-correlator receiver is seen to be far superior to that actually achieved by an FSK communication system operating at vlf. Although Watt, et al do not give all of the details of the particular FSK receiver employed, they indicate that it basically has the form described in Fig. 25, where a limiter performs the zero-memory nonlinear operation.

#### B. DETECTION AND ANALYSIS OF WHISTLER-MODE SIGNALS

In addition to the "known signal" detection problem considered so far, it is of interest to consider the application of the generalized "t" model to other signal analysis problems in the presence of additive atmospheric noise. One such problem is the estimation problem in which it is desired to find the "best" (in some sense) estimate to a transmitted signal that is not completely known a priori, given observations at the receiving site--i.e., given observations only after the atmospheric noise has been added. As an example of practical importance, we will consider the problem of detecting the presence of signals propagating in the whistler mode [Ref. 48] and in addition of measuring the defining characteristics of the detected whistler-mode signals. Although no analytical

results are as yet available on this estimation problem in the presence of additive atmospheric noise, it appears worthwhile to note the following: The whistler-mode signals which it is desired to analyze are described in detail by Helliwell [Ref. 48], and can be described for the purposes of this discussion as vlf signals possessing a very large time-bandwidth product, i.e., bandwidths of the order of 10 kc and durations of the order of one second. Furthermore, the name "whistler" stems from the fact that these signals typically consist of a gliding tone which sweeps across the vlf band from high to low frequencies producing an audible "whistle."

#### 1. Analysis of Typical Whistler Receivers

The purpose of this investigation of the whistler estimation problem is twofold: to consider the usefulness of the generalized "t" model in formulating a solution to this problem, and to use the insights gained in the known-signal problem for evaluating the performance of receiver forms presently used in whistler analysis. Thus in order to proceed, the receiver form typically used to study whistlers in the presence of additive atmospheric noise is presented in Fig. 26. The zero-memory nonlinear device normally used in this configuration is the wideband clipper described in connection with Fig. 25, so that this receiver will henceforth be called

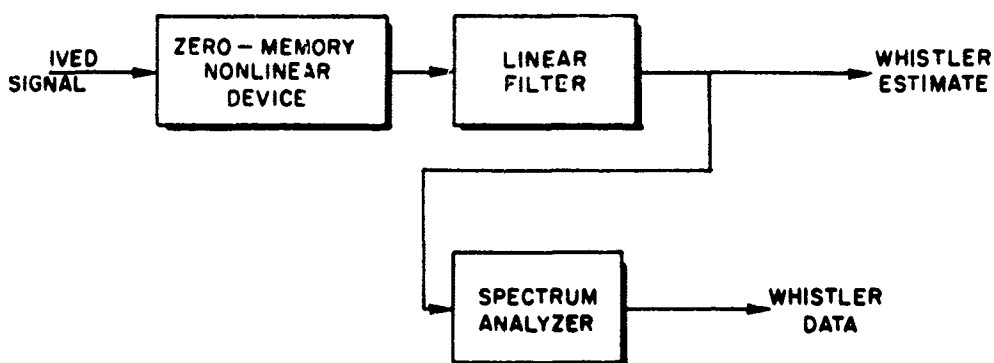


FIG. 26. BLOCK DIAGRAM OF CLIPPER RECEIVER COMMONLY USED TO ANALYZE WHISTLER SIGNALS.

a "clipper receiver." In order to proceed with the analysis of this receiver, it is first of all noted that the Case II known-signal results cannot be applied directly, since the information known about the whistler and of course that utilized by the clipper receiver is not sufficient to make the whistler a known signal. Rather, we can conclude that if the whistler to be analyzed can be further specified so that the problem becomes a known-signal problem, then the log-correlator receiver is the optimal receiver. Otherwise (as is usually the case since it is the detailed measurement of whistler parameters that is of scientific importance) the optimal receiver is not obvious, and the clipper receiver is a candidate whose use can be supported on physical grounds. In order to show this, it is noted that whereas the whistler is characterized by both a large bandwidth and long duration, the received whistler signal is contaminated by additive noise which primarily comes from two distinct sources:

1. Additive atmospheric noise: This noise, which is discussed in detail in Chapter II, has a bandwidth of the order of 10 kc (no narrowband assumption here) and can be characterized as a sequence of noise pulses, each of which has a duration of much less than one second.
2. Narrowband interfering signals: In contrast to the communication situation where a narrowband assumption is reasonable, the wide bandwidth of the whistler means that strong narrowband interfering communication signals may exist within the frequency band of interest.

With this description of the additive noise in mind, the performance of the clipper receiver can be investigated by examining the operations performed by the individual receiver components. This examination shows that in fact the clipper receiver is a good candidate for use in the presence of the additive noise described above, since it suppresses the effect of the noise on the spectrum analyzer output in the following ways:

1. The wideband clipper serves to reduce the effect of atmospheric noise pulses before these pulses can be "smeared" in time by the narrowband filters comprising the typical spectrum analyzer. It is clear that the usefulness of the clipper depends upon the ability of the operator to set the clip level close to the maximum level of the received whistler. This ability is a function of knowledge both of the level of the whistler signal and of the level of narrowband interfering signals. (The problem of optimally setting the clip level is discussed further below.)
2. The effect of narrowband interfering signals is suppressed by the fact that they contaminate only a small portion of the frequency

band examined by the spectrum analyzer. Thus the observer at the output of the spectrum analyzer is able to pick out the whistler signal by simply ignoring the spectral lines produced by the narrow-band interference.

It is important to note that although the above discussion indicates that narrowband interfering signals are not directly a problem, they may be an important factor in preventing an optimum setting of the clip level. Thus it is seen that the actual interfering signal environment is important in the analysis of the performance of the clipper receiver, and, of course, is also important in any analytical formulation of the whistler estimation problem. In fact, the above discussion dictates that the clipper receiver performs best when strong narrowband interfering signals are removed by selective linear filtering prior to the performance of the clipping operation. Having removed these strong interfering signals ("strong" refers here to the situation where the received interfering signal power is significantly greater than that of the received whistler), the performance of the clipper receiver becomes a function of how well the level of the whistler signal to be analyzed is known. In fact, if this level is known quite precisely, and if the setting of the clip level just above this known signal level results in clipping for only a small percentage of the time, then the clipper appears to be a good choice of nonlinearity that is effective in suppressing the additive atmospheric noise. On the other hand, if the whistler signal level is known only approximately (perhaps only statistically), or if the setting of the clip level just above the known signal level results in clipping a large percentage of the time, then it appears that there must certainly be another nonlinearity which performs better than the wideband clipper.

## 2. Conclusions

The foregoing discussion has been presented to specify an estimation problem of practical interest in the presence of additive atmospheric noise. The clipper receiver typically used in the analysis of whistlers has been examined in some detail, and is seen to operate on the received signal in a fashion that agrees both with intuition and with the results of the known-signal detection problem. However, the discussion also indicates that the clipper receiver is certainly suboptimal if either the power level of the

whistler signal is unknown or the whistler signal is a very weak signal-- i.e., if there is a very low SNR characterized by clipping for a large percentage of the time. Since usually the first and often both of these conditions are characteristic of the whistler estimation problem in practice, it is proposed that improved receiving techniques may result from applying the generalized "t" model to the whistler estimation problem. This possibility will be considered further in Chapter V.

## V. SUMMARY AND CONCLUSIONS

### A. THE GENERALIZED "t" MODEL FOR RECEIVED ATMOSPHERIC NOISE

This work has been concerned with the development and application of an analytical model for impulsive phenomena. In particular, the work has focused on a specific impulsive phenomenon, atmospheric radio noise.

In Chapter II a new model, called the generalized "t" model, was developed and was verified to be appropriate as a description of received atmospheric noise, i.e., atmospheric noise as observed through a given receiver passband. This generalized "t" model describes the received atmospheric noise  $y(t)$  as

$$y(t) = a(t) n(t) , \quad (2.3)$$

where  $n(t)$  is a zero-mean narrowband gaussian process with covariance function  $R_n(\tau)$  and  $a(t)$  is a stationary, slowly varying random process, independent of  $n(t)$ , that modulates  $n(t)$ . This modulating process  $a(t)$  is further described as

$$a(t) = 1/b(t) , \quad (2.72)$$

where the first-order statistics of  $b(t)$  are specified by the two-sided chi distribution given by Eq. (2.8).

The applicability of the generalized "t" model as a description of received atmospheric noise was considered in detail in Chapter II, and the pertinent results can be summarized as follows: The first-order statistics of the generalized "t" model are in good agreement with measured data on received atmospheric noise. This agreement is demonstrated in Figs. 4 to 13 and in Fig. 15, and it is noted that this agreement is particularly good at vlf and lf in those situations characterized by low-to-moderate local thunderstorm activity. In addition to this good agreement of first-order statistics, the higher-order statistics of the generalized "t" model can be specified to give good agreement with measured data on these statistics. This result is demonstrated in Fig. 18, where the plotted data indicate that the higher-order statistics of the modulating process  $a(t)$  can be

specified [it is noted that these statistics are not yet specified in Eq. (2.72) above] to reproduce the experimentally observed probability distribution of the interval between successive crossings of a fixed level by the envelope of the noise.

The investigation into the applicability of the generalized "t" model leads to the conclusion that this new model is an analytically attractive model that is appropriate for received atmospheric noise. Furthermore, it was pointed out in Chapter II that the generalized "t" model will be useful in the study of signal detection and estimation problems in the presence of additive atmospheric noise. This follows from the fact that limited spectrum availability generally dictates that the received signal be observed through a bandwidth that, in fact, is substantially smaller than the band center frequency.

#### B. DETECTION OF KNOWN SIGNALS IN ADDITIVE ATMOSPHERIC NOISE

Having developed and checked the applicability of the generalized "t" model in Chapter II, this model was applied in Chapter III to the detection of known signals in additive atmospheric noise. In particular, the problem of deciding between the two a priori equally probable hypotheses

$$\left. \begin{array}{l} h^{(1)}: x(t) = m(t) + y(t) \\ h^{(2)}: x(t) = y(t) \end{array} \right\}, \quad 0 \leq t \leq T \quad (3.2)$$

with the smallest probability of error was considered in detail. The additive atmospheric noise was represented by the generalized "t" model and two cases were identified:

##### 1. Case I: Short-Duration Signals

This case is characterized by the fact that the slowly varying modulating process  $a(t)$  in the generalized "t" model can be assumed constant for the duration of the transmitted signal. The familiar correlator receiver described by Eq. (3.23) was found to be optimum in this case, and the probability of error achieved by this receiver was calculated in Eq. (3.44). The probability of error result for high SNR is the result of most interest. It is given by

$$\lim_{\frac{E_w}{\gamma_w} \rightarrow \infty} P_{e|\theta=3} = \frac{\gamma_w^2}{E_w^2}, \quad (3.45)$$

where  $\gamma_w^2$  is proportional to the average received whitened noise energy and  $E_w$  is the energy of the known signal  $m(t)$  at the output of the whitening filter. The slow decrease with increasing signal energy of this  $P_e$  result, relative to the exponential decrease achieved by the correlator receiver in the presence of additive gaussian noise (see Fig. 22), leads to the conclusion that short-duration signals are not an optimal choice in the presence of additive atmospheric noise. This is, of course, physically reasonable since the distinctive impulsive nature of atmospheric noise suggests the use of signals of long duration relative to that of the typical noise pulse.

## 2. Case II: Long-Duration Signals, The General Case

This case is characterized by the fact that the slowly varying process  $a(t)$  is now allowed to vary during the signaling interval. In particular, Case IIa generalized "t" noise was considered in detail. It is specified to be that Case II noise whose complex envelope can be described by Eq. (3.76) in terms of 2TB statistically independent samples. This is proposed as the simplest representation of Case II signals of practical interest. The optimal receiver in this case was found to be a logarithmic-correlator receiver (see Fig. 23) that implements the rule:

Choose  $h^{(1)}$  iff

$$\int_0^T \ln[|x(t)|^2 + \gamma^2] dt \geq \int_0^T \ln[|x(t) - \mu(t)|^2 + \gamma^2] dt, \quad (3.97)$$

where  $|x(t)|$  is the envelope of  $x(t)$ ,  $|x(t) - \mu(t)|$  is the envelope of  $[x(t) - m(t)]$ , and  $\gamma^2$  is proportional to the average received noise power. An exponentially correct estimate of the probability of error

achieved by this receiver when the transmitted signal energy is distributed uniformly in the signaling interval is given by

$$\lim_{\substack{Y_0 B \\ Q} \rightarrow \infty} P_e \Big|_{\theta=3} \approx f\left(\frac{1}{\sqrt{2TB}}\right) \exp\left[-\frac{1.35 E}{Y_0}\right], \quad (3.138)$$

where  $f(1/\sqrt{2TB})$  is a polynomial in  $(2TB)^{-1/2}$ ,  $E = QT$  is the energy of the known signal  $m(t)$ , and  $Y_0 = 2\gamma^2/B$  is proportional to the average received noise energy. The exponential behavior of this  $P_e$  result is strikingly superior to that given by Eq. (3.45) for short-duration signals. Furthermore, it was shown (see Fig. 24) that this error performance predicted for the log-correlator receiver is significantly better than either that achievable by a matched-filter receiver or that actually achieved in practice by a typical FSK vlf communication system.

Also, to demonstrate that the asymptotic performance predicted by Eq. (3.138) for the log-correlator receiver can be closely approached in practice, we note the special case  $Y_0 B/Q = 3$ . It was shown in Chapter III that this special case is reasonably achieved in practice, and that it gives the result:

$$P_e \Big|_{\substack{\theta=3 \\ Y_0 B \\ Q = 3}} \approx f\left(\frac{1}{\sqrt{2TB}}\right) \exp\left[-\frac{1.15 E}{Y_0}\right]. \quad (3.141)$$

With the above probability of error results in mind, it is interesting to note that there is an alternate realization of the log-correlator receiver that is approximately equivalent to Eq. (3.97) when the condition  $(Y_0 B)/(4Q) \gg 1$  is satisfied. This realization takes the form:

Choose  $h^{(1)}$  iff

$$\operatorname{Re} \left\{ \int_0^T \frac{x(t) \mu^*(t)}{[|x(t)|^2 + \gamma^2]} dt \right\} \geq \int_0^T \frac{\frac{1}{2} |\mu(t)|^2}{[|x(t)|^2 + \gamma^2]} dt. \quad (3.98)$$

This receiver rule is of interest, since it may be easier to implement than Eq. (3.97), and since it has a realization closely related to the matched-filter realization of the correlator receiver rule.

The above summary of results on the general case of long-duration signals leads to the conclusion that the error performance predicted by Eq. (3.138) for the log-correlator receiver in the presence of additive atmospheric noise is a result of particular interest. This follows because Eq. (3.138) gives the only theoretical estimate known to the author of the error performance achievable in the presence of additive atmospheric noise. Furthermore, the reasonable simplicity of the log-correlator receiver indicates that this level of performance can be approached by practically realizable receivers.

#### C. RECOMMENDATIONS FOR FUTURE WORK

In Chapter IV, the operation of the log-correlator receiver was compared with that of a nonlinear receiver form commonly used in practice in the presence of additive atmospheric noise. A qualitative discussion was presented there to indicate why this commonly used receiver form must perform in a suboptimal fashion. However, the analytical difficulties involved in making this comparison quantitative, plus the need for experimental verification of the performance predicted by Eq. (3.138) for the log-correlator receiver, lead to the obvious recommendation that the log-correlator receiver be built and compared experimentally with receiver forms commonly used in the presence of additive atmospheric noise.

Also in Chapter IV, the statistical estimation problem in the presence of atmospheric noise was briefly considered as it pertains to the problem of obtaining the "best" (in some sense) estimate of a whistler mode signal that has been contaminated by additive atmospheric noise. As was pointed out there, the scientific importance of the whistler estimation problem indicates that the generalized "t" model can perhaps be fruitfully applied to the statistical estimation problem in the presence of additive atmospheric noise. Related to this problem, it is suggested that another problem of interest is the two-hypotheses communications problem, in which the signal whose presence is to be tested is taken to be random, i.e., is known only statistically. Furthermore, it is proposed that a procedure

that may give results applicable to the whistler estimation problem is to consider the two-hypotheses testing problem in which the random signal is taken to be a gaussian process.

Finally, returning to the generalized "t" model itself, it is proposed that an interesting problem consists of choosing the covariance matrices  $\Phi_v$  and  $R_b$  introduced in Chapter III in a manner which reproduces the probability distribution of the inter-level-crossing interval observed in practice for received atmospheric noise. In this regard it is pointed out that the calculations of the inter-level-crossing interval distribution in Chapter II indicate the existence of the desired covariance matrices.

## APPENDIX A. EVALUATION OF INTEGRALS

1. An integral that appears in consideration of the modified generalized "t" model has the form

$$I = \int_b^{\infty} x^{n/2} \exp[ax] dx, \quad n \text{ odd } \geq 1, \quad a < 0, \quad b > 0. \quad (\text{A.1})$$

This integral can be evaluated by parts, giving the result

$$\begin{aligned} I = \exp[ax] & \left\{ \frac{x^{n/2}}{a} - \frac{\left(\frac{n}{2}\right) x^{(n-2)/2}}{a^2} + \frac{\left(\frac{n}{2}\right) \left[\frac{(n-2)}{2}\right] x^{(n-4)/2}}{a^3} \right. \\ & - \dots (-1)^{(n-3)/2} \frac{\left(\frac{n}{2}\right) \left[\frac{(n-2)}{2}\right] \dots \left(\frac{5}{2}\right) (1) x^{3/2}}{(n-1)/2} \Bigg|_{x=b}^{x=\infty} \\ & + (-1)^{(n-1)/2} \frac{\left(\frac{n}{2}\right) \left[\frac{(n-2)}{2}\right] \dots \left(\frac{3}{2}\right) (1)}{a^{(n-1)/2}} \int_b^{\infty} x^{1/2} \exp[ax] dx, \end{aligned} \quad (\text{A.2})$$

and:

$$\int_b^{\infty} x^{1/2} \exp[ax] dx = 2 \int_{b^{1/2}}^{\infty} z^2 \exp[az^2] dz,$$

where:  $z^2 = x$

$$= 2 \left\{ \frac{1}{2a} z \exp[az^2] \Big|_{z=b^{1/2}}^{z=\infty} - \frac{1}{2a} \int_{b^{1/2}}^{\infty} \exp[az^2] dz \right\}$$

$$= \frac{z}{a} \exp[az^2] \Big|_{z=b^{1/2}}^{z=\infty} - \frac{1}{a} \left(-\frac{\pi}{a}\right)^{1/2} \int_{(-2ab)^{1/2}}^{\infty} \frac{1}{(2\pi)^{1/2}} \exp\left[-\frac{\tau^2}{2}\right] d\tau ,$$

where:  $\tau = (-2a)^{1/2} z$

$$= \frac{z}{a} \exp[az^2] \Big|_{z=b^{1/2}}^{x=\infty} - \frac{1}{a} \left(-\frac{\pi}{a}\right)^{1/2} \operatorname{erfc}(\sqrt{-2a} b) . \quad (\text{A.3})$$

Thus, substituting into (A-2);

$$I = \exp[ab] \left\{ -\frac{b^{n/2}}{a} + \frac{\left(\frac{n}{2}\right) b^{(n-2)/2}}{a^2} - \frac{\left(\frac{n}{2}\right) \left[\frac{(n-2)}{2}\right] b^{(n-4)/2}}{a^3} \right.$$

$$+ \dots (-1)^{(n-1)/2} \frac{\left(\frac{n}{2}\right) \left[\frac{(n-2)}{2}\right] \dots \left(\frac{5}{2}\right) (1) b^{3/2}}{a^{(n-1)/2}} \left. \right\}$$

$$+ (-1)^{(n-1)/2} \frac{\left(\frac{n}{2}\right) \left[\frac{(n-2)}{2}\right] \dots \left(\frac{3}{2}\right) (1)}{a^{(n+1)/2}} \left\{ -b^{1/2} \exp[ab] \right.$$

$$\left. - \left(-\frac{\pi}{a}\right)^{1/2} \operatorname{erfc}(\sqrt{-2a} b) \right\} . \quad (\text{A.4})$$

2. An integral that appears in the Case IIa probability-of-error calculations has the form

$$\begin{aligned}
 II &= \int_{-\infty}^{\infty} \frac{1}{(x^2 + a^2)[(x - b)^2 + a^2]} dx, \quad a^2, b \neq 0 \\
 &= \int_{-\infty}^{\infty} \frac{1}{(x + ia)(x - ia)(x - b + ia)(x - b - ia)} dx. \quad (A.5)
 \end{aligned}$$

This integral is easily evaluated as a contour integral as described in Fig. 27.

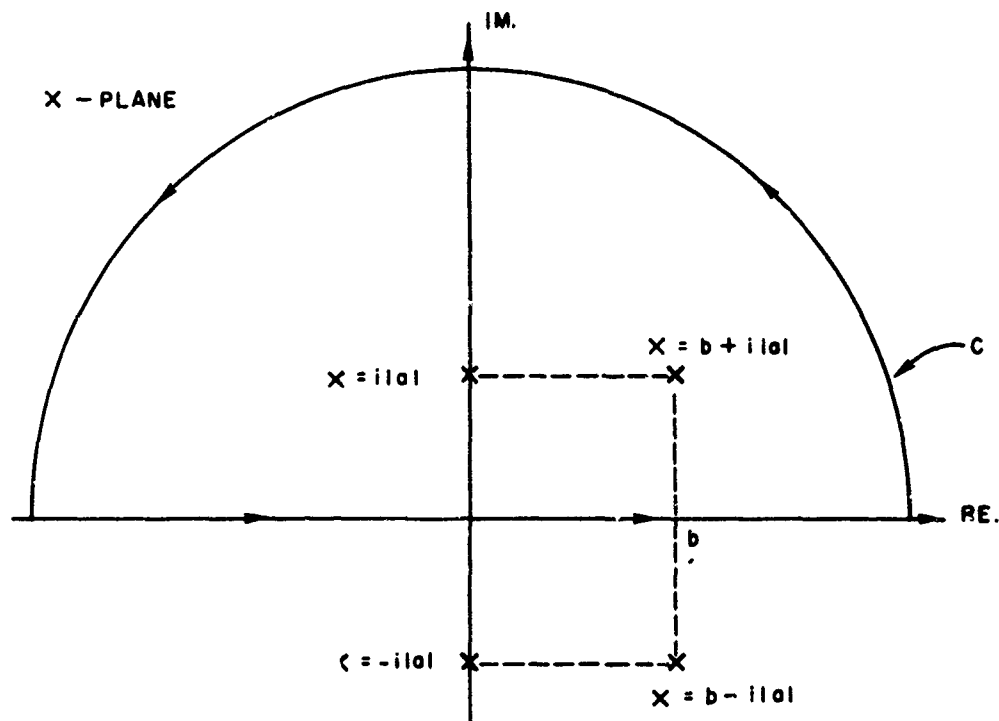


FIG. 27. DESCRIPTION OF CONTOUR OF INTEGRATION USED TO EVALUATE EQ. (A.5).

- Note: 1) The contour of integration C is closed at  $|x| = \infty$ .  
 2) The poles of the integrand plotted above are for the special case  $b > 0$ .

Now, it is clear that

$$II = \oint_C \frac{1}{(x + ia)(x - ia)(x - b + ia)(x - b - ia)} dx = 2\pi i \sum_{j=1}^2 K_j, \quad (A.6)$$

where

$$\begin{aligned} \frac{1}{(x + ia)(x - ia)(x - b + ia)(x - b - ia)} &= \frac{K_1}{x - i|a|} + \frac{K_2}{x - i|a|} \\ &+ \frac{K_3}{x + i|a|} + \frac{K_4}{x - b - i|a|} \end{aligned}$$

such that, for the residues  $K_1$  and  $K_2$  of interest:

$$K_1 = \frac{1}{2i|a|[(i|a| - b)^2 + a^2]} = \frac{1}{2i|a|(b^2 - 2i|a|b)} \quad (A.7)$$

$$K_2 = \frac{1}{2i|a|[(b + i|a|)^2 + a^2]} = \frac{1}{2i|a|(b^2 + 2i|a|b)} \quad (A.8)$$

Thus, substituting into (A.6) there results

$$II = \frac{2\pi}{|a|(b^2 + 4a^2)}.$$

APPENDIX B. PROOF THAT EQ. (3.126),  $\mu_N'(s) = 0$ , IS UNIQUELY SATISFIED  
BY  $s = 1$ .

In the calculation of the Chernoff bound on  $P_e$  in Case IIa, it is necessary to find the value of  $s(\text{finite}) > 0$  which satisfies the equation

$$\sum_{i=1}^N \frac{\int_{-\infty}^{\infty} dx \int_{-\infty}^{\infty} dy \frac{(x^2 + y^2 + \xi^2)^{s-2}}{[(x - \mu_i)^2 + y^2 + \xi^2]^s} \ln \left[ \frac{x^2 + y^2 + \xi^2}{(x - \mu_i)^2 + y^2 + \xi^2} \right]}{\int_{-\infty}^{\infty} dx \int_{-\infty}^{\infty} dy \frac{(x^2 + y^2 + \xi^2)^{s-2}}{[(x - \mu_i)^2 + y^2 + \xi^2]^s}} = 0 . \quad (\text{B.1})$$

Noting that the denominator of the summand is positive and finite for all  $i$  and all finite  $s$ , it is first of all concluded that each term of the sum must be zero if the sum itself is to be zero, since for any given  $s$  the sign must be the same for each term in the sum. Thus it is concluded that we desire that value of  $s > 0$  which satisfies the equation

$$I(s) \triangleq \int_{-\infty}^{\infty} dx \int_{-\infty}^{\infty} dy \frac{(x^2 + y^2 + \xi^2)^{s-2}}{[(x - \mu_i)^2 + y^2 + \xi^2]^s} \ln \left[ \frac{x^2 + y^2 + \xi^2}{(x - \mu_i)^2 + y^2 + \xi^2} \right] = 0 , \quad \forall i = 1, \dots, N . \quad (\text{B.2})$$

It will now be demonstrated that (B.2) is uniquely satisfied by  $s = 1$ .  
Setting  $s = 1$  in (B.2), it is desired to evaluate

$$\begin{aligned}
I(s) \Big|_{s=1} &= \int_{-\infty}^{\infty} dx \int_{-\infty}^{\infty} dy \frac{1}{(x^2 + y^2 + \xi^2)[(x - \mu_1)^2 + y^2 + \xi^2]} \\
&\quad \cdot \ln \frac{x^2 + y^2 + \xi^2}{(x - \mu_1)^2 + y^2 + \xi^2} \\
&= \int_{-\infty}^{\infty} dx \int_{-\infty}^{\infty} dy \frac{1}{(x^2 + y^2 + \xi^2)[(x - \mu_1)^2 + y^2 + \xi^2]} \\
&\quad \cdot \ln(x^2 + y^2 + \xi^2) \\
&\quad - \int_{-\infty}^{\infty} dx \int_{-\infty}^{\infty} dy \frac{1}{(x^2 + y^2 + \xi^2)[(x - \mu_1)^2 + y^2 + \xi^2]} \\
&\quad \cdot \ln[(x - \mu_1)^2 + y^2 + \xi^2] \\
&= \int_{-\infty}^{\infty} dx \int_{-\infty}^{\infty} dy \frac{1}{(x^2 + y^2 + \xi^2)[(x - \mu_1)^2 + y^2 + \xi^2]} \\
&\quad \cdot \ln(x^2 + y^2 + \xi^2) \\
&\quad - \int_{-\infty}^{\infty} d\tau \int_{-\infty}^{\infty} dy \frac{1}{[(\tau + \mu_1)^2 + y^2 + \xi^2](\tau^2 + y^2 + \xi^2)} \\
&\quad \cdot \ln(\tau^2 + y^2 + \xi^2)
\end{aligned}$$

where  $\tau = x - \mu_1$ . Therefore,

$$\begin{aligned}
I(s) \Big|_{s=1} &= \int_{-\infty}^{\infty} dx \int_{-\infty}^{\infty} dy \left\{ \frac{1}{(x^2 + y^2 + \xi^2)[(x - \mu_1)^2 + y^2 + \xi^2]} \right. \\
&\quad \left. - \frac{1}{y^2 + \xi^2[(x + \mu_1)^2 + y^2 + \xi^2]} \right\} \ln(x^2 + y^2 + \xi^2) \\
&= \int_{-\infty}^{\infty} dy \int_{-\infty}^{\infty} dx \frac{(x + \mu_1)^2 + (x - \mu_1)^2}{(x^2 + y^2 + \xi^2)[(x + \mu_1)^2 + y^2 + \xi^2][(x - \mu_1)^2 + y^2 + \xi^2]} \\
&\quad \cdot \ln(x^2 + y^2 + \xi^2) \\
&= \int_{-\infty}^{\infty} dy \int_{-\infty}^{\infty} dx \frac{2\mu_1 x}{(x^2 + y^2 + \xi^2)[(x^2 - \mu_1^2)^2 + (y^2 + \xi^2)(2x^2 + 2\mu_1^2)]} \\
&\quad \cdot \ln(x^2 + y^2 + \xi^2) . \tag{B.3}
\end{aligned}$$

Thus it follows directly that  $I(s) \Big|_{s=1} = 0$ , since the integrand above is seen to be odd in  $x$ .

Now, to show that this solution is unique, consider the following:

$$\begin{aligned}
\frac{d}{ds} I(s) &= \int_{-\infty}^{\infty} dx \int_{-\infty}^{\infty} dy \frac{1}{(x^2 + y^2 + \xi^2)^2} \ln \left[ \frac{x^2 + y^2 + \xi^2}{(x - \mu_1)^2 + y^2 + \xi^2} \right] \\
&\quad \cdot \left\{ \frac{d}{ds} \left[ \left( \frac{x^2 + y^2 + \xi^2}{(x - \mu_1)^2 + y^2 + \xi^2} \right)^s \right] \right\} \\
&= \int_{-\infty}^{\infty} dx \int_{-\infty}^{\infty} dy \frac{(x^2 + y^2 + \xi^2)^{s-2}}{[(x - \mu_1)^2 + y^2 + \xi^2]^s} \ln^2 \left[ \frac{x^2 + y^2 + \xi^2}{(x - \mu_1)^2 + y^2 + \xi^2} \right] . \tag{B.4}
\end{aligned}$$

Thus,  $d/ds I(s) > 0 \forall s$ , such that  $s = 1$  is shown to be the unique solution to  $\mu'_N(s) = 0$ , and the proof is thus complete.

APPENDIX C. PROOF THAT INFINITE RECEIVER BANDWIDTH ( $2B = \infty$ ) MINIMIZES  
THE CASE IIa  $P_e$  RESULT

In the  $P_e$  calculations of Case IIa, an exponentially correct estimate of the probability of error optimized with respect to signal shape is given by expression (3.135):

$$P_{e|_{\theta=3}} \approx f\left(\frac{1}{\sqrt{2TB}}\right) \left\{ {}_2F_1\left(1, \frac{1}{2}; \frac{3}{2}; 1 - \frac{Y_0 B}{Q + Y_0 B}\right) \frac{Y_0 B}{Q + Y_0 B} \right\}^{2TB}$$

$$= f\left(\frac{1}{\sqrt{2TB}}\right) \left\{ {}_2F_1\left(1, \frac{1}{2}; \frac{3}{2}; \frac{1}{1 + \frac{Y_0 B}{Q}}\right) \frac{\frac{Y_0 B}{Q}}{1 + \frac{Y_0 B}{Q}} \right\}^{2TB} \quad (3.135)$$

Noting that  $Y_0$  and  $Q$  are not functions of the receiver bandwidth  $2B$ , the optimal bandwidth can be determined by optimizing with respect to  $k$ , where  $k \triangleq Y_0 B/Q$ . Thus, in terms of this new parameter

$$P_{e|_{\theta=3}} \approx f\left(\frac{1}{\sqrt{2TB}}\right) \left\{ {}_2F_1\left(1, \frac{1}{2}; \frac{3}{2}; \frac{1}{1+k}\right) \frac{k}{1+k} \right\}^{\frac{2TQ}{Y_0} k}$$

$$= f\left(\frac{1}{\sqrt{2TB}}\right) \left\{ \left[ {}_2F_1\left(1, \frac{1}{2}; \frac{3}{2}; \frac{1}{1+k}\right) \frac{k}{1+k} \right]^k \right\}^{\frac{2E}{Y_0}}, \quad (C.1)$$

where  $E = QT$  is the energy of the known signal. Now, neglecting the  $f(1/\sqrt{2TB})$  factor, since it is of negligible importance in comparison to the factor that varies exponentially with  $2TB$ , the optimization problem reduces to that of finding the value of  $k \geq k_{\min}$  which minimizes the function

$$g(k) = \left[ \frac{k}{1+k} {}_2F_1\left(1, \frac{1}{2}; \frac{3}{2}; \frac{1}{1+k}\right) \right]^k, \quad (C.2)$$

where  $k_{\min} = Y_0/(2E)$ .<sup>†</sup>

Perhaps the simplest way to minimize  $g(k)$  is to plot it vs  $k$ , since it is seen in this way that in fact  $g(k)$  is a monotonically decreasing function of  $k \geq 0$ . From this it follows directly that the optimal choice for the receiver bandwidth is  $B = \infty$ , and the proof is thus complete. Such a plot of  $g(k)$  is not presented here, but a formula from which it can be easily prepared is presented as follows: Using Erdelyi [Ref. 49], items 2.8(18) and 2.8(16), it is seen that

$$\begin{aligned} {}_2F_1\left(1, \frac{1}{2}; \frac{3}{2}; \frac{1}{1+k}\right) &= {}_2F_1\left(\frac{1}{2}, 1; \frac{3}{2}; \frac{1}{1+k}\right) \\ &= \frac{(1+k)^{1/2}}{2} \ln \left[ \frac{(1+k)^{1/2} + 1}{(1+k)^{1/2} - 1} \right]. \end{aligned} \quad (C.3)$$

Thus:

$$g(k) = \left\{ \frac{k}{2(1+k)^{1/2}} \ln \left[ \frac{(1+k)^{1/2} + 1}{(1+k)^{1/2} - 1} \right] \right\}^k; \quad (C.4)$$

and, for particular values of  $k$  of interest, it is seen that (C.4) gives:

1.  $\lim_{k \rightarrow 0} g(k) = 1$ ;
2.  $g(0.125) \approx 0.821$ ;
3.  $g(0.5) \approx 0.684$ ;
4.  $g(5) \approx 0.544$ ;
5.  $\lim_{k \rightarrow \infty} g(k) \approx 0.5129$ .

<sup>†</sup>This minimum value results from the constraint that the receiver bandwidth must be at least as large as the signal bandwidth; i.e.,  $2B \geq 1/T$ , where, as mentioned in the text, the choice of  $T$  that minimizes  $\bar{P}_e$  is clearly  $T = \infty$ .

## REFERENCES

1. A. D. Watt and E. L. Maxwell, "Characteristics of Atmospheric Noise from 1 to 100 kc," Proc. of IRE, 45, June 1957, pp. 787-94.
2. H. Norinder, "The Waveforms of the Electric Field in Atmospherics Recorded Simultaneously by Two Distant Stations," Arkiv for Geofysik, 2, November 1954, pp. 161-95.
3. E. F. Florman, NBS Report No. 3558, 10 November 1955.
4. F. L. Hill, "Very Low Frequency Radiation from Lightning Strokes," Proc. of IRE, 45, June 1957, pp. 775-77.
5. D. Middleton, Introduction to Statistical Communication Theory, McGraw-Hill Book Co., Inc., New York, 1961.
6. K. Furutsu and T. Ishida, "On the Theory of Amplitude Distribution of Impulse Noise," J. of Applied Physics, 32, July 1961, pp. 1206-21.
7. B. A. Bowen, "Some Analytical Techniques for a Class of Non-Gaussian Processes," Queen's University Research Rept. No. 63-3, June 1963.
8. J. Galejs, "Amplitude Distributions of Radio Noise at ELF and VLF," J. Geophys. Res., 71, January 1966, pp. 201-16.
9. A. D. Watt and E. L. Maxwell, "Measured Statistical Characteristics of VLF Atmospheric Radio Noise," Proc. of IRE, 45, January 1957, pp. 55-62.
10. C. Clarke, P. A. Bradley and D. E. Mortimer, "Characteristics of Atmospheric Radio Noise Observed at Singapore," Proc. of IEE, 112, May 1965, pp. 849-60.
11. W. Q. Crichlow, A. D. Spaulding, C. J. Roubique and R. T. Disney, "Amplitude Probability Distributions for Atmospheric Radio Noise," NBS Monograph 23, 1960.
12. O. Ibukun, "Structural Aspects of Atmospheric Radio Noise in the Tropics," Proc. of IEEE, 54, March 1966, pp. 361-67.
13. J. G. Kneuer, "A Simplified Physical Model for Amplitude Distribution of Impulsive Noise," IEEE Trans. on Communication Technology, Com-12, December 1964, p. 220.
14. P. Beckmann, "Amplitude Probability Distribution of Atmospheric Radio Noise," Radio Science, 68D, June 1964, pp. 723-36.
15. G. Foldes, "The Lognormal Distribution and its Applications to Atmospheric Studies," Statistical Methods in Radio Wave Propagation, W. C. Hoffman, ed., Pergamon Press, Oxford, England, 1960, pp. 227-32.

16. T. Nakai, "The Study of Amplitude Probability Distribution of Atmospheric Radio Noise," Proc. Res. Inst. Atmos., (Japan), 7, January 1960, pp. 12-17.
17. R. M. Lerner, "Design of Signals," Lectures on Communication System Theory, E. J. Baghdady, ed., McGraw-Hill Book Co., Inc., New York, 1961, pp. 243-77.
18. P. Mertz, "Model of Impulsive Noise for Data Transmission," IRE Trans. on Communications Systems, June 1961, pp. 130-37.
19. P. Mertz, "Impulse Noise and Error Performance in Data Transmission," Rand Memorandum RM-4526-PR, April 1965.
20. B. Mandelbrot, "Self-Similar Turbulence and Non-Wienerian Conditioned Spectra," privately circulated IBM Research Paper, 1964.
21. B. Mandelbrot, "1/f Noises and the Infrared Catastrophe," privately circulated research note, full paper read at IEEE Symp. on Time Varying Channels, June 1965.
22. E. Parzen, Modern Probability Theory and Its Applications, John Wiley and Sons, Inc., New York, 1960.
23. H. B. Dwight, Tables of Integrals and Other Mathematical Data, 4th Edition, The Macmillan Co., New York, 1962.
24. S. O. Rice, "Mathematical Analysis of Random Noise," Bell System Tech. Journal, 23 and 24, 1944, 1945.
25. T. Nakai, "Calculated Statistical Characteristics of Atmospheric Radio Noise," Proc. Res. Inst. Atmos. (Japan), 10, January 1963, pp. 13-24.
26. N. Abramson, Course Notes EE251a, Stanford University, 1964.
27. J. Harwood, "Atmospheric Radio Noise at Frequencies Between 10 kc/s and 30 kc/s," Proc. of IEE, 105B, 1958, p. 293.
28. M. S. Longuet-Higgins, "The Distribution of Intervals Between Zeroes of a Stationary Random Function," Phil. Trans. of the Roy. Soc., London, 254, 1962, p. 557.
29. J. A. McFadden, "The Axis Crossing Intervals of Random Functions," IRE Trans. on Information Theory, IT-2, December 1956, pp. 146-50.
30. W. B. Davenport and W. L. Root, Random Signals and Noise, McGraw-Hill Book Co., Inc., New York, 1958.
31. H. O. Pollak, H. J. Landau, and D. Slepian, "Prolate Spheroidal Wave Functions, Fourier Analysis, and Uncertainty - I, II, III," Bell System Tech. Journal, 1961-62.

32. E. J. Baghdady, "Analog Modulation Systems," Lectures on Communication System Theory, E. J. Baghdady, ed., McGraw-Hill Book Co., Inc. New York, 1961, pp. 439-555.
33. A. N. Shchukin, "On a Method of Combatting Impulse Interference in Radio Reception," Ann. USSR, Phys. Ser., 19, (trans. by P. E. Green and W. Dolye).
34. A. J. Nicholson and M. J. Kay, "Reduction of Impulse Interference in Voice Channels," IEEE Trans. on Communication Technology, December 1964.
35. B. Shepelavey, "Non-Gaussian Atmospheric Noise in Binary-Data Phase-Coherent Communication Systems," IEEE Trans. on Communications Systems, CS-11, September 1963, pp. 280-34.
36. L. R. Halsted, "On Binary Data Transmission Errors Due to Combinations of Gaussian and Impulse Noise," IEEE Trans. on Communication Systems, December 1963, pp. 428-35.
37. P. E. Bello, "Error Probabilities Due to Atmospheric Noise and Flat Fading in HF Ionospheric Communication Systems," IEEE Trans. on Communication Technology, 13, September 1965, pp. 266-79.
38. A. M. Conda, "The Effect of Atmospheric Noise on the Probability of Error for an NCFSK System," IEEE Trans. on Communication Technology, 13, September 1965, pp. 280-84.
39. P. M. Woodward, Probability and Information Theory with Applications to Radar, Pergamon Press, Oxford, England, 1953.
40. C. W. Helstrom, Statistical Theory of Signal Detection, Pergamon Press, Oxford, England, 1960.
41. T. Kailath, Course Notes EE 253a, b, c, Stanford University, 1965.
42. U. Grenander, "Stochastic Processes and Statistical Interference," Arkiv fur Matematik, 1, 1950, pp. 195-277.
43. G. E. Shilov, An Introduction to the Theory of Linear Spaces, Prentice-Hall, New York, 1961.
44. B. V. Gnedenko and A. N. Kolmogorov, Limit Distributions for Sums of Independent Random Variables, Addison-Wesley, Reading, Mass., 1954.
45. R. M. Fano, Transmission of Information, MIT Press, Cambridge, Mass., 1961.
46. A. Erdelyi, ed., Tables of Integral Transforms, McGraw-Hill Book Co., Inc., New York, 1954.

47. A. D. Watt, R. M. Coon, E. L. Maxwell and R. W. Plush, "Performance of Some Radio Systems in the Presence of Thermal and Atmospheric Noise," Proc. IRE, 46, December 1958, pp. 1914-23.
48. R. A. Helliwell, Whistlers and Related Ionospheric Phenomena, Stanford University Press, Stanford, Calif., 1965.
49. A. Erdelyi, ed., Higher Transcendental Functions, Vol. I, McGraw-Hill Book Co., Inc., 1953.

Security Classification

DOCUMENT CONTROL DATA - R & D

(Security classification of title, body of abstract and indexing annotation must be entered when the overall report is classified)

1. ORIGINATING ACTIVITY (Corporate author) Stanford University Stanford Electronics Laboratories Stanford, California 94305		2a. REPORT SECURITY CLASSIFICATION UNCLASSIFIED	
		2b. GROUP	
3. REPORT TITLE  A NEW MODEL FOR "IMPULSIVE" HOENOMENA: APPLICATION TO ATMOSPHERIC-NOISE COMMUNICATION CHANNELS			
4. DESCRIPTIVE NOTES (Type of report and inclusive dates) Scientific Interim			
5. AUTHOR(S) (First name, middle initial, last name)  Harry M. Hall, Jr.			
6. REPORT DATE August 1966		7a. TOTAL NO. OF PAGES - 176	7b. NO. OF REFS 49
8a. CONTRACT OR GRANT NO. AF 49(638)-1517- <del>XXXXXX</del>		9a. ORIGINATOR'S REPORT NUMBER(S) SEL 66-052	
b. PROJECT NO. 9768			
c. 61445014			
d. 681305		9b. OTHER REPORT NO(S) (Any other numbers that may be assigned this report) <b>AFOSR 67-0753</b>	
10. DISTRIBUTION STATEMENT  1. Distribution of this document is unlimited.			
11. SUPPLEMENTARY NOTES  TECH, OTHER		12. SPONSORING MILITARY ACTIVITY AF Office of Scientific Research (SREE & SFMA) 1400 Wilson Boulevard Arlington, Virginia 22209	
13. ABSTRACT This work is concerned with the development and application of an analytical model for atmospheric noise, which is radio noise originating in lightning discharges. The generalized "t" model resulting from our approach is in good agreement with measured data and describes the received atmospheric noise $y(t)$ as  $y(t) = a(t) n(t),$ where $n(t)$ is a narrowband gaussian process and $a(t)$ is a slowly varying random process, independent of $n(t)$ , that "modulates" $n(t)$ .  The detection of known signals in additive generalized "t" noise is considered, and the receiver that minimizes the probability of error found to be a nonlinear "logarithmic-correlator" receiver. Analytical and experimental results indicate that the probability of error achieved by this receiver in the presence of additive atmospheric noise.			

Security Classification

14.

KEY WORDS

LINK A

LINK B

LINK C

ROLE

WT

ROLE

WT

ROLE

WT

Noise Model  
 Impulse-Noise Model  
 Atmospheric-Noise Model  
 Signal Detection  
 Additive-Atmospheric-Noise Channel